DEVELOPING A 3D MULTI-BODY SIMULATION TOOL TO STUDY DYNAMIC BEHAVIOUR OF HUMAN SCOLIOSIS

KHATEREH HAJIZADEH

NATIONAL UNIVERSITY OF SINGAPORE

2013

DEVELOPING A 3D MULTI-BODY SIMULATION TOOL TO STUDY DYNAMIC BEHAVIOUR OF HUMAN SCOLIOSIS

KHATEREH HAJIZADEH
(B. E, Isfahan University of Technology, Isfahan, Iran)
(M.S., Isfahan University of Technology, Isfahan, Iran)

A THESIS SUBMITTED

FOR THE DEGREE OF DOCTOR OF PHILOSOPHY

DEPARTMENT OF MECHANICAL ENGINEERING

NATIONAL UNIVERSITY OF SINGAPORE

2013

Declaration

I hereby declare that this thesis is my original work and it has been written by me in its entirety. I have duly acknowledged all the sources of information which have been used in the thesis.

This thesis has also not been submitted for any degree in any university previously.

Khatereh Hajizadeh

List of Publications

Journal Paper

1- **Khatereh Hajizadeh**, Ian Gibson, Gabriel Liu "*Developing a 3D Multi-Body Model of the Scoliotic Spine with Lateral Bending Motion for Comparison of Ribcage Flexibility*" International Journal of Advanced Design and Manufacturing Technology, Vol 6, No 1 (2013).

Book Chapter

1- I. Gibson, **Khatereh Hajizadeh**, K. T. Huynh, B. N. Jagdish, M. J. Huang, "*Development of a Human Spine Simulation System*", in Advances in Therapeutic Engineering, Taylor & Francis Group (Book Chapter).

Conference Papers

1- **Khatereh Hajizadeh**, Gabriel Liu, Ian Gibson, Mengjie Huang "*Development of A Virtual Musculo-skeletal, Multi-body Scoliotic Spine Model*", Proceedings of the 6th International Conference on Rehabilitation Engineering & Assistive Technology (2012)

2- **Khatereh Hajizadeh**, Huang Mengjie, et al, "*Developing A 3D Multi-Body Model of A Scoliotic Spine During Lateral Bending for Comparison of Ribcage Flexibility and Lumbar Joint Loading to the Normal Model*" in ASME 2013 Mechanical Engineering Congress & Exposition, November 2013, San Diego, California.(Accepted for publication)

3- **Khatereh Hajizadeh**, I. Gibson, et al, "*Developing A 3D Multi-Body Model of the Scoliotic Spine to Simulate the Distribution of Loads on The Spine During Normal Walking*", ASME 2012 Mechanical Engineering Congress & Exposition, November 2012, Huston, Texas.

4- **Khatereh Hajizadeh**, I. Gibson, et al, "*Developing A 3D Multi-Body Model of The Scoliotic Spine with Lateral Bending Motion for Comparison of Ribcage Flexibility*" in ICMEAT 2012 International Conference on Mechanical Engineering and Advance Technology, October 2012, Isfahan, Iran (invited).

5- Mengjie Huang, Taeyong Lee, Ian Gibson, **Khatereh Hajizadeh**, "*Effect of Sitting Posture on Spine Joint Angles and Forces*" Proceedings of the 6th International Conference on Rehabilitation Engineering & Assistive Technology

Acknowledgements

I would like to express my sincere thanks and gratitude to many people who have directly or indirectly helped me in fulfilling my dream of completing my PhD. First, I would like to thank my graduate advisors, Dr. Ian Gibson and Dr. Gabriel Liu, and Dr. Lu Wen Feng for their guidance, encouragement and support throughout the period of my PhD. Their inspiring guidance, solid encouragement, and helpful insights have paved way for me to complete this research. I am grateful to the Gait Analysis Lab officer, Ms. Grace, for her support and assistance in gait analysis experiments. I would also like to express my gratitude to the graduate office staffs, Ms. Teo Lay Tin, Sharen and Ms. Thong Siew Fah, for their support.

I am very much indebted to my family, my parents, my sister and my brother who encouraged and helped me at every stage of my personal and academic life, and longed to see this achievement come true. I would like to highly thank my friends, Fatemeh Jamshidian, Ahmadreza Pourghaderi, Saeed Arabnezhad, Sara Adibi, Huyhn Kim Tho, Wang Xue and especially Huang Mengjie for their tremendous support, both physically and emotionally.

Last but certainly not least, my gratitude goes to my husband, Ehsan, for his love, support and encouragement throughout my PhD candidature. No words are sufficient to express my gratitude and thanks for his support. I am truly appreciative to all that he has done for me over the years. I could not have reached my goal without his help, support and love.

Above all, I owe it all to God for granting me the wisdom, health and strength to undertake this research task and enabling me to its completion.

Table of Contents

Summary

Knowledge of the movements of whole spine is important for evaluating clinical pathologic conditions that may potentially produce unstable situations in human body movements. At present these are few studies that report systematic three-dimensional (3D) movement analysis of the whole spine. Scoliosis is one of the asymmetric conditions in the spine. Scoliosis is a complicated condition characterized by a lateral curvature of the spine and accompanied by rotation of the vertebrae about its axis.

The objective of this study is to simulate a 3D multi-body model of the human body, especially body with spine deformity (scoliosis) for investigating various medical applications. This personalized multi-body scoliotic spine model is developed based on patient anthropometric data. Such a model is able to capture the dynamic interactions between vertebrae, muscles, ligaments, and external boundary conditions. In this study, the scoliotic spine of three patients was modeled using 2D X-ray images to investigate the biomechanics of abnormal spines which were examined in upright posture. The spine joint forces and torques were found in this posture for all models and the results were discussed. Furthermore, the biomechanics of human scoliotic and normal spine in daily maneuvers such as flexion, bending and twisting exercises were investigated with conducting musculoskeletal model with motion capture data of the subjects. The range of motion (ROM) of the patient was compared with the ROM of the healthy subject with similar anthropometric data in all exercises. The force and torque in lumbar joints from scoliosis simulated model in these exercises were compared to those of the normal one. Finally, this simulation model was used to study the effect of corrective spine surgery (instrumentation) on the spinal forces and range of motion. This model can be used as a tool for wheelchair design or other seating systems design which may require attention to ergonomics as well as assessing biomechanical behaviour between normal and scoliotic spines.

List of Tables

List of Figures

Chapter 1: Introduction

1.1 Overview of Clinical Spinal Problems

Investigation into the biomechanics of human spine in different postures is becoming increasingly important. The human spine is an essential bodily component which undertakes complex motions and provides stability and protection for the spinal cord during a variety of loading conditions. However, it is also a very vulnerable part of our skeleton that is subject to many medical problems such as whiplash injury, low back pain and scoliosis. People with sedentary jobs may spend hours sitting in a chair in a relatively fixed position, with their lower back forced away from its natural lordotic curvature. Sustained lumbar flexion (Adams and Dolan 1995) and static loading (Callaghan and McGill 2001) suggest possible risks linking prolonged sitting with lower back disorders. Extensive studies have been conducted to investigate the biomechanics of the human spine in different sitting postures.

In clinical spinal problems, "*scoliosis*" is a less common but more complicated disease in comparison with low back pain or whiplash injury. Scoliosis is generally defined as a three-dimensional deformity of the spine and trunk affecting 1.5% to 3% of the population most commonly occurring in young women (Weinstein, Dolan et al. 2008). Scoliosis is basically a source of instability in the vertebral column. This instability may cause other diseases which are not well understood yet. Current scoliosis treatments are mostly mechanical, i.e. based on external load application that can potentially be long and uncomfortable for the patients. Severe cases of scoliosis are generally treated by spinal instrumentation and fusion to stabilize and straighten the curve in 3D space (Chen, Chen et al. 2005, Desroches, Aubin et al. 2007). Decisions on instrumentation parameters such as position of instrument, the number of implants, type and shape of the rod, etc. mainly depends on the surgeons' experience. The experience and preferences of the surgeon, the objectives of surgical correction as well as the lack of standardized strategies of instrumentation can be the main reasons for variability in the operation strategy and outcome.

Therefore, collaboration between mechanical, computer engineers and orthopedic surgeons is inevitable in this field. Because of the limitations of the treatment methods, biomechanical modeling and simulations has found great importance to give future spine surgeons training before the real surgical operation. The computer models have been capable of simulating various scoliosis treatments including bracing (Perie 2004) and

instrumentation (Aubin 2003, Lafage 2004, Desroches, Aubin et al. 2007). To help surgeons gain insight into complex biomechanics of scoliotic spines and to propose better surgical plans before spine correction operations, development of a virtual bio-fidelity musculo-skeletal multi-body scoliotic spine model would be very helpful.

1.2 Biomechanical Models of Human Spine

Knowledge of the movements of the whole spine and lumbosacral joint is important for evaluating clinical pathologic conditions that may potentially produce unstable situations in human body movements. In addition, evaluation of internal actions such as contraction force of muscles, force and stress interactions in body joints (e.g. articular joints) plays an important role in understanding, treatment and physical rehabilitation of biomechanically related diseases. Despite the great importance of understanding these parameters, there are limited feasible experimental techniques for quantitative (or even qualitative) evaluation of internal interaction between bonds, cartilages, joints and soft tissues (muscles, tendons, etc.) directly and in a painless fashion. This important requirement, as well as lack of a proper understanding of the biomechanics of the human body was the main reason for emerging computational biomechanics and developing biomechanical models to evaluate the behaviour of the different parts of the body.

Computer modeling simulation has been also applied to try and help to solve some spine problems (Fagan, Julian et al. 2002). Multi-body and finite element models, or a combination of the two, are popular simulation tools that can contribute significantly to our understanding of the biomechanics of the spine. Although a great deal of computational power may be required, finite element models (FEMs) are helpful in understanding the underlying mechanisms of injury and dysfunction, leading to improved prevention, diagnosis and treatment of clinical spinal problems. These models often provide estimates of parameters that *in vivo* or *in vitro* experimental studies cannot obtain easily. Although they can predict internal stresses, strains and other biomechanical properties under complex loading conditions, they generally only consist of one or two motion segments. At present there are few studies that report systematic three-dimensional (3D) motion analysis of the whole spine.

Compared to FEMs, multi-body models have advantages such as less complexity, less demand on computational power, and relatively simpler validation requirements. Multi-

body models possess the potential to simulate the kinematics and kinetics of the whole human body.

1.3 An introduction about multi-body for spine

In one early model, Chaffin represented a very simple spine in which back extensors were represented by a single muscle equivalent (Chaffin 1969). One of the first attempts to construct a more realistic model incorporated the geometry of individual muscle fascicles derived from McGill's own cadaver dissections (McGill and Norman 1986). This work describes a dynamic model of the low back that incorporates extensive anatomical detail of a three-dimensional musculo-ligamentous-skeletal system. The study suffered however from not explicitly reporting the anatomical information used. Since then, the anatomy of the lumbar erector spine and the lumbar multifidus has been described in great detail (Bogduk 1980, Macintosh and Bogduk 1986, Macintosh and Bogduk 1987) and this information has become a common basis for detailed biomechanical models (Bogduk, Macintosh et al. 1992a, Macintosh, Bogduk et al. 1993, Stokes and Gardner-Morse 1995, Van-Dieen 1997). These models excluded quadratus lumborum muscles and later, Zee et al. (Zee, Hansen et al. 2007) presented a more detailed spine model incorporating most of the necessary lumbar muscles. In most of the previous models, only a portion of the spine (for example the lumbar spine) was modeled, whereas the other regions (e.g. thoracic spine and cervical spine) were left as rigid segments.

Based on the studies presented above, it is found that modeling of a detailed whole human spine has not been completely investigated. Although there were finite element spine models created for the whole spine, the influence of spinal muscles as well as ligaments was not fully taken into account in these models. Furthermore, in multi-body methods, many authors have attempted to develop human spine models. Nevertheless, these models are still incomplete.

This project mainly focuses on developing a 3D multi-body simulation tool to study dynamic behaviour of human musculoskeletal system. In this work, a detailed realistic 3D model of the whole spine is designed which enables us to consider the effects of structural abnormalities of scoliosis as well. This model is constructed based on measurements of the anatomical (biomechanical) parameters of healthy and scoliosis real subjects and is developed in the *LifeMOD* Biomechanics Modeler (LifeMOD). *LifeMOD* is a dynamic modeling tool (software). It is a plug-in module to ADAMS (Adams) and is able to

construct multi-body model of the human musculoskeletal system with different boundary conditions and/or environments. The kinetics and kinematics of the developed model in this system can be analyzed by a combination of inverse and forward dynamics (Roberson and Schwertassek 1988).

Recently, LifeMOD Biomechanics Modeler (LifeMOD) has been popularly used as a multi-body dynamic simulation platform in numerous modeling researches. A dynamic simulation of the cervical spine containing a disc implant was performed using *LifeMOD* to understand the intradiscal forces/pressures, bending moments and vertebral body rotation (De-Jongh, Basson et al. 2007). In a similar manner, a human-wheelchair musculoskeletal model was generated with *LifeMOD* to analyze the cervical spine of a wheelchair user subjected to frontal and side impacts (Kim, Yang et al. 2007).

The main goal of this research work is to investigate and develop a simulation tool to study biomechanics, more specifically kinematics, of the human body with scoliosis spine models. This model is able to provide valuable information such as internal forces between vertebrae, joints, relation between the angles of the joints and muscle tensions and joint torques. It also has the potential to calculate the forces resulted from interaction between rods, screws, and implants used for instrumentation correction of the spine deformity. The outcomes of this simulation and analysis tool can be useful for orthopedists or surgeons to acquire valuable information about the biomechanics of the body which may enable them to plan the operation/treatment more accurately, to optimize the design procedure of the biomechanical correction devices (braces, implants, etc.), or to predict the results of the treatment.

The necessary factor to build such a simulation tool is in developing a realistic model of the human body in which all biomechanical and geometric details of the spine and its deformities has been taken into account. In the current work *LifeMOD* was used as a platform to create a "multibody" biomechanical model of the spine in which the scoliosis deformity of the spine can be considered. Real-time motion capture analysis of the real subject (base on whom the model has been constructed) have been used for validation of the results of this multibody model.

The personalized multi-body scoliotic spine models represented in this study are based on patient anthropometric data. These models are able to capture the dynamic interactions between vertebrae, muscles, ligaments and external boundary conditions (e.g. representing the probable instrumentation of external forces).

It is noteworthy that this research was done in close relationship with National University Health Center (spine center) and we took the benefit of medical advices from Dr. Gabriel Liu who is a surgeon specialist in scoliosis spine treatments. This model can furthermore be used as a tool for wheelchair or other seating systems design which may require attention to ergonomics as well as assessing biomechanical behaviour between normal and scoliotic spines. The force in lumbar joints from scoliosis simulated model in daily maneuvers such as flexion/ extension, bending and twisting were compared to those of the normal one.

1.4 Outline of thesis

In this study, a multi-body spine model presents to quantify the various biomechanical aspects which are important in scoliosis assessment. As mentioned earlier, this model is capable of providing fundamental biomechanical information about the scoliotic spine which can be required for optimization of the spine deformity treatments methods.

Chapter 2 gives an overview of biomechanics of spine and spine deformity, Biomechanical models of spine deformity and a review of methods for quantitative evaluation of scoliotic spine curvature.

The concepts of the spine biomechanics and modeling methods have been explained in chapter 3. It presents the investigation on simulation tools which are used in this study followed by the development of the detailed scoliosis modeling method in various stages. The procedure of constructing of the final multibody model has been described in chapters 3 and 4. In these chapters, initially the general structure of the model in the light of different anatomical structures has been described and the assumption and simplifications considered in the simulation process have been explained. Chapter 3 is concluded by validation of the model and discussion about the role of soft tissues (ligaments and back and lumbar muscles) and intra-abdominal pressure on the stability of the model.

Being a generic model, the geometrical aspects of the model (e.g. the severity of the scoliosis deformity) can be easily changed in this model. In chapter 4, two methods for modeling of the scoliosis spine were presented. The loading condition in sagittal and frontal planes on hypothetic scoliosis spine with different Cobb angle was investigated in this chapter as well.

Simulation results of the detailed (refined) spine model of normal and scoliosis conditions tested in different body motions and configurations has been reported in chapter 5. In this chapter the related simulation challenges and limitations has been also discussed.

Furthermore, the performance of the model with scoliosis condition is tested as the final goal of the musculoskeletal model with conducting it with Mocap data. Dynamic behavior of the scoliosis subject during daily activities like bending and twisting was investigated and the mechanical behavior of the scoliosis spine was compared to those of the healthy spine in this chapter. According to the results subjects with scoliosis condition endure higher force during bending and twisting movements compared to normal ones.

In chapter 6, the presented results and methods in the previous chapters as well as the strength and limitations of the developed models will be discussed. Summarizing the findings of the work, recommendations for improvement of the current method in the future works has been presented. Further information about the modeling and simulation details steps has been extensively presented in Appendices. The appendices give other relevant information including a step by step guide to the modeling technique.

Chapter 2: Literature review

2.1 Spine Physiology and Biomechanics

Understanding the physiology and biomechanics of the spine is necessary to get insight into the motion and load carrying capacity limitations of the spine. The main function of the spine together with the trunk muscles surrounding the spine is to support the weight of the head and upper extremity limbs and their consequent forces and moments to maintain the upright body posture. In addition, spine is responsible to control the relative motion of the head, neck, trunk and the pelvic region. It also provides a base for ribs and connects the upper and lower body via the sacrum which connects the spine to the pelvis. Last but not the least, the spine has the very important role of protecting the spinal cord against any physical damage due to shocks or excessive movements (Panjabi 1990).

The human spine is made up of 24 vertebrae which are stacked on top of one another to create the spinal column. The bones of the spine, the vertebrae, are the hard elements of the structure which are separated from each other by soft inter-vertebrae disks. While vertebrae support the loads as levers, the intervertebral disks act as confined joints between the vertebrae. The unique combination of vertebrae and the disks provides numerous degrees of freedom to the human body such as forward-backward and lateral bending, turning and rotating (twisting) around the body's central axis. The spine is tied together by ligaments and actuated by muscles (Edidin, Kurtz et al. 2006). The muscles attached to the spine act as actuators which provide the required forces (moments) and stiffness required for different modes of body mobility (e.g. standing, bending, twisting, etc.) and more importantly stability of the body.

Applying external loads or relative movements to the spinal system, imposes internal tensions and stresses to the components of this system (i.e. vertebrae, disks, ligaments, and muscles). If these loads are greater than the maximum magnitude that a disk, vertebra or ligament can support, the whole system or a part of that will fail.

The spine is divided into cervical, thoracic, lumbar, and sacral regions. Figure 2.1 shows the different regions of the human spine. The seven cervical vertebrae of the neck provide maximum flexibility and range of motion for the head. These vertebrae are nominated C1 through C7. The 12 thoracic vertebrae (T1 through T12) support the ribs and the organs that hang from them. The five vertebrae under the thoracic region constitute the lumbar

region. These five lumbar vertebrae (L1 through L5) are subjected to the highest forces and moments. The lumbar section of the spine has the critical responsibility of supporting the total weight of the trunk and upper extremity limbs of the body and also provides the maximum capability of bending and twisting as compared to the other parts of the spine. Hence, they are the largest and strongest vertebrae of the spine. These bones (vertebrae) are optimized for structural support rather than flexibility. At the lower extremity of the spine, Five bones that are joined together in adults form the sacrum and three to five bones fused together to form the coccyx or tailbone.

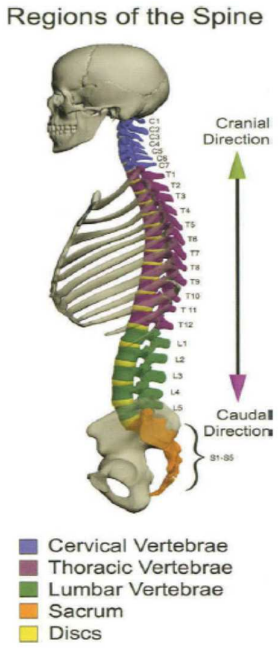

Figure 2.1 Cervical, thoracic, lumbar and sacral region of the spine (Edidin, Kurtz et al. 2006)

From the back view, the vertebrae form a straight column keeping the head centered over the body. From the side view however, the spine is consisting of different curves as can be seen in Figure 2.2. These natural curves position the head over the pelvis and work as shock absorbers to distribute mechanical stress during movement (Edidin, Kurtz et al. 2006).

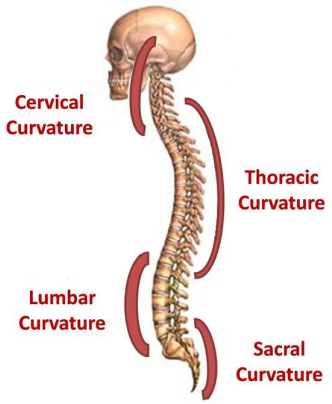

Figure 2.2 Side view of the spine showing the natural curvatures of the spine

All vertebrae have almost a similar geometry. The main section of each vertebra (anterior section) is a round block of bone, called the vertebral body that is optimized for sustaining compressive loads. The size of the vertebra gradually increases from the neck to the lower parts of the spine. This increased size helps to maintain the balance of the spine and also supports the larger muscles that are connected to the lower parts of the spine. The posterior elements of the spine are optimized to provide the maximum protection of the spinal cord and also proper connection points for attachment of the muscles (Kurtz and Edidin 2006). The structure of a typical vertebra is shown in Figure 2.3.

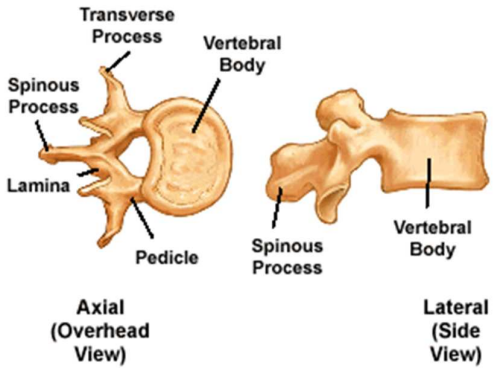

Figure 2.3 The structure of a typical vertebra showing the anterior and posterior sections of the spine (figure from http://www.coloradospineinstitute.com/)

2.1.1 Interbody Joints

As mentioned earlier, because of its flexibility, the spine allows relative motion of limbs connected to that with respect to each other or with respect to the rest of the body. The

flexibility of the spine itself sources from the relative motion of the vertebrae with respect to each other which is controlled through interbody and facet joints (Figure 2.4).

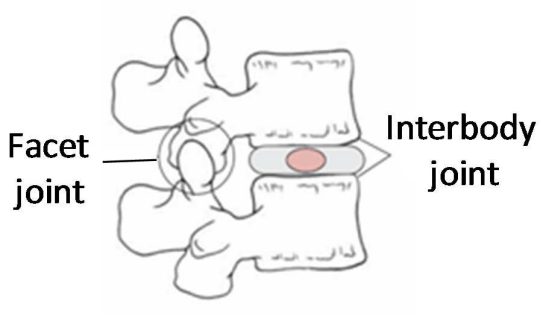

Figure 2.4 Interbody joint and facet joint (Pamela K. Levangie 2005)

The facet joints are composed of the articulations between the right and left superior articulating facets of a vertebra and the right and left inferior facets of the adjacent cranial vertebra. The facet joints are diarthrodial joints and have regional variations in structure (Wooley, Grimm et al. 2005).

Interbody joints are composed of two successive vertebral bodies, the gaps between which are filled with intervertebral disks. The intervertebral discs form a viscoelastic cushion which separates the vertebrae from each other and provides a higher range of motion (Figure 2.5). The other important function of the intervertebral disk is to transfer the load from upper vertebra to the lower one in a smooth and attenuating manner. The intervertebral disks constitute about 20-30% of the total height of the spinal cord. The size and thickness of the disk is not uniform and changes based on the amount of load which should be supported by the disk and also the motion range of the specific spine region. Therefore by increasing the load, the thickness of the disk gradually increases from ~ 3 mm in the cervical region with minimum weight load to about 9 mm in the lumbar region with maximum weight-load capacity (Panjabi 1990). The relation between the motion range and the thickness of the disk is not straight forward. An important factor which determines the maximum range of motion is the disk thickness to vertebra height ratio (Kapandji and Honore 1981), the greater the ratio, the greater the mobility. This ratio is the greatest in the cervical region followed by the lumbar region and is the minimum in the thoracic part of the spine.(Pamela K. Levangie 2005)

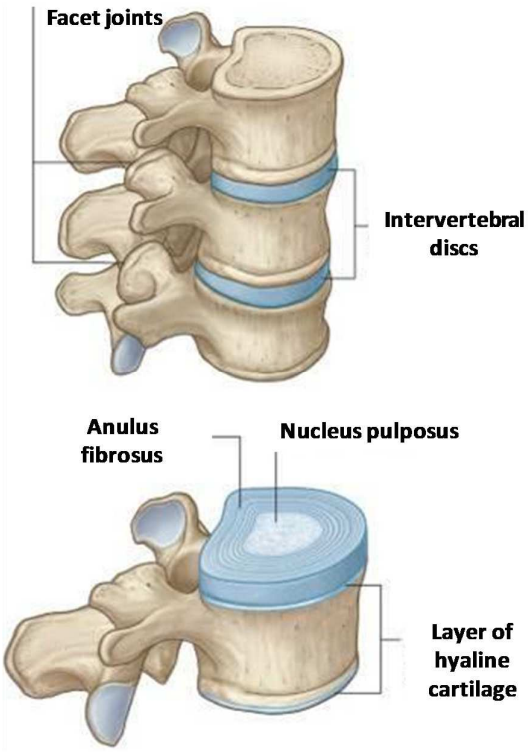

Figure 2.5 Intervertebral disc (http://www.naturalheightgrowth.com/)

Function of interbody joints provide different kinds of motions such as gliding, distraction, and tilt motion. Gliding motion is a relative linear movement of the vertebrae in sagittal and frontal (lateral) planes. Tilt motion is rotation of the vertebra in sagittal, frontal, and transverse planes. Distraction (compression) is linear displacement of the vertebrae in the axial direction. Combination of these motions provides six degree of freedom as can be seen in Figure 2.6. The magnitude of these motions is generally a function of structure of the disk and vertebral body and also the support of the ligaments (Panjabi 1990). In the current study, interbody and facet joints are referred to as "intervertebral" joints.

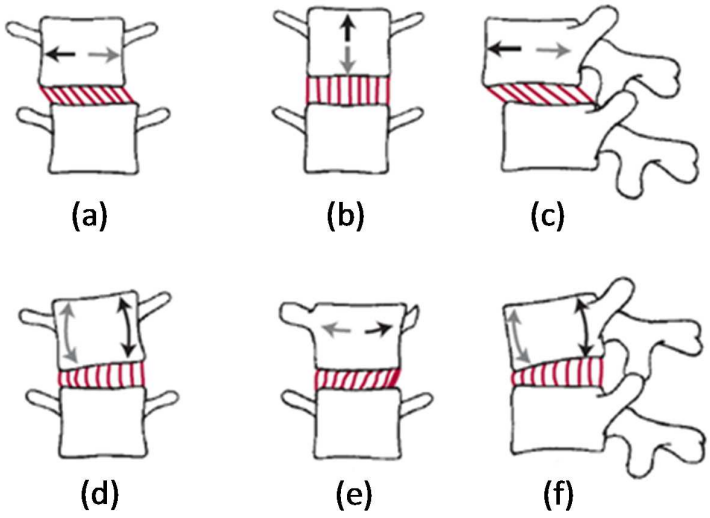

Figure 2.6 Translations and rotations of one vertebra in relation to an adjacent vertebra (a) Side-to-side translation (b) Superior and inferior translation (c) Anteroposterior translation (d) Side- to-side rotation (e). Transverse rotation (d). Anteroposterior rotation (Pamela K. Levangie 2005)

2.1.2 Ligaments and Joint Capsules

Ligaments are one of the important parts of the spinal system. The main function of the ligaments is to connect the separate bones of the joints (i.e. facet and interbody joints) together and to limit the mobility of the articulations and prevent the severe movements of the bones (vertebrae). Depending on the position and performance of different regions of the spine, shape, number and physiological properties of the ligaments may change. Generally spinal ligaments can be categorized into 6 different groups as depicted in Figure 2.7. The ligaments which connect the anterior and lateral surfaces on the vertebral bodies are referred to as “anterior longitudinal ligament (ALL)” and “posterior longitudinal Ligament (PLL)”. ALLs and PLLs start from the sacrum and continue up to the second cervical vertebra.

The thick and elastic ligament which connects the laminae (see Figure 2.3) of two neighboring vertebrae together is called ligamentum flavum which extends from C2 to the sacrum and covers the anterior wall of the spinal canal (Olszewski, Yaszemski et al. 1996). The considerable elasticity of these ligaments remarkably contributes to preserve the upright posture, and also helps the spine to recover the upright position after flexion.

The ligament which connects the spinous processes (Figure 2.3) of two adjacent vertebrae together is called the interspinous ligament which plays an important role to maintain the stability of the lumbar spine. The tips of the spinous processes of the vetrbrae from C7 to L3 (or L4) are connected together via the strong cord-like supraspinous ligaments.

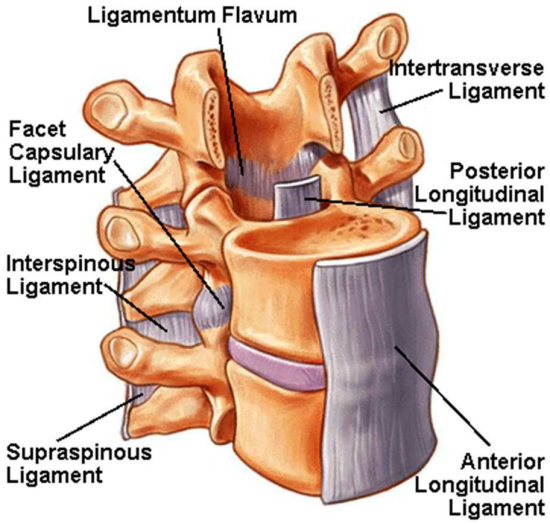

Figure 2.7 Six types of spine ligaments (Chiropractic 1997)

Generally, these ligaments function as elastic bands which can only support tension forces and control/limit the movement and deformation of the spine and in this way provide the spine stability (Panjabi 1990).

2.1.3 Muscles of the vertebral columns

In the spinal system, muscles act as actuators that depending to their position (spine regions), may act to maintain the proper posture of the head and the spine, control the movement of the trunk, and/or to protect the spine against external shocks and forces. The cervical spine muscles basically are responsible for accurately positioning of the head in space and maintaining the upright position of the head against gravity. In addition to the above mentioned responsibilities, the thoracic muscles serve to stabilize the neck and move the scapula. Movement of the trunk is produced and controlled by means of the lower spine muscles. These muscles are also functioning to maintain stability of the trunk during the motion of the lower extremities and damping the extensive forces that are imposed to this area (Pamela K. Levangie 2005). Generally, the large muscles create larger trunk

movements and provide stiffness, and the small muscle groups are responsible for precise control of movements (Panjabi 1990).

2.2 Spine deformity

As explained in the previous sections, the spine is a very complicated system consisting of several components of different biomechanical properties. While this complexity is necessary for proper functioning of the spine, it makes the spine very sensitive to any abnormality in terms of shape of the vertebrae (i.e. irregular development of the vertebrae), stiffness of the ligaments and muscles (i.e. too soft or too stiff ligaments or very weak muscles), flexibility and shape of the disk, etc. These abnormalities may directly result in abnormal spine shapes (deformities) which on the other hand can affect the normal performance of the spine and/or other organs such as heart, lung, back muscles, hip alignment, etc.

Generally, an arbitrary spine deformity consists of a combination of abnormal curvatures in three different biomechanical planes (e.g. coronal, sagittal, and transverse) as shown in Figure 2.8. Based on the plane in which the abnormal shape has taken place, the spine deformities can be categorized into three major groups of kyphosis, scoliosis, and kyphoscoliosis.

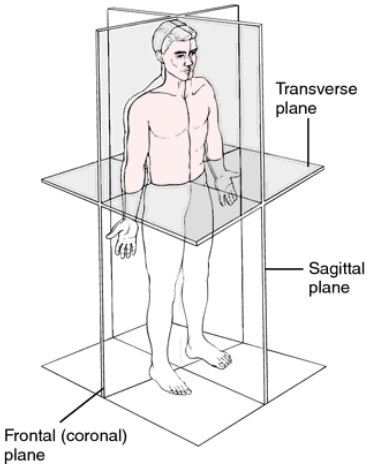

Figure 2.8 Biomechanical planes (Villafranca, Ballasteros et al. 2000)

2.2.1 Kyphosis

Kyphosis or abnormal thoracic spinal curvature is characterized by the presence of a hump in thorax or chest region in the sagittal plane (Figure 2.9) which can be considered as an exaggerated backward curvature in the thorax region. A patient with such spinal deformity may experience difficulties in lying on the back. This abnormality can mainly be attributed to degeneration of the disks and/or vertebrae, developmental problems of the vertebrae in the thorax region, or poor standing/sitting postures.(Ryan and Fried 1997)

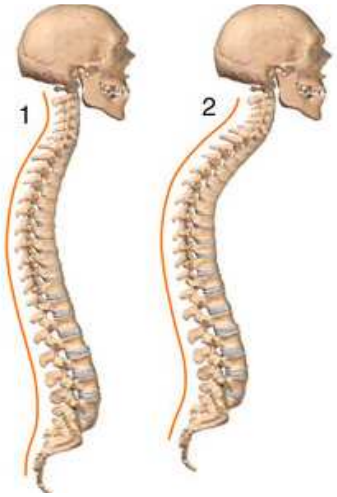

Figure 2.9 lateral view of (1) normal spine and (2) spine with kyphosis (figure from http://www.activeforever.com/a-kyphosis)

2.2.2 Scoliosis

Scoliosis is a complex 3D deformity that can be generally characterized as deformation (curvature) of the spine in the frontal plane (Figure 2.10). This displacement of the vertebrae can be accompanied by the rotation of the vertebra around its axis. In an x-ray image which is taken from the back, a normal spine should be like a straight line; however, from this view, a scoliosis spine looks like a “C” or “S”. In most cases, scoliosis is not painful, but there are certain types of scoliosis such as degenerative that can cause back pain.

2.2.3 Kyphoscoliosis

A combination of abnormal curvatures in both coronal and sagittal planes is clinically referred to as “kyphoscoliosis”(Dickson 2009).

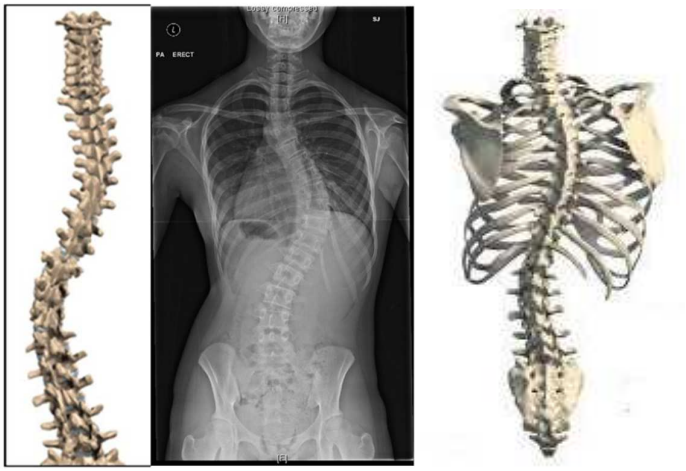

Figure 2.10 back view of the spine with Scoliosis deformity

2.3 A review of methods for quantitative evaluation of scoliotic spine curvature

As compared to lower back pain, scoliosis is a less common but a more complicated spinal disorder affecting between 1.5% and 3% of the population. Scoliosis can be categorized in three major groups of adult, infantile, and elderly. Adolescent idiopathic scoliosis (AIS) is the most common type among scoliosis types (about 80% of the scoliosis cases). In this type, the cause of scoliosis is unknown (Weinstein 1986). Although many different conditions such as genetics, abnormal growth hormone discharge, wrong nutrition regimes (e.g. lack of calcium), neurological problems, continuous and repetitive cycles of lifting heavy items (e.g. heavy bags or back-packs), incorrect sports activities, and poor standing/sitting postures have been implemented as the causes of scoliosis, none of them has been known as the certain cause of AIS (Keim 1982, Machida 1999).

In most of the cases, AIS starts at the age of 10-18. It is more common among girls and is not a function of race. This abnormal spine deformities at early ages (when the curve has not been developed), does not show any side effect such as bone or joint problem and in the case of early identification can be treated or controlled by intervention which fixes the spine and prevent further progression of the curvature (Lenke, Betz et al. 2001). However,

if not controlled, the progression of scoliosis may lead to large deformities which consequently may impose excessive pressure on the internal organs such as heart, lungs and liver and cause side effects such as chest pain or shortness of breath.

Identifying the curve pattern, age, and level of severity (progression) of the curve are the most important roles in taking the proper decision about the treatment method (syndrome Homocystinuria 2001, Weinstein, Dolan et al. 2008, Weiss, Bess et al. 2008). For example, while the slight curve progression are not painful and can be easily monitored or treated by physiotherapy, in the more severe (moderate) cases bracing has to be used to hinder or stop the curve progression (Maruyama 2008, Sponseller 2011). In very severe cases where the curve is progressive, the curvature is corrected or controlled with fusion of vertebrae in which the vertebrae are fixed to each other using metallic implants (instrumentation) through a surgical operation. One of the common instrumentation methods to fix the severe curvature of the scoliosis spine was "Harrington instrumentation" (Harrington 1962). In this method, fixation was done by applying compression and distraction forces by means of a series of rods, wires and hooks. The main drawback of this method was considerable reduction of the mobility of the spine after the surgery. To address this problem, Dwyer and Newton (Dwyer, Newton et al. 1969, Dwyer 1973), developed an anterior system with a lower level of fusion. While this method was able to support the spine with the same level of correction as that of Harrington method, it limited the mobility of the spine to a lesser extent. In this method, plate segments were horizontally installed across the vertebral bodies only on the convex side of the curve by means of screws and the correction force was applied by means of a tensioned cable. By replacing the cables by flexible rods and nuts, Zielke (Zielke 1982) modified the anterior approach and further increased the mobility of the treated spine.

Decisions on instrumentation parameters such as position of instrument, the number of implants, type and shape of the rod, etc. mainly depends on the surgeons' experience. Therefore, the experience and preferences of the surgeon, the objectives of surgical correction, and the lack of standardized strategies of instrumentation result in strategy and outcome variability of the operation.

This should be noted that while the first two techniques (physiotherapy and brace) are feasible during the growth age, the latter case (diffusion) surgery is only possible when the growth is completed (King, Moe et al. 1983). It is noteworthy that these treatment methods are not meant only for correction of the spine deformity, but also to balance the posture and maintain the mobility of the patient. As can be seen, the treatment methods may drastically

change based on the severity of the scoliosis curve progression (Stokes 1994). This necessitates a quantitative definition rather than qualitative expressions to define the severity of the scoliosis curvature.

Because of their cost effectiveness and ease of availability, two-dimensional (2D) images are widely being used in clinical examination. Since most of the important components of the scoliosis deformity are detectable in the coronal cross-sections, the 2D images taken in the frontal (coronal) plane have been extensively used to evaluate the spinal curvature and deformation severity of a scoliotic spine (Vrtovec, Pernuš et al. 2009).

One of the earliest methods to evaluate the spine deformity in the coronal plane was proposed by Ferguson (Ferguson 1930). This method evaluates the deformity by measuring the angle between two straight lines that connect the centers of the end vertebrae with the center of the apical vertebra (Figure 2-11 (a)). A similar method was proposed by Cobb (Cobb 1948), where the deformity was measured by the angle between the two straight lines that are tangent to the superior and inferior endplate of the superior and inferior end vertebra, respectively (Figure 2-11(b)). As both Ferguson and Cobb methods are based on manual identification of the end vertebrae, their variability and unreliability are relatively high (Vrtovec, Pernuš et al. 2009).

Short-segment or small spinal curvatures can be measured by means of "Green index" technique which evaluates the deformity at individual vertebrae (Greenspan, Pugh et al. 1978). In this method centers of the vertebrae at the beginning and end of the curved region of the spine are connected by an orthogonal line which is called "spinal line" (Figure 2.11 (c)). By dividing sum of the length of the lines which are drawn from center of each vertebra perpendicular to the spinal line to the total length of the spinal line, one can calculate the index of deformity of the spine. For a normal spine this value has to be zero.

A new method for measuring coronal curvature in radiographs was developed by Diab et al.(Diab, Sevastik et al. 1995). They compared it to the Cobb and Ferguson method. This method consisted of identifying the four vertebral body corners of the apical and end vertebrae.

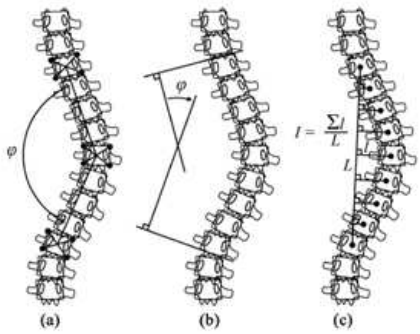

Figure 2.11 Evaluation of coronal spinal curvature in 2D images (Vrtovec, Pernuš et al. 2009), (a) Ferguson method (Ferguson 1930), (b) Cobb method (Cobb 1948), (c) Greenspan index (Greenspan, Pugh et al. 1978)

Among all measuring methods, Cobb method has been the most popular method in the publications. Instead of measuring the changes in the spinal curvature, this method is able to show changes of the final inclination of each vertebra and represents maximal deviation of the spine in the frontal plane as described in Figure 2.11.

The main reasons of popularity of the Cobb's method are its ease of application, repeatability of the measurements, and its capability to measure large deformities. Because of all these advantages, Scoliosis Research Society (SRS) in 1966 adopted this method as the standard method for evaluation of the deformities of the spine with scoliosis conditions (Vrtovec, Pernuš et al. 2009). According to the Scoliosis Research Society standard definition, scoliosis is diagnosed when the Cobb angle of the spine is greater than 10 degrees (Cobb 1948, Kane 1977). Deformations between 10 and 25 degrees are considered as mild; curves with Cobb angle between 25 and 45 are moderate and curvatures with Cobb angles greater than 45 degrees are considered as severe scoliosis cases.

2.4 Biomechanics, modeling and simulation of the scoliotic spine

Distribution of different loads on the spine is one of the important factors in the field of orthopedics, physiotherapy, and ergonomics. It has been shown that overloading the spine is one of the major risk factors resulting in disk degeneration (Marras, Lavender et al. 1995, Hoogendoorn, van Poppel et al. 1999, Bakker, Verhagen et al. 2009).

Majority of the early biomechanical studies of the spine focused on prediction of local kinematic and dynamic responses of a certain part of the spine under load. One of the oldest techniques to experimentally study the biomechanics of the spine in different static or

dynamic postures was conducted by Nachemson and Elfstrom in 1970 (Nachemson and Elfstrom 1970). In this method, needle electrodes were inserted into the intervertebral disks of the lumbar region to measure the disks internal pressure in different postures and actions such as sitting, standing, lying, jumping, etc. In 1987 Glashen et.al studied the load/displacement behaviour of the lumbosacral joint of the spine in a cadaveric investigation. In their experiments, different external forces and moments in different directions were applied to the L5/S1 joint and six consequent displacements of this joint were measured and finally the stiffness of the L5/S1 joint in segments in flexion extension, and lateral bending were calculated (McGlashen 1987). Measurement of the intradiscal pressure at different single joints of the spine was conducted by insertion/implantation of sensitive transducers into the body of the subject and recording the pressure during different sitting postures. (Sato K 1999, Wilke HJ 1999, Wilke, Neef et al. 2001). Despite its importance, direct quantification of the spinal loads of a living subject is not possible as the load transducers always requires an invasive process and there are few examples in which the spinal loads in certain regions of the spine have been evaluated by *in vivo* measurements (Stokes and Gardner-Morse 2004).

This limitation has urged researchers of this field to develop analytical musculoskeletal simulation models of the spine to estimate/simulate its bio-mechanical behavior (which are impossible or difficult to measure) in simplified conditions (McGill 1987, Stokes and Gardner-Morse 1995, Daggfeldt and Thorstensson 1997, Fagan, Julian et al. 2002, Rohlmann, Petersen et al. 2012). These techniques can be considered as the only method to investigate the internal interactions (loads) between the spine system members (i.e. among vertebrae, ligaments, disks, etc.) which are impossible through *in vivo* experiments. Due to complexities in terms of structure, shape, diversity of the bio-mechanical properties and dynamics of the human body and more specifically the human spine, up until now it has been impossible to develop a full realistic biomechanical model of the whole spine. To address these limitations, researchers have tried to develop simplified models of a certain part of the body (e.g. intervertebral disks, muscles, or a region of the spine) insulated from the rest of the body. These simplified models usually consider the very basic constituting elements (e.g. vertebral bodies, disks, main active muscles, etc.) and neglect the less important elements such as soft tissue, passive muscles (McGill 1987, Cholewicki, McGill et al. 1995, El-Rich, Shirazi-Adl et al. 2004, Shirazi-Adl, El-Rich et al. 2005).

These models have been basically used to help the researchers and physicians to measure or estimate the parameters which are very difficult or even impossible to be measured by

common experimental methods. Intradiscal pressure, joint reaction forces (Nachemson 1966, Nachemson 1981, Sato K 1999, Wilke HJ 1999, Wilke, Neef et al. 2001), or interactive forces between the implants which internally fix the vertebral bodies together are a few examples of these parameters which are difficult to be measured by experiments (Rohlmann, Bergmann et al. 1999, Rohlmann, Graichen et al. 2000, Rohlmann, Gabel et al. 2007). A variety of assumptions and simplifications that are used to develop these models in conjunction with the mechanical complexities have resulted in remarkable variations in the results obtained from different models which are studying the same region of the body.

In most of these biomechanical models, the spine is studied in the static mode (activities with permanent static posture) in which the posture of the body and consequently the internal and external loads do not change. Investigation into the dynamics of the spine can be done using two main simulation/modeling approaches of Finite element (FE) modeling (Belytschko, Kulak et al. 1974, Ahmed, Shirazi-Adl et al. 1986, Bozic, Keyak et al. 1994, Goel, Park et al. 1994, Yoganandan, Kumaresan et al. 1996, Maurel, Lavaste et al. 1997, Pankoke, Buck et al. 1998, Kumaresan, Yoganandan et al. 1999, Seidel, Hinz et al. 2001, Teo and Ng 2001, Zander, Rohlmann et al. 2002, Ng and Teo 2005, Natarajan, Williams et al. 2007, Greaves, Gadala et al. 2008, Schmidt, Heuer et al. 2008) and multi rigid body or multi-body models (MBM) (Chaffin 1969, Garcia and Ravani 2003, Aubin and Labelle 2004, Desroches, Aubin et al. 2007, Abouhossein, Weisse et al. 2011).

Multi-body and finite element models, or a combination of the two, are popular simulation tools that can contribute significantly to understanding of the biomechanics of the spine. Finite element models (FEMs) are helpful or sometimes are the only tool to understand the underlying mechanisms of injury and dysfunction, leading to improved prevention, diagnosis and treatment of clinical spinal problems. These models often provide estimates of parameters that *in vivo* or *in vitro* experimental studies cannot obtain easily. The FEM models generally are more detailed in representing spinal geometries (Belytschko, Kulak et al. 1974, Ahmed, Shirazi-Adl et al. 1986, Bozic, Keyak et al. 1994, Yoganandan, Kumaresan et al. 1996, Kumaresan, Yoganandan et al. 1999, Teo and Ng 2001, Natarajan, Williams et al. 2007, Greaves, Gadala et al. 2008). Although this type of models can predict internal stresses, strains and other mechanical properties under complex loading conditions, they generally consist of only one or two motion segments and do not provide insight for the whole spinal column. Furthermore this technique suffers from considerable computational effort and convergence problems (Aubin, Goussev et al. 2004).

In contrast, the Multi-body models study the dynamics of interconnected bodies - generally a series of rigid bodies (vertebrae or bones) connected by soft or flexible tissues which may undergo large translational and rotational displacements. In this method, the rigid bodies are considered as solid elements and the flexible elements are modeled as springs (Jerkovsky 1978, Goel, Park et al. 1994, Maurel, Lavaste et al. 1997, Pankoke, Buck et al. 1998, Seidel, Hinz et al. 2001, Zander, Rohlmann et al. 2002, Ng and Teo 2005, Schmidt, Heuer et al. 2008). In this method, each element (body) is defined based on two important terms of degree of freedom and motion constraints. The degree of freedom determines the minimum number of parameters which are required to define the location of the body in the space and constraints are defined as the limitations of degrees of freedom of one or more articulated bodies. Despite FEMs, MBM is relatively simpler and with less computational complexity and easier for validation.

The kinematics of the multibody methods is basically originated from the classical mechanics. The simplest multibody system is comprised of free particles. Such a system can be modeled by Newton's laws. In 1775, Euler introduced the concept of the rigid bodies (Euler 1776) which can be considered as the principal element of the more realistic multibody systems. A combination of both methods which is known as Newton-Euler equations is used for modeling of the systems with joints or constraints. In this method all the interactive and constrain forces have to be taken into account and the momentum and force balance equations are needed to be written for all the elements of the system. This makes the Newton-Euler method a tedious approach when a system with many bodies is supposed to be dealt with or when only a few of the force of momentums of a complex system are supposed to be found.

As the first try to develop the principle of virtual work for dynamic systems, in 1743, d'Alembert separated the applied and reaction forces in the constrained rigid body systems and stated that the work of sum of differences between the external applied forces (deriving forces) and inertia forces for an arbitrary virtual displacement is zero (this displacement has to comply with the constraints of the system). This method is known as called d'Alembert's principle and demonstrates that the constraint forces is not needed to be considered (d'Alembert).

In 1953, Lagrange introduced mathematical form of the principle of d'Alembert's principle of virtual work as set of second order ordinary differential equations (Lagrange 1853). He did the first systematic analysis of the constrained multibody systems at 1788 (Lagrange 1853). By considering Newton and d'Alembert principles, Lagrange developed a set of

equation which could represent the dynamics of a multibody system in a simple form disregarding of the coordination (in a generalized coronation). Considering the kinetic constrains of the system, he applied the variation principles to the total kinetics and potential energy of the system. The resultant equations were either a set of differential algebraic equations (DAE) or a set of ordinary differential equations (OED) which are also known as which was resulted in first and second kind of Lagrange equation respectively. By differentiating the scalar kinematic and potential energy parameters, Lagrange's equation do not take the effect of the constraints or interactive forces which do not perform work. However, differentiating the scalar energy functions can be considered as the main disadvantage of the Lagrange equations when a large multibody system is to be solved.

In order to eliminate the limitations of both techniques (Newton-Euler and Lagrange methods), Kane et.al developed a simpler method based on d'Alemberts principle. In this method, the translational and rotational velocities of a nonholomonic multibody system where considered and the partial derivatives of the position vectors were replaced with partial derivatives of velocities with respect to time derivative of the position vector. Doing so, Kane proposed the concept of generalized forces (Kane and Levinson) in which there was no need to consider the interactive and constraint forces and also no need to differentiate the energy functions. Simplicity of formulation (ordinary differential equations (OED)) less number of variables and parameters (as compared to Lagrange method), and availability of many efficient algorithms to calculate the partial derivatives (compute velocities and accelerations), has made this method very popular for computational forward dynamics multibody systems. This method soon founds its position in simulation of complex robotic, biomechanical and control systems.

As one of the early applications of rigid multibody methods, dynamics of the human walking was modeled by Fischer et.al in 1906 (Fischer 1906). In the second half of 20th century, computational modeling of dynamics of biomechanical systems using multibody methods became an interesting topic for researchers, especially those who work in the field of athletic training or designing of sport equipments. Simulation of gross body motions by Chaffin (Chaffin 1969), falling cat phenomena by Kane (Kane and Scher 1969), stability analysis of the biped human locomotion Vukobratovic et al. (Vukobratovic, Frank et al. 1970) are a few examples of the early works done in this field in late 1960s and early 1970s (Schiehlen 1997).

Multibody methods were used to simulate kinematics and kinetics of the whole human body (Roberson and Schwertassek 1988). As one of the early works in this field, using

anthropometric data of a human subject, Chaffin developed a full human body model consisting of seven solid bodies (links) which were articulated at ankles, knees, hips, shoulders, elbows and wrists (Chaffin 1967). In the first attempts to consider the effect of muscles in the multibody model of the human body, McGill and Norman used muscles forces from EMG measurements and incorporated the geometry of the individual muscles in a two dimensional model to simulate symmetrical body positions lifting conditions dissections (McGill and Norman 1986).

The first multibody models of the human spine were developed in which all the back extensor muscles were modeled with an equivalent muscle to estimate the forces at the L5/S1 joint (Chaffin 1969) and (Chaffin 1967). Later models tried to include more anatomical details of different regions of the spine in multibody models (Bogduk 1980, Macintosh and Bogduk 1986, Macintosh and Bogduk 1987) and (Bogduk, Macintosh et al. 1992a, Macintosh, Bogduk et al. 1993, Stokes and Gardner-Morse 1995, Van-Dieen 1997). In the next years, the research in the field of multibody dynamics of biomechanical systems was more focused on addition of more realistic conations to the models such as considering complicated boundary conditions (e.g. nonholonomic constraints), friction, impact, and contact forces. New recursive methods were developed to calculation of reaction forces and torques of the close loop multibody systems. In addition to formulation improvements, considerable computational efforts were done for pre- and post-processing of the results and visualizing the simulation methods by means of CAD methods, animations, and signal analysis. All these improvements resulted in evolution of more detailed and realistic models in the recent years that enabled researchers to simulate more complicated cases such as walking or calculation of the spinal loads in changing position to study the effect of physiotherapeutic instructions and body supports on the spinal loads (Rohlmann, Petersen et al. 2012).

2.5 Spine model with using motion capture system

Developing a complete real model of the human body with real daily activities details requires complete and accurate static and dynamic sets of information about the motion and displacement of the different parts of the body during a defined movement scenario. This set of data together with the static properties of the body (such as weight and inertia of the parts), and mechanical properties of the soft tissues (such as stiffness of the muscles and tendons and ligaments) can be used to extract/calculate the internal force, torques, and

momentum in different joint or limbs of the body during a specific activity. In other words, in order to develop a realistic dynamic biomechanical model of the human body, body motion information has to be accurately coupled with the different parts of the model to drive the body in a real manner. Doing so, the internal force and torques can be calculated using inverse dynamic methods. Acquiring the 3D motion information of the body is commonly known as "body motion capture". Optical tracking (Balan, Sigal et al. 2005), radiology (Zheng, Nixon et al. 2003), electromagnetic techniques (Klein, Broers et al. 2003), inertial sensors (Lee, Laprade et al. 2003), and goniometry are some of the conventional techniques for conducting motion capture analysis and measurements. Goniometry method is basically a static method which measures the initial and final angles of a certain joint. The main drawback of this method was its high positioning error and also this fact that the measurement apparatus are imposing mechanical constraints on the moving segments of the body. In the radiology method, snapshots of the initial and final position of the body (bones) are captured and therefore the kinematics of the motion is not captured. In addition, since the subject is always exposed to hazardous x-ray radiation the number and duration of the experiments will be limited in this method.

Among these methods, optical tracing is more prevalent to capture dynamics of the real time human body with the minimum interference between the measurement apparatus and the measured motion in an accurate and non-invasive manner. In this study, a Vicon MX motion analysis system was used to find the motion data from the real subjects. After acquiring the experimental motion data in different activities (e.g. lateral bending, bending forward and backward, twisting and walking), the motion map of the subject was created using the Nexus motion capture system and processed using Vicon BodyBuilder.

Optical track motion capture which hereafter will be referred to as motion capture (Mocap) in this thesis, has been extensively used to study different biomechanical (kinematic and kinetics) aspects of the human spine system. In 1993, Khoo and Goh used Vicon motion analysis to capture 3D co-ordinate and ground reaction force of the human body during normal level walking. Using the motion capture results, they developed a biomechanical model of the spine to estimate the joint forces in the lumbosacral spine during the stance phase of walking (Khoo, Goh et al. 1995). According to their results, the maximum of the joint loads was in the range of 1.45-2 times of the body weight of the subject.

In 1998, Goh and Thambayah used the motion capture experiments to develop a biomechanical model which was capable of determining the effect of various back pack weights on the joint forces of lumbosacral (joint force at L5/S1) during walking. In their

experiments, the body motion and trajectories of the body segments was acquired by means of a 5-camera Vicon motion analysis system and two Kistler force plates (Goh, Thambyah et al. 1998). According to their results, walking with back packs of 15% and 30% of the body weight resulted in an increased lumbosacral load of 26% and 64% as compared with that of the subject walking without any back pack.

In order to measure the 3D real time motion of the spine in a portable and non-invasive fashion, Goodvin et.al (Goodvin, Park et al. 2006) developed a magnetic based postural analysis method. In this method, the magnetic sensors were mounted on a wearable frame which exerts a level inconveniency and constant load on the subject. The results and performance accuracy of this method were verified by repeating the similar experiment using a Vicon optical motion tracking system which demonstrated a maximum error of ~ 3° in the tracking of segment orientation.

Using BodyBuilder for Biomechanics Language, and taking into account the anatomical motion limitations of the spine, Dlugosz et.al (Dlugosz, Panek et al. 2012) developed a kinematic model which was able to graphically present a realistic 3D animation of the spine movement in dynamic activities such as walking and lateral bending.

Most of these methods have been developed to study the dynamics of the normal spine and very less attention has been paid to developing a simulation technique to study the musculoskeletal interactions during dynamic activities (moving postures such as bending, walking, sitting, etc.) of the scoliosis subjects. The aim of this study is to present the musculoskeletal normal spine and also a spine model with scoliosis condition to measure the loads on a certain intervertebral joint during change of body position from upright to lateral, or during flexion, extension or rotating position while standing. The term "intervertebral joint" in this study is taken to include not only the intervertebral disc, but also the facet joints between the two adjacent vertebrae.

2.6 Spine models with scoliosis condition

Current scoliosis treatments are mostly mechanical, i.e. based on external load application. This makes the collaboration between mechanical, computer engineers and orthopedic surgeons inevitable in this field. In recent years, many models have been developed to simulate scoliosis conditions (Gréalou, Aubin et al. 2002, Rohlmann, Zander et al. 2008, Robitaille, Aubin et al. 2009). Each model was validated for special activity or posture based on *in vivo* information or by comparing the results with other researcher's findings.

However, the whole scoliotic spine with a complete set of muscles and ligaments has not been presented so far.

Because of the limitations of the scoliosis treatment methods, biomechanical models have been mainly developed to help researchers and surgeons in investigation and better understanding of scoliosis condition. For example, reliable and validated biomechanical models and simulation techniques can potentially be used to train spine surgeons before the real surgery operation. The computer models have been capable of simulating various scoliosis treatments including bracing (Perie 2004, Clin, Aubin et al. 2011) and instrumentation (Aubin 2003, Lafage 2004, Desroches, Aubin et al. 2007, Lalonde, Villemure et al. 2010). In order to personalize the evaluation and to improve the design of the treatment methods, optimization techniques have been applied to determine patient specific material properties (Lafage 2004, Petit, Aubin et al. 2004, Duke 2005).

In 2003, Delphine developed a personalized biomechanical model in order to improve the efficiency of the brace design process for a specific patient (Perie, Aubin et al. 2004). In this method, using a multi-view radiographic reconstruction technique, they re-constructed the 3D geometry of the spine and the ribcage of three different scoliosis subjects. Effect of the brace on the biomechanical model was simulated by applying equivalent compression forces to certain nodes of the model. These forces were calculated by measuring the pressure (using pressure gages) which was applied by the brace to different regions of the spine of the subjects.

In 2007, Clint et.al developed a 3D patient specific finite element model of the spine, rib cage, pelvic and abdomen to optimize the brace design parameters (to achieve the maximum brace efficiency). In this model, the effect of the brace on the body (trunk) of the subject was simulated as a point-to-surface contact interface (Clin, Aubin et al. 2007).

The process of instrumentation and surgical corrections of the scoliosis spine has been simulated by different mathematical models. In one of the early simulation attempts, Belytschko (Belytschko, Andriacchi et al. 1973) and Schultz (Schultz, Belytschko et al. 1973) and (Schultz and Hirsch 1973, Schultz and Hirsch 1974) simulated the Harrington correction by developing a 3D deformable model of the thoracolumbar spine and compared the effect of lateral and longitudinal forces on the level of correction.

Vanderby et al. (Vanderby Jr, Daniele et al. 1986) used radiographs which were taken from a preloaded spine before the operation to develop a 2D model to determine the *in vivo* segmental properties of the scoliosis spine. Viviani et al. (Viviani, Ghista et al. 1986) and Stokes and Laible (Stokes and Laible 1990) presented a 3D finite element model to simulate

the Harrington correction of the thoraco-lumbar spine. In both of these cases, a personalized geometry of the subjects was re-constructed based on stereo-radiographic Direct Linear Transformation reconstruction method. However, in these studies, the mechanical properties of the model segments were obtained from the results of other researchers which were acquired from normal subjects. According to the results of these studies, adopting a correct value for the stiffness of the segments is of a great importance in predicting the effect of the surgery. Similar conclusion has been drawn by Poulin et al. (Poulin, Aubin et al. 1998).

2.6.1 Finite element (FE) scoliosis models

Finite element models have been extensively used in modeling of scoliosis conditions (Gardner-Morse and Stokes 1994, Wang, Liu et al. 2008, Driscoll, Aubin et al. 2010). Using a flexible mechanism, Aubin et al (Aubin, Petit et al. 2003) developed a kinetic model of the spine to address the intrinsic convergence problem of these finite element based spine simulation methods. This personalized model of the spine was composed of rigid bodies corresponding to the thoracic and lumbar vertebrae, and flexible elements representing the intervertebral structures.

Stokes et all (Stokes and Gardner-Morse 1991) developed a finite element model of the scoliosis spine to study the interaction of the lateral and axial deformities of the idiopathic scoliosis spine to answer the question of whether external forces can be the cause of scoliosis. To answer this question, predetermined displacements were applied to the model to reconstruct a scoliosis curve. In this experiment, the force which was needed to deform the normal (straight) spine to double curve scoliosis with Cobb angle of 10 degree was calculated. It was found that generating such a curvature implies exertion of a load of 20 N at 40 mm in front of the center of the vertebral body. According to the authors of this work, occurrence of such situation is almost impossible and therefore it is very unlikely that scoliosis can be caused by acting external forces. Although this model used realistic elastic properties of the segments, the effect of rib cage, muscles were not taken into account in the simulation. Gignac et al (Gignac, Aubin et al. 2000) developed a finite element model of the spine and rib cage to investigate the biomechanics of the correction of the scoliosis curves by means of bracing. This model was used to optimize the personalized braces. As one of the rare cases in which finite element method is used to model the whole spine, Lafage et al. (Lafage 2004) developed a 3D model to simulate the Cotrel–Dubousset

scoliosis correction surgery (Cotrel, Dubousset et al. 1988). Their study demonstrated the necessity of using specific personalized mechanical properties of the subject to accurately simulate the correction process.

2.6.2 Scoliosis gait analysis

Effect of scoliosis condition of the gait pattern of the subject is one of the important factors in gait pathology and many researchers have investigated the potential alteration of the gait pattern in scoliosis patients. For example, in the very recent studies, Malgorzata Syczewska et al (Małgorzata Syczewska 2007) used a dynamic motion capture technique (Helen Hayes marker set-model) to study the study gait pattern of the scoliotic subjects.

Later P. Mahaudens et al (Mahaudens, Banse et al. 2009) studied the effect of scoliosis and severity of the spine deformity on dynamic and electromyographic (EMG) parameters of walking of several AIS subjects with different curve structure such as thoracolumbar or lumbar. Similar experiments were repeated for the subject with normal results. They found the motion restrictions in scoliosis subjects compared them to those of to the subjects with normal spine. In addition, they found that the muscle activation was increased by 21-61% in scoliosis subjects which can result in stiff dynamic behaviour of the lombo-pelvic segment.

In order to study the effect of severity of the scoliosis spine deformity on the gait pathology of the AIS subjects, Syczewska et.al (Syczewska, Graff et al. 2012) designed an experiment by using a VICON 460 system to analyze parameters such as gait velocity, step length, ankle dorsiflexion, pelvic tilt, etc. According to their results, severity of the scoliosis double curve and also the deformity of the pelvic are two important parameters that can affect the gait pathology.

Recently, *LifeMOD* Biomechanics Modeler (LifeMOD) has been popularly used as a multi-body dynamic simulation platform in numerous modeling researches. A dynamic simulation of the cervical spine containing a disc implant was performed using *LifeMOD* to understand the intradiscal forces/pressures, bending moments and vertebral body rotation (De-Jongh, Basson et al. 2007). In a similar manner, a human-wheelchair musculoskeletal model was generated with *LifeMOD* to analyze the cervical spine of a wheelchair user due to frontal and side impacts (Kim, Yang et al. 2007). In a research to conduct complex biomechanical analysis of surgical techniques using *LifeMOD*, the

muscle-skeleton model was integrated with motion capture in a system designed to analyze the surgeon's skill. The loads on the bones, fatigue on the muscles and the ergonomics of surgical instruments were also assessed in this simulation (Cavalloa, Megalia et al. 2007). Although in many applications, *LifeMOD* has been used to model the whole spine as a multibody structure, these models have been quite basic and none of them were fully discretized to the level of single vertebrae.

As mentioned in the earlier sections of this chapter, understanding the kinematics and kinetics of the spine (the whole spine or a certain area of the spine) is an important rule especially for the surgeons to have better and clearer understanding about the existing condition as well as prospect of any effective treatment on the spine. This necessitates development of a detailed spine model in which biomechanical properties of different members of the spine system such as vertebrae, ligaments, muscles and disks is taken into account. Such a model can be used in different medical applications such as wheelchair design based on posture, implant, and brace design or even planning of surgical operations to help surgeons gain insight into complex biomechanics of scoliotic spines and to propose better surgical plans before spine correction operations.

The main focus of the current study is to develop a personalized fully discretized musculo-skeletal multibody scoliotic spine model using *LifeMOD* and *Nexus* (motion capture) softwares. In this study, a Vicon MX motion-tracking system and Nexus software package which was specifically designed for life science studies have been used to conduct the Mocap analysis. Vicon is a marker based motion capture set up which because of its high accuracy and precision is being used in a wide variety of life science and animation applications (VICON). This Vicon system tracks the dynamic 3D position of the moving markers with an acquisition rate of 100 frame/s (100 Hz). While in the conventional modeling technique, developing a personalized model of a certain subject is a tedious process, in this work an attempt has been made to develop a technique to automatically create a personalized model based on anthropometric data of the subject. Such a model is able to capture the dynamic interactions between vertebrae, muscles, ligaments and external boundary conditions (e.g. representing the probable external forces of instrumentation of external forces) and provide more realistic response predictions.

2.7 Summary

As mentioned at beginning of this section, some of the biomechanical parameters pertinent to muscular activities such as muscles and tendons of the spinal system are not easily measurable or in some cases such as internal forces and torques in the joints it is almost impossible to be calculated in an noninvasive manner. On the other hand, such information is of a great importance in the biomechanical, orthopedic and rehabilitation applications. This necessitates development of computational simulation techniques to create biomechanical models of the whole or a certain part of the body to evaluate the biomechanics of the human body and more specifically the spinal system. Constructing such a model requires a thorough understanding about the spinal system segments and their independent and group functions. In addition, understanding the kinematics of the spine requires inverse dynamic analysis of the spine model that on the other hand needs accurate description of the kinetics of the parts of the real subject as the input. While the spine is modeled either by finite element or multibody models, the body motion information (to drive the model) is usually acquired from motion capture analysis of the real subject.

In spite of much work which has been done in the biomechanical modeling of the human spine with scoliosis deformity using finite element or multibody models, considerably less progress in development of detailed model of the whole spine with scoliosis deformity has been observed. Although more details in terms of mechanical properties and shape of the different elements (segments) of the spine can be considered in finite element methods, these models have been basically successful in static analysis of an isolated region of the spine (e.g. lumbar region or cervical region of the spine on a certain loading condition) to calculate parameters such as internal stress or deformities. Nevertheless, these methods were not that successful to efficiently model the whole spine (e.g. to consider the effect of muscles and ligaments) and provide reliable kinematic results.

In contrast, although multibody models are not able to provide detailed information about internal interactions of the parts which can be useful to study the source of injury mechanisms, they are very strong in providing information about the kinematics of the spine under different motion and loading conditions. The main shortcoming of this model can be summarized as oversimplification of the spine model (in terms of number of the bodies and also the effect of muscles and ligaments) when the whole spine is supposed to be modeled. For example, in many of the multibody models, only a certain part of the spine model is refined to the vertebrae level and the rest of the regions are considered as a single

solid body. Such assumption and simplifications compromise on the accuracy and reliability of the results.

Based on these limitations, the main goal of this PhD work was to develop a three dimensional, detailed, bio-fidelity multibody model of the whole human spine with scoliosis condition in which the effect of all vertebrae and also the role of soft tissues such as muscles, ligaments and tendons has been taken into account. This work comprises developing a realistic model based on the X-ray images of the scoliosis subjects by means of *LifeMOD* simulation tool and also Vicon motion capture system. Using the *LifeMOD* simulation tool, the influence of the environment (boundary condition, constraints, motion agents, etc) on the body is considered and the biomechanical unknowns such as muscle forces, joint torques, etc. are calculated by means of inverse dynamic techniques.

Our detailed spine simulation system was evolved in a number of stages. The first stage of developing a realistic and detailed normal spine model was started in 2008 (Tay, Gibson et al. 2009). This model was built using *LifeMOD* by discretizing the default spine model and adding necessary ligaments. Although this model was more realistic than the initial default one, it experienced stability problems when subjected to external forces. To address this problem, an entirely discretized musculo-skeletal multi-body spine was developed in 2010 (Tho 2010) in which Intra abdominal pressure (IDP) and abdomen and lumbar muscles were considered and added to the model .

In the previous applications of *LifeMOD*, a predefined (default) standard model of the software has been used to simulate the normal human body. However, in the current study, the model of the human body with scoliosis spine condition has been specifically designed and refined based of the X-ray images of the real scoliosis subject. In order to drive the model in a certain pre-defined motion, the motion of the real subject has been captured using the VICON motion capture system and the recorded trajectories have been applied to the model. In order to increase the time efficiency of the modeling (to increase the number of the cases that can be studied in a limited time), instead of manual locating of the vertebrae, the process of generating personalized scoliosis spine model has been automated.

In the next chapter, the procedure to construct a kinematic model of the spine in *LifeMOD* software and also application of motion capture technique to apply the motion trajectories to the developed model will be discussed

Chapter 3: Scoliotic spine model development in LifeMOD and integration with Motion Capture

3.1 Introduction

Nowadays, many different biomechanical aspects of the human body such as ergonomic analysis, comfort studies, motion analysis, impact simulation, surgery simulation and planning can be systematically studied by means of various commercial or custom-built software applications. Continuous advancement and development of these softwares enables the users to model the human body (completely or partially) and also to analyze the interaction between the body and external objects (i.e. environment, bed, chair, wheelchair, rehabilitation devices, surgical devices, etc) to simulate and measure many of the effects or parameters that are not directly assessable or measureable *in-vivo*.

Depending on the application, type of analysis may typically include finite elements or multibody kinematic analysis. Finite element is used to analyze the stress and deformation in human body parts and kinetics or kinematics is used to study the motion of the body segments, forces and interaction of the body with external constraints. In this study multibody kinematic analysis is used to calculate displacement, force and torque distribution on spinal joints.

Among many different biomechanics simulation softwares, *LifeMOD* from Biomechanics Research Group is a powerful tool for kinematics and kinetics analysis of the human body to calculate displacement, velocities, accelerations, angles and force and torque distribution on different parts of the human body model. This software is basically a plug-in module to the ADAMS physics engine (from MSC Corp.) which makes it a suitable tool for kinematic simulation of human-machine interaction.

By defining some descriptive variables of the subject, such as age, height, weight, and gender, *LifeMOD* automatically creates a basic (default) virtual human model using its anthropomorphic database (Cheng, Obergefell et al. 1994). Furthermore, the user has the option to refine the segment parameters and the body characteristics. One can move this model into the desired positions, such as sitting, walking, or bending, etc. and also can create different environments (constraints) with which the human model can interact. As the result, this simulation tool is able to produce diagrams of displacement, velocities, accelerations and angles of the limbs as well as internal forces and torques at the joints and

tension in the soft tissues (mussels, ligaments, etc.). Figure 3.1 shows some application of this software in simulating musculoskeletal human models in relation to different environments or mechanical systems. Generally *LifeMOD* is used for the integration of the normal human model with the immediate surroundings. It is noteworthy that in this study, according to our knowledge of current literature, for the first time *LifeMOD* is used for detailed modeling of the scoliosis condition.

Although the *LifeMOD* default human model is able to simulate basic kinematic performance of the human body, it fails to provide accurate outcome when more detailed understanding of a sophisticated part such as spine is required. This default model consists of 19 segments. Based on location of the center of mass and orientation of the segment, mass properties of each segment are estimated using ellipsoids. In this system (default model), the spinal column is modeled with only 3 segments.

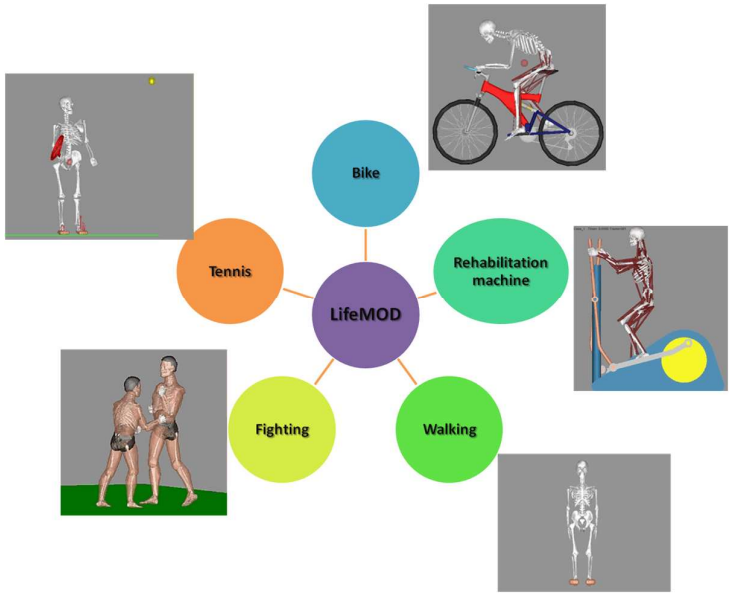

Figure 3.1 *LifeMOD* applications (LifeMOD)

This chapter mainly focuses on developing a realistic model for human spine which is able to be modified to show the scoliosis effect with different levels of severity. The main purpose of developing such a model is to study the dynamic behaviour of human scoliosis in order to help researchers to have a better understanding about biomechanics of the scoliotic spine.

In order to solve this problem, one should overcome the drawbacks of the default model. This task may generally include discretization (refining) of the spine to single vertebrae and addition of necessary muscles, ligaments, and capsules. In this chapter, development

of detailed scoliotic and normal musculoskeletal multi-body models and combining them with motion capture experiments are explained in brief. This method is capable of building a patient specific model to investigate the biomechanics of a specific scoliosis patient. Using this method, different scoliotic models can be developed based on anthropometric information of the patient and X-ray imaging of the patient's spine. Further details about the modeling process can be found in the Appendix.

In this work the trajectories of the body segments were acquired from motion capture data of a real subject and applied to a model comprising of the same anthropometric parameters. This enables us to validate the developed model by comparing the outcomes of the simulation and motion capture experiment results. In this study, a Vicon MX motion analysis system was used to find the motion data from the real subject. After acquiring the experimental motion data in different activities (e.g. lateral bending, bending forward and backward, twisting and walking), the motion map of the subject was created using the *Nexus* motion capture system and processed by Vicon BodyBuilder. Finally, a set of motion capture results was imported to *LifeMOD* to drive the human body model with the developed detailed (refined) spine. It should be noted that this is the first time that such a detailed model has been constructed according to the known literature.

3.2 General human modeling paradigm

A pre-default multi-body model is generated in *LifeMOD* based on the user's anthropometric input. In *LifeMOD*, 19 body segments (constructing the whole body) are generated by default, represented by ellipsoids which include characteristics like mass, principal moments of inertia, location of center of gravity, and orientation of the principal axes. In addition, the model consists of 118 muscles attached to the body at anatomical landmarks. In *LifeMOD*, first a base level segment set (19 segments) is generated using data from the anthropometric databases (Cheng, Obergefell et al. 1994). Secondly, joints and soft tissues are generated and finally, the contact elements between the environment and the model were created. Figure 3.2 shows the default spine model and also the discretized one with all ellipsoidal segments of 24 vertebrae in the cervical, thoracic and lumbar regions.

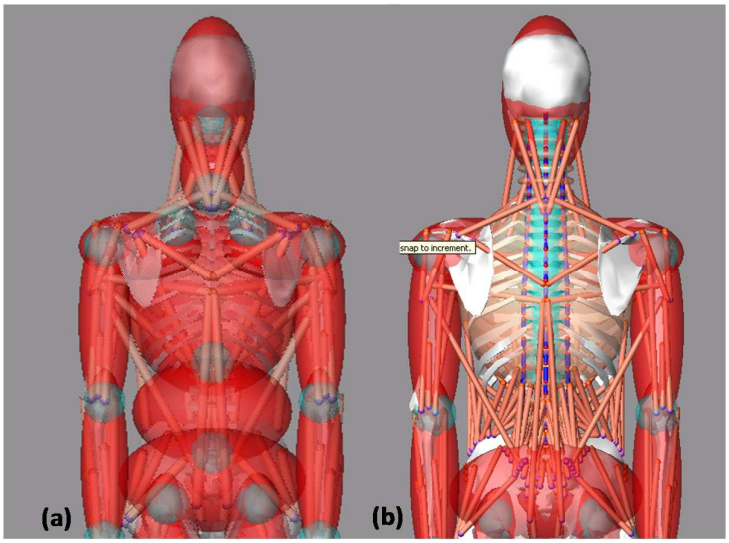

Figure 3.2 Back view of (a) the default model and (b) complete discretized spine model

Generally, two types of dynamic simulation can be performed in *LifeMOD*, active and passive simulation, as illustrated in the simulation flowchart in Figure 3.3.

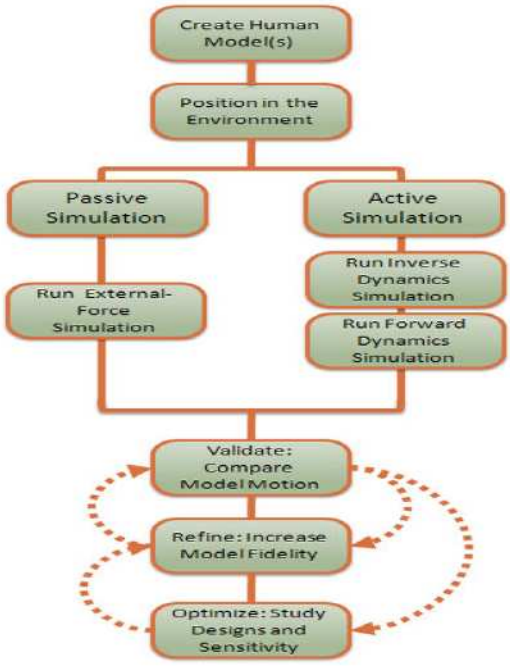

Figure3.3 Simulation flowchart (LifeMOD)

Passive dynamics generally studies the reaction of the model with respect to the environment and/or stimulators. In this method the response of the body to the forces and torques (boundary conditions) which are imposed to the model segments are studied. For

example, having the external forces imposed on the segments, one will be able to calculate the acceleration, and internal forces and torques in the joints. It should be noted that in this method, the body itself does not drive or cause any motion. This analysis mode is usually used when severe external forces (much greater than the internal ones such as muscles or ligament forces) are imposed to the model in an injury-producing event such as vehicle crashes. In the passive simulation, forward dynamics is enough to resolve the dynamics of the human body system.

In contrast, in active simulation, the muscles are active and able to cause reaction in relation with the environment (e.g. when a model is lifting a weight in a sport exercise). In this type of simulation, proper motion agents position different segments of the body model to drive the desirable movement and teach the muscles, ligaments, and other soft tissues as well as the joints how to move. In order to precisely simulate the muscle and joint movements, the joint angulations and muscle contraction histories for each body segment are first calculated in an inverse dynamics simulation. In comparison with the passive method, both forward and inverse dynamics processes are required to simulate and solve the dynamics of the developed model of the human body. After recording the required movement parameters during the inverse dynamics simulation, these compiled motion histories will be used to run the forward dynamic simulation which examines the model of the subject in the predefined motion or environment. During the forward dynamic simulation, the model is guided by the internal forces (joint torques and/or muscle forces) and is influenced by the external forces (gravity, contact, etc.).

Conducting the simulation, the user may check the results and compare them with the physical expectations and/or the experimental results for validation. In the cases that the results do not satisfy the biological (biomechanical) requirements or are not in agreement with the experimental results of the same conditions, the user has to take proper actions to improve the performance of the model and simulation. This improvement (correction) can be done by refining the model to more specific segments, addition of more detailed joints, soft tissues, boundary conditions, or modification of the environment.

3.3 Modeling methods

Generally developing a model in *LifeMOD* can be done in three different ways of Passive Joint, Recorded Joint (trainable passive), and Trained Muscle. Details of these three methods are briefly explained as follows:

3.3.1 Passive Joint

Passive joint models are usually exploited in passive simulations in which the body is not supposed to internally drive the model. As mentioned earlier in this chapter, this type of simulation is very common in passive injury activities such as sporting activities or car crash experiments.

3.3.2 Recorded Joint Models

These joints are able to record the information which is required to drive the model and are mainly used in the simulation models where the muscles themselves are the source of motion. In this model, a desirable motion pattern (for example walking or bending) is applied through a pre-defined trajectory or motion capture data. While these motion agents are driving the model segments, the joint angle histories are being recorded. This information later will be used to generate proper torques at the joints to drive (enforce) the model to follow the pre-defined displacement. This torque is generated in the joints by means of a set of proportional-derivative (PD) controllers.

3.3.3 Trained muscle

Similar to "recorded joint" models, "trained muscle" are also used for active simulation of the human body in almost any kind of activities. In this model, a pre-defined motion pattern (motion agent or motion capture data) is dictated to the segments of the multi-body model. The resultant joint angulations and muscle contractions will be recorded to the model segments and later will be used to drive the joints and muscles of the model with proper torques (in joints) and also forces (of the muscles). These torques and forces are generated by PD controllers. In this process, the force of the muscles are continuously checked and controlled to keep their values smaller than the maximum capability of the tissue of that specific muscle.

As this model (Trained muscles) simultaneously considers the effect of muscles and joints, we have used this technique in developing the detailed human spine model to acquire more accurate and realistic results. As mentioned before, there are two ways to assign a motion pattern to the multi-body model 1) to apply a pre-defined movement trajectory to the

segments or 2) to use the motion capture data from a real subject with the same anthropometric parameters.

3.4 Fully Discretized Musculo-Skeletal Multi-Body model

In this study, in order to improve accuracy of the simulation, the spine was refined into individual vertebra segments, cervical (C1-C7), thoracic (T1-T12) and lumbar (L1-L5). Rotational joints representing the intervertebral joints are kinematic constraints which are used to connect two vertebra segments were added to the model. Theoretically (as explained in chapter 2), each intervertebral disk has 6 degree of freedom consisting of 3 rotational and 3 translational degrees of freedom. A vertebral unit with all available degrees of freedom is shown in Figure 3.4.

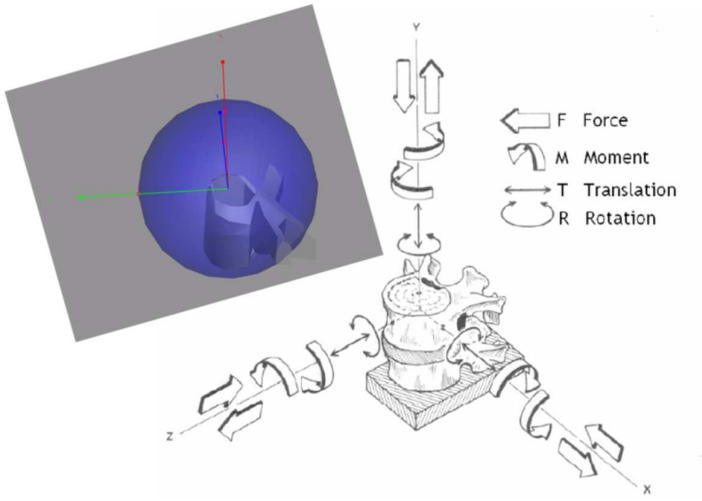

Figure 3.4 A functional spinal unit

Rotational degrees of freedom are able to create larger displacement as compared to the translational ones and enable the flexion/extension (forward/backward) bending, lateral (side) bending, and axial bending. Since scoliosis is mainly concerning about rotation of the vertebrae, in this study the main focus of the modeling in the current work is on rotational movements. In each segment of the spine, the anatomical constraints limit the range of the motion of the joints (segment motions). This rage of motions varies in different regions of the spine for different directions and is more limited in the thoracic region because of attachment of the ribs. In addition to motion constraints, muscles and ligaments provide further stability by restraining the segmental motions.

In this study, the spinal kinematic joints are modeled as 3 DOF trainable passive joints. The trainable passive jointed action can be defined with user-specified stiffness, damping, angular limits and limit stiffness values. These will be used in an inverse dynamics analysis to record the joint angulations during simulation. In the inverse dynamic simulation, motion capture data is used to drive the model and train the joints by assigning specific angulation patterns to joints. Later, the trained joints in which the motion has been recorded act as actuators to repeat the recorded motion trend in the forward dynamic stage of the simulation (Jerkovsky 1978, Roberson and Schwertassek 1988). These trainable passive joints are necessary to stabilize the model during the inverse dynamics simulation and also to provide proper joint friction stiffness in the forward dynamic section of the simulation. Tuning the stiffness value of these joints is an important factor which can affect the simulation results. The majority of the muscle-skeletal segments such as muscles, cartilages, ligaments, and bones have viscoelastic mechanical properties. This behaviour in most of the biomechanical models can be modeled as a combination of springs and dampers with proper stiffness and damping values. In the current study, mechanical properties (damping and stiffness values) of the joints which have been used as initial values in the forward dynamic analysis have been selected based on relevant values taken from the literatures (Panjabi 1976, Berkson 1979, Schultz 1979, McGlashen 1987, Moroney 1988, Schultz 1991). As mentioned in the previous section, these values may change after applying motion agents to the model (in the inverse dynamic mode). Clinical conditions such as scoliosis or muscle weakness may affect stiffness values of the joints.

LifeMOD has a detailed set of 118 muscles from which we can select the proper muscles to be attached to the segments of the model. The muscles are attached to the landmarks of associated bones on the body segments. This set is scalable with the skeletal geometry. By refining the spine segments to the level of a single vertebra, the connection position of the muscles to body segments has to be modified (considering the anatomical landmarks) in such a way that muscles are attached to the specific positions of the newly created vertebrae. In addition, the default muscle sets are not sufficient to help the human body to perform some activities without using Mocap.

Among many different types of the muscles (in terms of function, size, shape, etc.), back muscles (postvertebral muscles) are of a great importance in biomechanical performance of the spine and consequently in creating a biomechanical spine model. These muscles act as extensors and are responsible for straightening the spine and mandating the upright

position of the head. In addition these muscles have an important role in controlling the back movement and also assist the respiratory functions (Panjabi 1990).

Another group of muscles which are connected to the spine is the abdomen muscles. These muscles are responsible for controlling of the motion and also to help expiration and inspiration (Cheng, Chen et al. 2006, Mutluay, Demir et al. 2007). These muscles were modeled by means of an artificial segment with a zero mass and inertia (Zee, Hansen et al. 2007) to simulate the role of the rectus sheath on which the abdominal muscle is attached. Each of the obliquus externus and internus are divided into 6 fascicles (Stokes and Gardner-Morse 1999). Four of the modeled fascicles of the obliquus externus run from the costae and end in the artificial rectus sheath and the other two originate on the costae and end to the iliac crest on the pelvis. Obliquus internus modeled as six fascicles, three of them run from the costae to the iliac crest and the other three originate of the iliac crest and end in the artificial rectus sheath. Figure 3.5 displays the full body muscles.

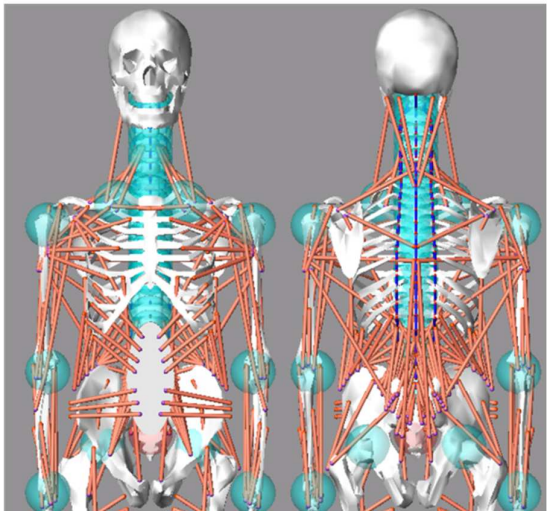

Figure 3.5 Front and back view of the abdomen and lumbar muscles

In addition to the back muscles, five types of ligaments, (interspinous, flaval, anterior and posterior, longitudinal and capsular spinal), two types of abdominal muscles, (obliquus internus and obliquus externus), and four types of the lumbar muscle, (psoas major, erector spinae, multifidus and quadrates), were implemented into the model. These ligaments and muscles surround the spine and guide segmental motion and contribute to intrinsic stability of the spine by limiting its excessive motion (Tho 2010). The initial stiffness of the ligaments can be obtained from the results of other studies (Pintar, Yoganandan et al. 1992, Yoganandan 2001). These values may change after applying motion agents to the model

based on the clinical condition of the subject. Figure3.6 displays side and rear view of ligaments attached to vertebrae in the cervical spine region.

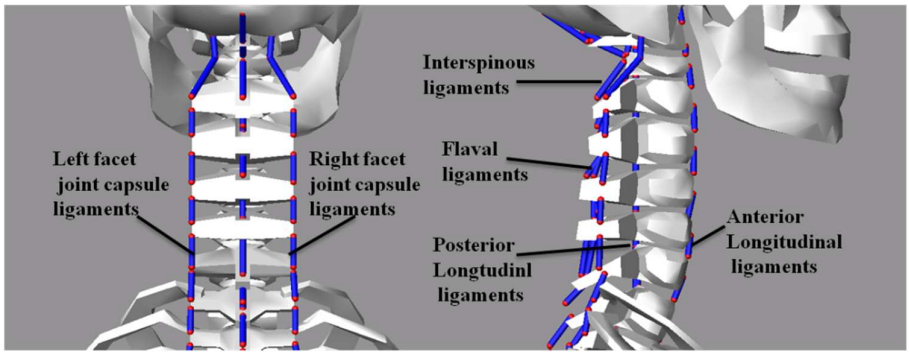

Figure 3.6 Side and back view of ligaments in the cervical region

Previous studies have shown that in addition to muscles and ligaments, intra-abdominal pressure (IAP) is a necessary factor for maintaining the stability of the lumbar spine (Cholewicki, Juluru et al. 1999, Hodges, Cresswell et al. 2001, Arjmand and Shirazi-Adl 2006). Therefore, in order to increase the fidelity of the model, intra abdominal pressure was implemented in the model. It should be noted that, application of the intra-abdominal pressure is only necessary for passive dynamics simulation in which no motion trajectory was used to drive the model. Otherwise, in the active simulation of this study where the model is being driven by the motion agents (as if it is alive); the spinal loads are in the range of *in-vivo* experiment results. Therefore, the lumbar muscle and abdomen muscle group will stabilize the spine and using the intra-abdominal pressure is not necessary. In the static simulation of this study, a bushing element is used instead of IAP.

In order to model the intra-abdominal pressure, one needs to calculate the abdominal volume and cross-section, construct a spring structure and calculate the stiffness of the springs, and finally use an equivalent bushing element (Tho 2010, Huynh, Gibson et al. 2013). It should be noted that the effect of abdominal cavity on the shape of the spine is a personalized effect which is different among the subjects. It can be considered by changing the property of the bushing element based on the anthropometric data of the subject. As can be seen in Figure 3.7 bushing joint represents the IAP.

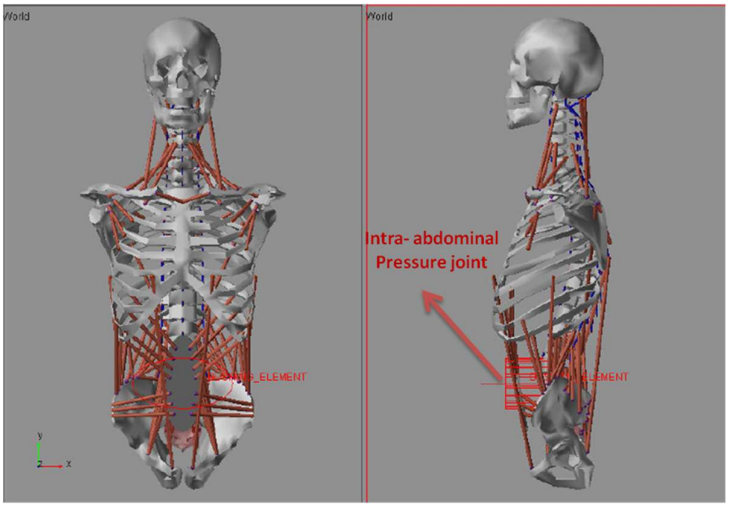

Figure 3.7 Intra abdominal pressure joint in front and side view

Finally, assigning the proper values to the model parameters (i.e. stiffness, damping, etc.) is very critical for developing a realistic simulation with reliable results. This requires a massive effort of optimization of the key parameters of the engaging parts (joints, muscles, ligaments, motion agent stiffnesses, etc.) which requires changing the parameters and monitoring the effect of this change on the behaviour of the model and continuous comparison between the obtained results and the experimental ones or results from other validated simulation models. Figure 3.8 shows the flowchart of modeling detailed human body before doing the analysis.

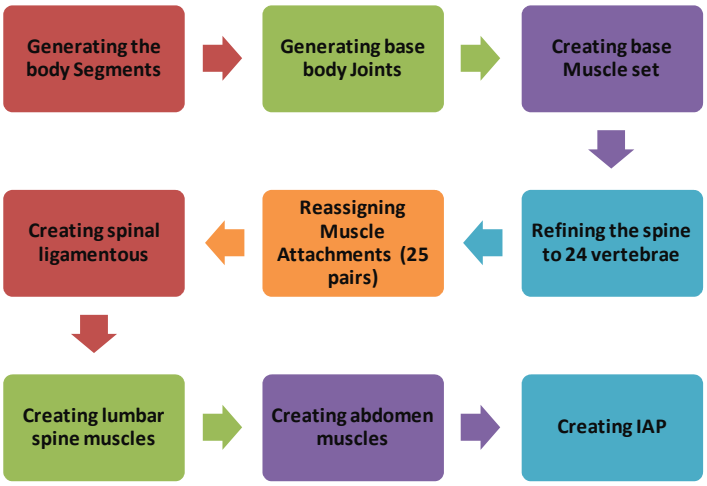

Figure 3.8 Flowchart of modeling a detailed human model

3.5 Muscle formulation

The contribution of the muscles in the biomechanical models developed in *LifeMOD* is modeled using a so called "net force" approach. In this scheme, the muscle is isolated from its environment (as free body) and the effect of the boundary conditions is introduced as external forces. Calculation of the muscle force is conducted in two steps of passive (training) and active (driving).

In the passive step, muscles are connected to the physiological landmarks but they do not contribute in the body motion. Each muscle acts as a trainable element which records muscle contraction while the body is being driven by means of an external force or a set of motion agents (containing displacement history data) attached to a certain body segment. Motion agents can be extracted from motion capture analysis of the real subject or from a custom-designed trajectory defined by the user. During the movement of the body segments, the muscles act as training elements in which the velocities, displacements, and length changes are recorded. This process can be referred to as "inverse dynamic" process. The recorded motion pattern (including muscle shortening/lengthening) later in the active (forward dynamics) step will be used to generate muscle forces to drive the body segments. As the inverse dynamics simulation has been performed, the model will be prepared for forward dynamics simulation using the muscles to include the proportional-integral-differential (PID) controllers or "trained muscles" as drivers in the simulation. In other words, each muscle acts as an actuator to apply the required force which is necessary to regenerate the predetermined motion of the body segment. In the active muscle step, the muscle (actuator) generates a force (tension) to minimize the error between the current length and the desired (recorded) length of the muscle.

The physiological and mechanical parameters needed to run the forward dynamics step are defined as bellow:

- Fi: force in the i^{th} muscle
- p_{CSA}: physiological cross sectional area of the muscle
- M_{stress}: maximum tissue stress
- F_{Max}: maximum physiological force limit of the muscle = $p_{CSA} \times M_{stress}$

In this algorithm, during the forward dynamic step, a controller senses the instantaneous length (L) and speed (rate of the length change: $\dot{L}$) of the muscle and compares it with the desirable instantaneous muscle length and speed which has been recorded in the inverse

dynamic step. Among these parameters, p_{CSA} and M_{stress} can be found from *LifeMOD* database in which they are assigned to the model based on the anthropometric data of the subject (height, weight, age, and gender). The controller calculates the required force to minimize the calculated error in the muscle length and rate of muscle length change based on equation 3-1.

The magnitude of the muscle force is controlled in such a way that it does not exceed the maximum physiological limits for that muscle, otherwise the F_1 is considered to be equal to F_{max}. The calculated force of the muscles will converge to the physiological (real) values by increasing the number of the muscles to that of the actual condition.

$$F_1 = \begin{cases} F_{max} & if\ F_1 \geq F_{max} \\ P_{gain}(L_{desired} - L_{actual}) + D_{gain}(\dot{L}_{desired} - \dot{L}_{actual}) & if\ F_1 < F_{max} \\ 0 & if\ L_{desired} \geq L_{actual} \end{cases} \quad Eq\ 3.1$$

3.6 Scoliosis condition

In order to create a model for scoliosis spine, two different methods for constructing of the scoliosis curvature have been investigated in this study: 1) modeling based on X-ray images of the subject or 2) constructing the model based on the motion capture results. In some cases, the combination of both methods has been used to develop the spine model with scoliosis curvature. This model can be used by orthopedic surgeons to study the dynamic behavior, the effect of different forces, and the changes of curvature resulting from different external boundary conditions. This virtual platform enables users to gain insight into the complex biomechanics of scoliosis spines and analyze loads acting on the intervertebral joints, corresponding angles between vertebrae and tension in the spine muscles for different patients with different spine conditions.

Manually generating of the human model is a tedious process because it is needed to create the body segments, joints and markers one by one based on the anthropometric parameters of the subject and then locate the segments based on the coordination of the vertebrae in the corresponding X-ray images. This problem will cause more difficulties when one needs to generate different models of different patients with different anthropometric information and different scoliosis curves. In order to address this problem, in this study, a partially programmable technique was developed to automate the process of construction of the scoliosis spine based on the anthropometric information of the subject and position information of the vertebrae. The position of the vertebrae can be obtained from the X-ray images (method 1) or from the motion data of the subject during specific exercise (method

2). This automation was done by developing proper script commands for each necessary step of the model generation process. By developing this code (script), for creating a model of a new subject, it is only needed to update the anthropometric results and also to key in the new coordinates of the spine segments to create the model. In this technique the required time to develop the model was reduced by a factor of 10 as compared to the common visual based methods. It is noteworthy that this method has the potential to be parameterized to the model various cases with different anthropometric inputs. Details of all the steps to generate script code to generate the models are explained in the Appendix.

3.6.1 Method 1: Reconstruction of the spine based on X-ray images of the scoliosis subject

In this method, before conducting the analysis, the positions of the vertebrae are found from X-ray images of the subject (in lateral and sagittal planes) based on which the vertebrae are rotated/displaced in the simulation model accordingly. This method will be further discussed in chapter 4. Figure 3.9 shows the scoliotic spine model which was created based on the X-ray images. It should be noted that only Cartesian coordinates (displacement) have been applied to the model thus far.

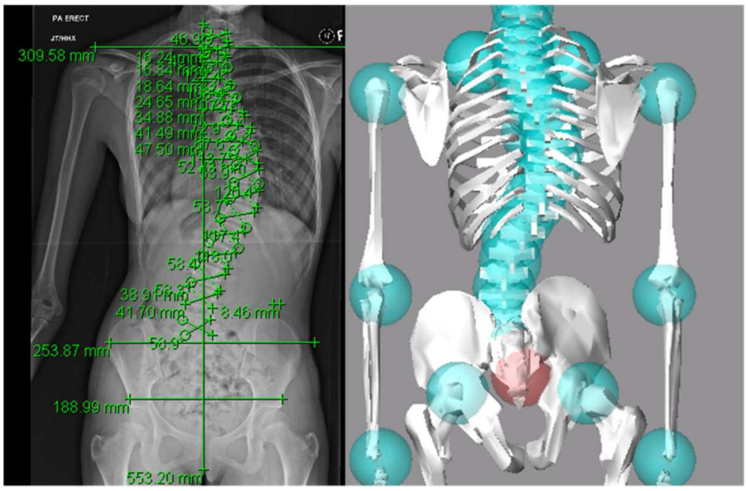

Figure 3.9 The scoliotic spine model which created based on the X-ray images

Since the ribcage in this model is one segment, it was connected to the spine with one joint. The joints keep the ribs in connection with the spine during the full range of spine motion. In this method, if the asymmetry of the spine in sagittal and frontal planes is huge, the ribcage cannot follow the same movement of the spine and the simulation will fail.

Therefore this model only can be used in specific posture and static simulations such as up right standing posture and also in the models which have a small scoliotic curvature in thoracic region.

3.6.2 Method 2: Using motion capture (Mocap) data

In this method, the motion data of the scoliosis subject is used to construct the deformity of the spine. The simulation will be done based on the motion data from Mocap experiments. In this method, tracking the position of the body segment in a given activity is used to predict the kinematics of the body. Some markers are attached to certain posits of the body (body segments) to make the motion of that certain point detectable for a number of cameras which can record the motion (trajectory) of that point in a 3D space at different moments. By using proper number of markers on the pre-defined positions of the body, one can accurately measure (capture) the subject's motion. Furthermore, in this study, the plug in protocol and a custom-built template called scoliosis-specific model were created to track realistic scoliosis patient movement. In the plug-in model, there are only two markers on the spine, one on C7 and the other on T10. We have added 4 more markers on the spine to capture the spine movement in a more accurate and realistic manner.
In this study the combination of these two methods (X-ray and motion capture) was used to model the scoliosis condition according to the type and size of the spine curvature. If the curvature is in the lumbar region or small curvature in thoracic region, repositioning of the vertebrae based on the X-ray images is possible and can be done by rotating the ribcage by a small angle to maintain the connection between the ribcage and the spine. However for larger Cobb angles, in thoracic region, method one will not work because of the ribcage connection problem and for these models only method two can be used.

3.7 Motion capture system (motion capture model)

Motion capture analysis of this study was done in National University Hospital (NUH) motion and gait analysis laboratory. Using NUH motion capture facilities and requesting the patients to participate in this experiment requires official authorization from National Healthcare Group (NHG) Domain Specific Review Board (DSRB). NHG is one of the main organizations responsible for public healthcare in Singapore. DSRB is an independent committee of medical and non-medical members which is responsible for protection of the

rights, safety, and well-being of the human subjects who are participating in the research experiments. All research protocols, plans, methods, and materials should be supervised and approved by this board before taking the informed consent from the research subject. In this study, subjects gave informed consent for participation in this experiment. The activities of the patient during the experiment are recorded (camera recording). This data enables us to extract the maximum possible information about the activities of the subject later even without presence of the subject. The patients were videotaped during the experiments. This also allows a detailed evaluation later on without the patient needing to be present.

3.7.1 Motion capture system

In this study, a Vicon MX motion-tracking system and *Nexus* software package which was specifically designed for life science studies have been used to conduct the Mocap analysis. Vicon is a marker based motion capture set up which because of its high accuracy and precision is being used in a wide variety of life science and animation applications (VICON).

This Vicon system tracks the dynamic 3D position of the moving markers with an acquisition rate of 100 frame/s (100 Hz). The main advantages of this system over older motion tracking systems are its speed and flexibility (McNamara, Feng et al. 2007).The tracking mechanism is based on shining a near infrared light to the spherical retro-reflective markers and recording the trajectory of the reflected light with a set of cameras. In this work, 6 cameras (3 pairs) mounted to the walls and tripods all were used to capture the motion of the markers. The cameras are equipped with a ring of light emitting diodes (LEDs) that flash the near infrared light. This eliminates the effect of the background light of the room or in other words makes the experiment independent of the background light of the lab. The specification sheet of the cameras using in MX Vicon system were shown in Table 3.1.

Before starting the motion capture experiment, the cameras and the view (tracking) volume has to be calibrated. The calibration is done in two steps. First, an “L” shape 2D structure which is shown in Figure 3.10 is waved throughout the tracking volume while snapshots are taken with all connected cameras.

Table 3.1 T-Series camera performance

	Vicon MX T-Series Camera				
Performance	T160				
Sensor resolution (pixels)	4704 H × 3456 V				
Sensor size (mm)	8.35 H × 13.48 V 22.77 (diagonal)				
Maximum Frame Rate (fps) at full resolution	120	515	690	1000	250

The L shape constituent markers are used to calculate and eliminate the non-linear effects of the lenses by acquiring the error feedback from each camera. Next, this L shape structure will be fixed in a certain position (e.g. on the floor) and considered as the origin (reference) for the geometry of the tracking space for the Vicon motion capture system (Figure 3.11).

Figure 3.10 “L” shape 2D structure

Figure 3.11 5-marker L-frame used to calibrate the cameras and set the Vicon origin

Current commercially available full body Mocap systems rely on a pre-defined skeleton model. These models are consisting of a small number of markers that must be attached to predetermined fixed landmarks on the subject body. In this predefined models, it is assumed that the subject has a normal body, so the motion data contains the minimum information to define the motion of the normal body sections. However, application of standard models will not be accurate when the model is supposed to be used for patients with body abnormalities (deformities) or when more details about the motion of a certain part of the body (e.g. the spine) is of the interest.

The common method to generate a skeleton model based on the motion capture data is to calculate the center of rotation between bones defined in their position and rotation by three or more optical markers (Silaghi, Plänkers et al. 1998, Ringer and Lasenby 2002, Cameron and Lasenby 2005). In these methods, positions of the joints were determined by considering two neighbor vertebrae the least square fitting technique. This default model is able to capture simple motion activities of the normal body. However in cases where the effect of a certain part of the subject is to be studied in more details, this method fails to accurately capture such details (due to lack of enough number of markers to be fixed on the small features of that certain region). For example in the case of scoliosis condition, the standard method may not be able to identify the less severe curves, because only two markers have been attached to the vertebrae.

In our study, in order to overcome the limitations of the conventional modeling schemes and to analyze the actual motion of the spine with scoliosis condition (to take the asymmetry of scoliosis deformity into account) and to create a realistic model, a new labeling template called "scoliosis specific model" was developed in Vicon *Nexus* software. This scoliosis specific model was made by addition of several new markers to the conventional Plug-in Gait models. In order to capture the deformity (asymmetry) of the spine in thoracic region, in addition to the marker on T10 (in plug in gait model), two more markers were attached to T1 and T6. To capture the effect of the curvature of the lumbar region, two more markers have been attached to L1 and L5. In addition, to capture the hump, two markers were attached to right and left side of the rib cage. Disregarding these changes, the rest of the Plug-in-Gait model remain the same as the conventional one which enables the user to use the modified Plug-in-Gait for the normal subject as well. In other word, while the modified plug-in is able to capture the effect of the deformities of the spine, it is still able to capture the general motion of the rest of the body (as in the normal case).

3.7.2 Motion Capture analysis

In this study, first the standard plug-in gait marker protocol was applied during the motion capturing, in which 35 markers were attached at specific landmarks on the subject's body. In this protocol, only two markers attached to the spine. Therefore, for scoliotic spine which has asymmetry, it cannot reflect the real motion. To address this issue, we have added four more markers, two on the thoracic region and two on the lumbar region to capture the scoliosis spine movement in a more accurate fashion during the exercises. The position of each marker (as x, y, z coordinates) and their orientation (as yaw, pitch, roll) is recorded every 0.01 s and stored as one frame in the system.

Based on the information from all the cameras, the location of each marker is calculated and highly accurate 3D trajectories are established in Vicon *Nexus*. This software has been used and validated over the years and in many different bio-mechanical applications and now is known as a reliable tool for musculoskeletal studies such as gait analysis and rehabilitation. Figure 3.12 shows the plug in and the scoliosis specific models which were created in Vicon Nexus from motion data.

Motion capture analysis using Vicon system consists of four main steps:

Step1: Calibrate the system- before starting the motion capture experiment in which the cameras and the view (tracking) volume has to be calibrated.

Step2: Patient preparation- in this step, anthropometric information of the subject such as age, weight, length and gender is collected. Later, a set of markers (based on the standard protocol) are attached to the pre-determined positions on the subject body. Plug in standard protocol is shown in Figure 3.13.

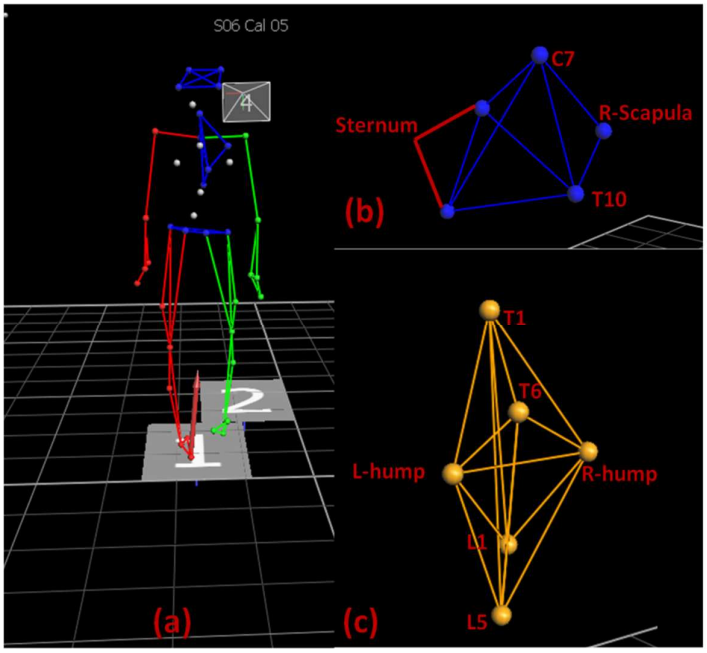

Figure 3.12 The model which is in Vicon Nexus from motion data (a) plug in model (b) spine in plug in model (c) spine in scoliosis-specific model

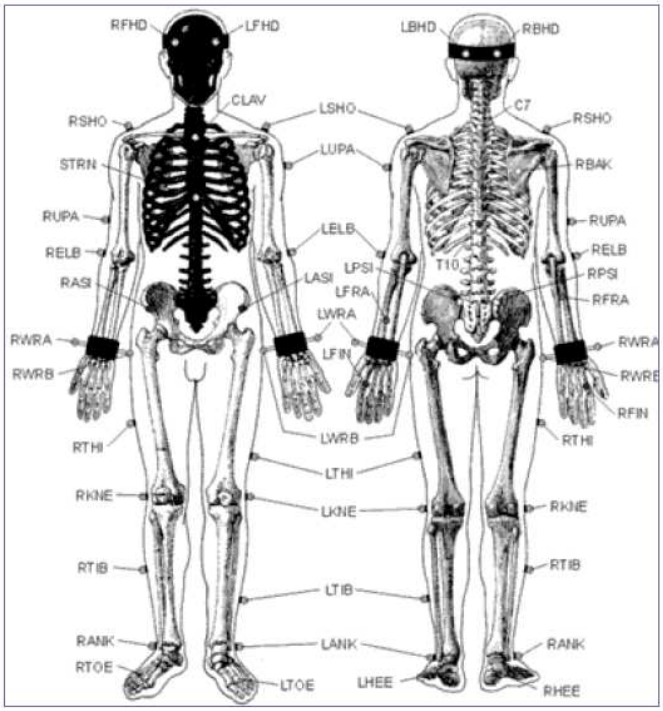

Figure 3.13 Standard plug-in-Gait marker placement protocol

Step3: Data recording- in this step the subject is asked to perform a certain motion. Prior to the motion, a static analysis is done which is followed by the main motion analysis. This

step may be repeated many times until the acceptable result in which all the markers have been seen by the cameras during the motion is captured.

Step 4: Post-processing the data. In this step the recorded data will be processed and the data points are connected to each other to form the moving body structure and extract the kinetics information of the subject such as joint angulations, speed, and displacements.

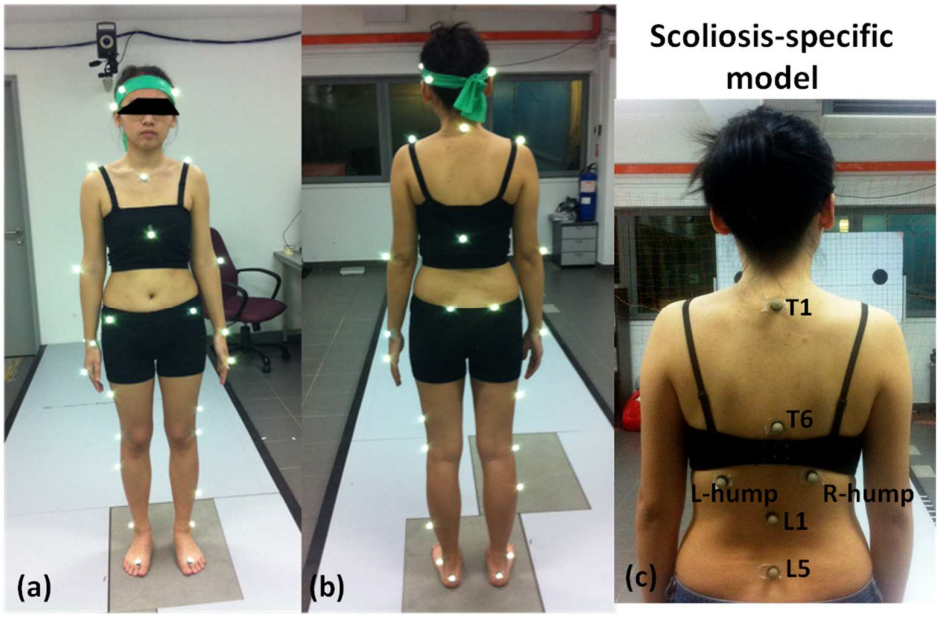

Figure 3.14 A subject marker sets (a) Front and (b) back view of a subject with plug in marker set (c) back view of a subject with scoliosis- specific marker set

In this study, the subjects were asked to perform some typical tasks such as bending forward and backward, bending to the sides and rotating which are requested by clinicians to assess the severity of scoliosis condition. First, plug-in Gait modeling in the Vicon Nexus generated the segments of the human body model according to the anthropometric input and the virtual marker trajectories which indicate kinematic and kinetic quantities, such as angles, moments etc. Secondly, the scoliosis-specific model was reconstruct based on the six extra markers which were added to the original plug in model. Figure 3.14 shows the front and back view of one of the subjects with markers attached to her body.

After capturing the motion of each exercise, the recorded data will be processed and the data points are connected to each other to form the moving body structure and extract the kinetics information (joint angulations, speed, and displacements) of the subject. It is very common that some of the markers become hidden from the view of one or more cameras

or in other words, one or more cameras cannot see some of the markers for a while. This situation usually takes place when a part of the body (e.g. hand of the subject) or a piece of the clothing of the subject obstructs the line of sight of cameras. This implies that the data motion of those markers (at least a short period of time) is not recorded. In other words, the motion of those markers is lost. This may result in discontinuity in the trace of the makers and causes problems in post processing of the results. In the existing Vicon model, the problem has been addressed by "gap filling" process (spline or pattern fill) in such a way that if one or more markers cannot be detected in some frames they can still be tracked. This can be done by using the information of the other markers which are visible in those frames to predict the position (trajectory) of the lost marker to make the motion continuous. This can be very helpful to find the hidden markers in the post processing analysis.

In addition to gap filling, in order to obtain meaningful results, all the artifacts resulted from vibrations of the markers or displacement of the markers due to skin deformation are detected and filtered from the raw data. This process may be repeated (optimized) by making many trials to become sure that the obtained marker positions are consistent with general motion trend of the subject. This is where the expertise of the user to use the proper gap filling and filtering routines will come into play. Most of the filtering routines of Vicon are able to fill the small gaps as well. For example, in this project, the Woltring quintic spline routine was used for filtering the artifacts and at the same time filling the trajectory gaps smaller than 10 frames (Woltring 1986). Although filtering is able to recover the small gaps, for large gaps, it is recommended to use the routines which are specifically written for gap filling. Among many gap filling algorithm, "Spline Fill" and "Pattern Fill" are the most common methods. While the "spline" method is more accurate for filling the small gaps, the "pattern" fill is more efficient for the large gaps.

The spline fill algorithm is an automatic method which works based on the extrapolations of the known trajectories. In this method the missing trajectory is estimated to be located on an extrapolated spline between the point after which the trajectory has been lost and the first point of re-appearing. This method is very efficient for gap instances of ≤ 60 frames and its accuracy decreases by increasing the gap size (Gait 2010). In the cases that the existing motion at a few frames before the gap is very irregular and unpredictably changing (erratic motion), the spline method fails to predict the motion of the lost targets. This is because this method estimates the trajectory of the lost markers by extrapolating the known trajectories of the few frames before the gap starts. It is noteworthy that most of the gaps are the result of disappearing of the markers during the erratic motions.

In such cases (large gaps or erratic motions), the pattern fill method is more accurate. In this method, the missing trajectory will be reconstructed (estimated) based on the trajectory of a similar known (visible) marker which was supposed to have a motion trajectory similar to that of the missing marker. For example, in the cases that two markers have been attached to a rigid segment (i.e. a bone) and one of them has been hidden for a long time, the trajectory of the other marker can be used to regenerate the trajectory of the missing one. In this study the second method (pattern fill) has been used to fill the gaps.

3.8 Conducting Musculo-skeletal Human-Body with Mocap data

After conducting the motion capture experiment and data processing, the data obtained from the motion analysis of the real subject were imported to the *LifeMOD* software as an SLF format to create the human body model from the measurements. SLF file contains information about the subject name, gender, age, height and weight, as well as the motion trajectories of the body segments. *LifeMOD* uses this information to extract body segment dimensions and mass properties from its internal anthropometric database. The motion data (Mocap) for the specific motion is imported into the model and used to drive the motion agents created on the human-body model.

After building the model in *LifeMOD*, the motion agents of the subjects were added to drive the muscles (inverse dynamics). It is noteworthy that in all experiments of this study, the subjects were asked to do motions normally (i.e. lateral bending, flexion, extension and rotating, they are used to perform the tasks as they would do in their normal daily activities). For this model, trainable passive joints were created for the inverse dynamics simulation. The trainable passive joint consists of a torsional spring force which includes angulation stops, stiffness and damping torques. As mentioned earlier, these joints are being used in the inverse dynamics simulation to record joint angulations while the model is being driven by the motion agents obtained from motion data analysis. These joints will be later removed and replaced with Servo-type torque generators for the "trained" phase. The joint angle and muscle activity (contraction) histories recorded from the inverse-dynamics simulation will be used in a proportional-derivative controller (servo-controller) to produce required torques and forces to recreate the motion history. The trainable joints may be re-installed according to the applications and data sets. Therefore, the user is able to run the inverse-dynamics simulation for another set of data, boundary conditions, etc. In other words, the

joints can be converted from trained to training (trainable) for an un-limited number of iterations.

To produce smooth simulations for both the inverse-dynamics and forward-dynamics simulations, an equilibrium simulation was initially performed to equalize the forces in the model. These forces occur due to displacement of the contact ellipsoids and balancing the pre-loaded soft tissues, etc. This is a dynamics analysis which holds the positions of the data-driven motion agents fixed, while finding the minimum energy configuration in the springs of the motion agents. The motion is imposed to the segments of the model by means of so called "motion agents" which are mass-less elements attached to the body of the segments. In order to address the differences in the geometry of the model and the real subject and also the discrepancies of the motion agents, the motion agents are connected to the segments by means of spring elements. The trajectories of the markers obtained from the motion capture experiments are used to drive these motion agents. Therefore the motions against can be considered as motion influencers rather than motion governors.

Tuning of the stiffness value of the motion agents is an important factor which can affect the simulation results. For example if this value is selected too high, the motion agent stiffness may not be able to overcome such a large joint stiffness and therefore it will not be able to move the body segments connected to each other with that joint.(see Figure 3.15)

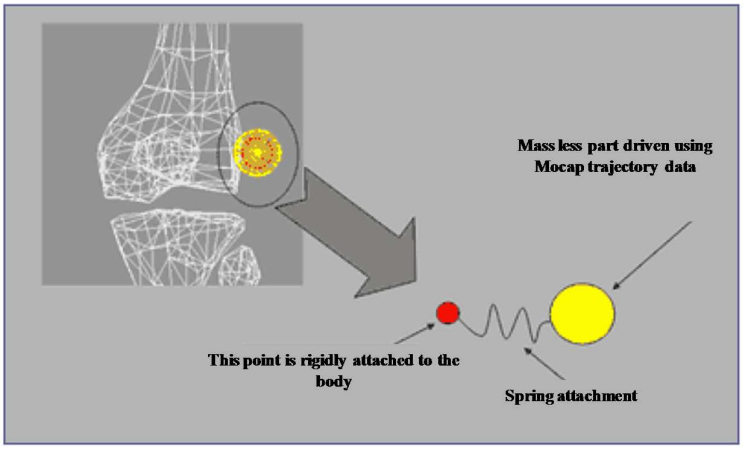

Figure 3.15 Motion agent configuration (figure taken from *LifeMOD* website)

After equilibrium analysis, contact constraints (e.g. ground contact constraints) were added to the simulation and inverse dynamics was performed for each simulation model. The process entails removing of the Motion Agents and updating the joints to include the proportional-differential (PD) controllers or "trained joints" and the muscles to include the

proportional-integral-differential (PID) controllers or "trained muscles". With the trained joints and muscles based on the recorded motion from the inverse-dynamics analysis, the model is now ready for forward-dynamics simulation. Conducting all the above mentioned stages, a musculo-skeletal model with fully discretized spine was constructed and driven based on a certain motion which was obtained from a real subject. As such, the force and torque distribution of spine vertebrae can be obtained for further investigation. Similar to any other simulation method, before utilizing this model and interpreting its results for clinical applications, its performance have to be validated which will be the main topic of the next section.

3.9 Validation of the Spine Model

Validation of the forces and torques obtained from the simulation is presently impossible due to lack of experimental data, variety of the physical conditions of the subjects and environments. In this study, joint reaction forces were compared against relative intradiscal pressures measured *in-vivo* (Nachemson 1981, McGill 1987, Wilke, Neef et al. 1999, Wilke, Neef et al. 2001) and the results from the simulation spine model in the literature (Hansen, De Zee et al. 2006). Subsequently, dynamic behaviour of the spine during lateral bending while standing with carrying different dead weight and without it were investigated. Later on in chapter 5, simulation and analysis of dynamic behaviour of the spine model is conducted in daily activity such as bending and twisting by means of motion capture data.

3.9.1 Compare the results with simulation models and experimental data

One of the simple validation approaches is to compare the outcome of the simulation (e.g. maximum extension moments) in a certain position (e.g. upright position) with similar results obtained from experiment in the same condition. In the first attempt for validation, an increasing horizontal force in the posterior-anterior direction (in sagital plane) was applied to the vertebra T7 of the model as shown in Figure 3.16. Applying this external force, the resulting moment, axial and shear forces around the L5-S1 joint were calculated.

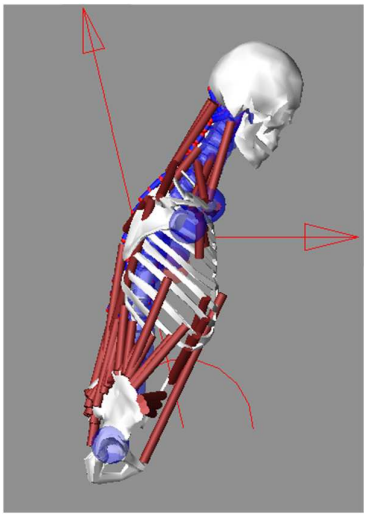

Figure 3.16 Spine model under external force applied on T7

Applying an extension moment of 238 nm, Zee'e model (Zee, Hansen et al. 2007) calculated axial and shear forces at L5-S1 joint to be about 450N and 639 N respectively. In order to impose a similar extension moment to our model (to be comparable to the results of Zee's model), an equivalent external posterior-anterior force of 1260 N has to be applied to T7 vertebrae in the sagittal plane. Application of this external force to our model resulted axial and shears forces of 4582 N and 625 N at the in L5-S1 joint. These results are lying within in the range of the forces that was estimated by McGill et.al ($3929 < F_{axial} < 4688$ N and $F_{shear} < 650$ N) (McGill 1987) or presented in the Hansen's review (Hansen, De Zee et al. 2006).

3.9.2 Comparison of the results with experimental data (*in-vivo* experiment)

Another example for performance validation of the current model is to compare its results with that of the Wilke et al. (Wilke, Neef et al. 2001) during a dead weight holding condition. In their study to measure the internal joint forces, Wilke et.al simulated a case in which a male subject of 70 kg weight and 174 cm height was holding a crater of beer of 19.8 kg 60 cm away from his chest. Performing the simulation, they calculated the L5-S1 intradiscal pressure as 1.8 MPa. Considering the disk area of 18 cm^2, the corresponding axial force at this joint is about 3240 N. Using our developed multibody model with similar body mass and height, the similar loading condition was simulated and the L5-S1 axial force was calculated as 3161.6 N which is in close agreement with Wikle's results.

Further validation needs to be done in order to use this model for clinical applications. In the next section, the validated model has been used to simulate the kinematic behaviour of the whole spine under external forces applied at different directions to certain vertebrae.

3.10 Loading on the spine

During daily activities, the spine is subjected to different loadings including axial (compression or tension) and shear (lateral or anterior posterior) forces as well as moment (bending or torsion) torques. The way that the different regions of the spine react against these loads to maintain its normal position and performance depends on many different functions such as the type, magnitude, and the rate of the external loads, anthropometric specification of the body (age, weight, height), the posture of the spine at and during the loading, and last but not the least biomechanical properties of the spinal system segments (disks, muscles, vertebrae, ligaments, and capsules) (Parnianpour, Nordin et al. 1988).

Axial load (in most of the cases compression) is the category of the forces with their direction parallel to the long axis of the spine and normal to the intervertebral disks. The main sources of the axial forces are gravity force, ground reaction, and axial components of the muscles and ligaments tensions. The major portion of these axial loads is supported by the vertebral bodies and intervertebral disks. It is noteworthy that the force corresponding to the pressure that disk is supporting is much greater than the magnitude of the external applied loads (Nachemson 1976). The direction of the axial force and its consequent compression deformation/displacement is shown in Figure 3.17(a).

The forces whose direction is parallel to the surface of the intervertebral disks are referred to as shear loads. These forces are responsible for in-plane deformation of the disk which results in sliding of one vertebra against the other one as it is shown in Figure 3.17. This deformation (displacement) may take place in lateral direction (in lateral plane) or in anterior/posterior direction (in sagittal plane).

While forces are responsible for translational deformations, torque and moment are responsible for rotation or twisting of the body around an axis. Moment (or torque) of a force applied to a certain point of the body can be considered as the effect of a force which has been applied to a point with a certain perpendicular distance with respect to the direction of the force. This distance is known as moment arm (MA). The subsequent internal effect of the toques and moments can be induction of internal shear or axial stresses (Serway and Jewett Jr 2009).

Flexion/extension, medial/lateral rotation, and abduction/adduction are technical terms to describe the direction of the moment or torque which has been applied to a joint (see Figure 3.18). The word "moment" and "torque" are considered as synonym in this thesis and can be used alternatively. For example a moment in flexion direction of the joint may be equally referred to as flexion moment or flexion torque.

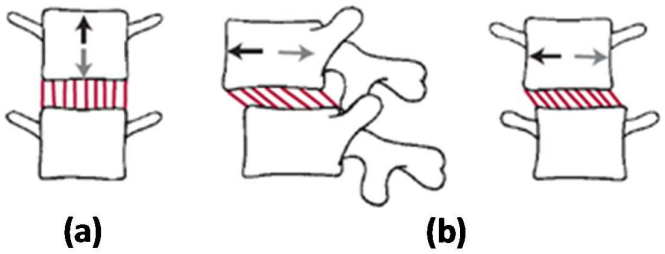

Figure 3.17 Schematic illustration of the loads applied on the disc (a) Compression load (b) Shear forces (Pamela K. Levangie 2005)

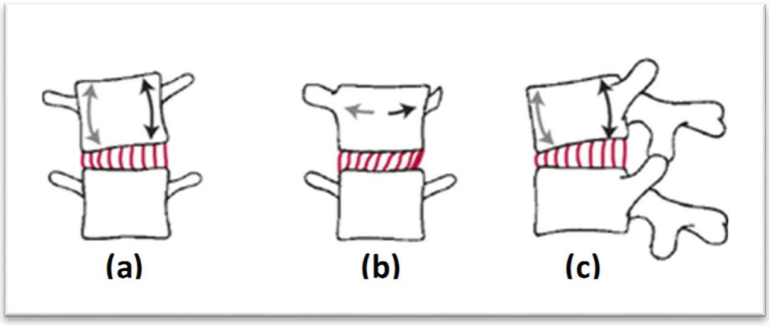

Figure 3.18 Schematic illustration of the torques applied on the disc (a) Abduction/ adduction (b) Medial/lateral rotation, or (c) Flexion/extension

3.11 Lifting activity during lateral bending exercise

In this exercise, a female healthy subject with no back pain experience performs the lateral bending exercise whilst holding a weight on her left hand. The dead weights of 1 kg, 2 kg and 3 kg were used in this experiment. After conducting the motion capture experiment, the data obtained from the motion analysis of the real subject were imported into the *LifeMOD* software. The motion trajectory data is used to drive the motion agents created on the human-body model. Then equilibrium analysis and inverse dynamics analysis were

done. The Motion Agents were removed and the proper PD and PID servo-controllers (representing joints and muscles) got trained to run the model. With the trained joints and muscles based on the recorded motion from the inverse-dynamic analysis, the model is now ready for forward dynamics simulation. As such, for each exercise the process repeats to find set of parameters which work for all these four experiments. This set of parameters link the proportional and derivative values for joints and muscles. This set of parameters reduces the angulation error of the spinal joint to less than 0.3˚ in all of the simulations.

The motion was simulated and the force and torque distribution of spine vertebrae can be obtained for further investigation. According to the results (Figure 3.19 – 3.21), as the deadweight increases, the joint force in the lumbar region also increases in both left and right bending. According to the results, by increasing the deadweight, the compression load on the lumbar joints will increase. The amount of increasing this load is higher than the amount of the lifting weight. For example after applying 1kg (~100 N), the compression load on L5/S1 increase around 400 N in left bending and around 200 N in right bending. These differences are due to the momentum produced by the weight being held in one hand. Therefore, maintaining the stability of the posture in this condition required higher muscle activity and ligament tension which implies more energy consumption and increased compressive loads on the spine segments (Pamela K. Levangie 2005).

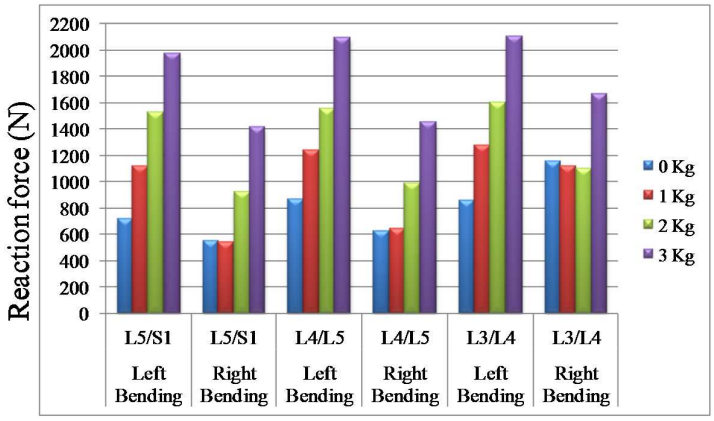

Figure 3.19 Reaction force on the three lower lumbar vertebrae in lateral bending exercise with different weight lifting

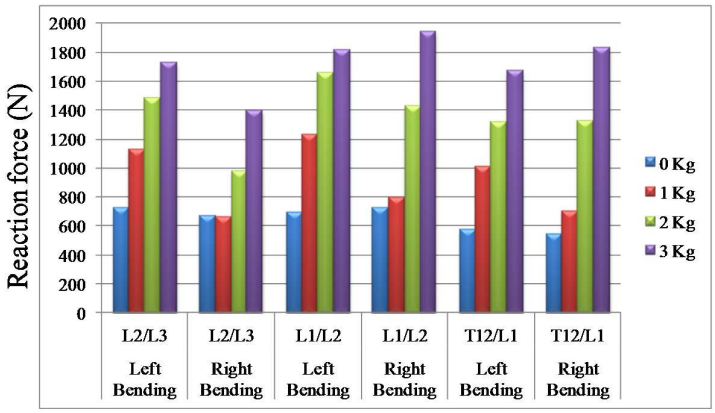

Figure 3.20 Reaction force on the two upper lumbar vertebrae joints and thoracolumbar joint in lateral bending exercise with different weight lifting

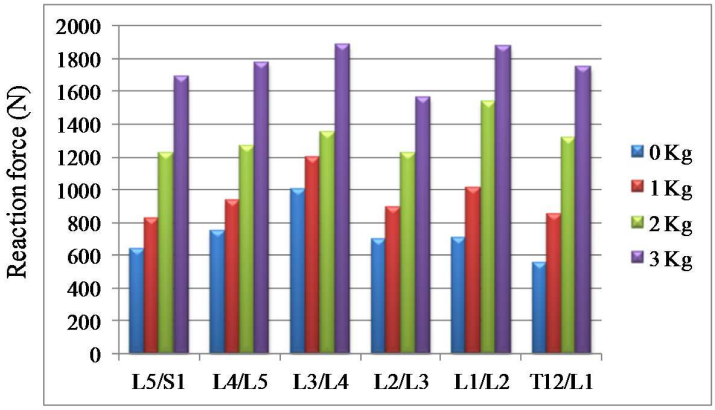

Figure 3.21 Reaction force on the lumbar vertebrae joints and thoracolumbar joint in lateral bending exercise with different weight lifting (average of value in left and right bending)

3.12 Summary

In this chapter, an overview of *LifeMOD* was introduced which helps users to understand fundamental concepts and modeling methods. Then, the modeling process was presented briefly and the references that the model was validated with them were introduced. Finally the motion capture system which was used in the experiments was introduced and the method of conducting musculo-skeletal human body with Mocap data was presented in brief.

Chapter 4: Modeling hypothesis scoliosis spine and test the stability under static loads

4.1 Introduction

The situations in which the spine is not able to maintain its normal displacement pattern to prevent severe deformities, excessive neurological deficit, and severe pain under physiological loads is referred to as spine clinical instability (Panjabi 1990). The spine instability conditions which occur due to deformation of the spine to excessive forces usually results in severe back pain. This can be considered as a diagnostic sign of the instability. In addition to excessive force, other physiological irregularities and disorders such as osteoporosis and especially scoliosis are able to contribute in the spine instability. Although it can be indirectly diagnosed by monitoring different physiological and orthopedic outputs, none of these can ultimately determine the instability as accurately as dynamic motion and force analysis of the spine.

In this chapter, 2D x-ray images of three scoliotic subjects (patients) were used to construct the 3D multi-body detailed spine model using *LifeMOD*. The developed models were tested for static stability analysis and the spine joint forces and torques were calculated for upright posture. Finally, the effect of severity of the scoliosis condition (Cobb's angle) on the lumbar joint forces was studied using the three scoliosis models hypothetically developed with left thoracic curvature. To achieve this goal, three hypothetical scoliosis models with different Cobb angles of 38°±2, 52°±2 and 62°±2 and one normal subject with a healthy spine (as a control model) were created. Effect of asymmetry on the scoliotic spine was evident in the resultant forces and momentums.

4.2 Curve patterns of scoliotic spine

The degree of curvature in scoliotic spine is usually measured using Cobb's method (Vrtovec, Pernuš et al. 2009), which is the angle of intersection of lines drawn perpendicular to the vertebral end plates that represent maximal deviation of the spine. The degree of Cobb angle identifies the type of treatment that doctors use to treat the patient (see Figure 4.1).

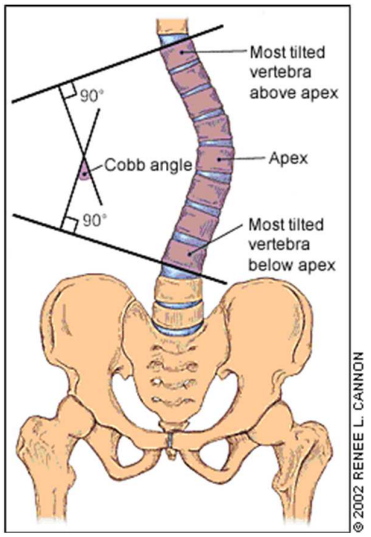

Figure 4.1 Cobb angle of a scoliotic spine in frontal plane (Patias, Grivas et al. 2010)

The curve patterns of idiopathic scoliosis may be called "primary" and "compensatory. Larger curves in magnitude are referred to as "Primary curve" which generally have more cosmetic deformity. These cases are more rigid on side bending in the supine posture (James 1951, Weinstein 1986). "Compensatory curves" are those that are more flexible on supine side bending and smaller in magnitude (James 1951). The position of the scoliosis curve is commonly identified by the position at which the apex of the curve is located. In other words, position of the curve is known as the name of the vertebra at which the spine has the maximum off-centricity. For example a curve which has its apex in the thoracic region is referred to as "thoracic curve".

Most of the scoliosis curves have a dual curve pattern which consists of a curve in thoracic (rib cage area) region and another one with opposite direction in the lumbar (lower back) region. These curves are known as "thoracolumbar curve" and their different curvature direction balances the total spine orientation in a way that the head still remains centered over the pelvic region (Figure 4.2). On the other hand, other scoliosis patterns may consist of only one curve which usually may lead to a considerable degree of imbalances in the upper extremity parts of the body as well as the head.

Based on their location, shape, pattern and cause, idiopathic scoliosis curve patterns can be classified into four classical curve patterns: thoracic, thoracolumbar, lumbar and double (primary and thoracic primary) (Kurtz and Edidin 2006).

Thoracic curve (Goel and Press. 1980): This curve typically extends from T5 or T6 to T11 or T12, with the apex at T10 or higher.

Thoracolumbar curve*:* The curve extends from about T8 to L3. The apex of this "C-shape" curve is usually located at the junction between the thoracic and lumbar spine (T12 or L1, or the T12-L1 disc space). Patient with this curve pattern usually suffer from cervical or lower back pain.

Lumbar curve: This curve typically extends from about T11 to L4. It may be in either direction but is more commonly to the left that may force the right hip toward to the left. This unbalance situation of the hip usually causes a severe pain in the lumbar region of the spine.

Double primary curve: This "S-shape" curve pattern has a right thoracic curve that usually extends from T5 to T12 and a left lumbar curve from T12 to L4. The right thoracic curve usually causes pain in the lungs due to compression in the ribcage.

Double thoracic primary curve: This curve pattern has two primary curves in the thoracic region. The upper one is to the left, extending from about T2 to T5, whereas the lower one is to the right (from T5 to T10) (Edidin, Kurtz et al. 2006).

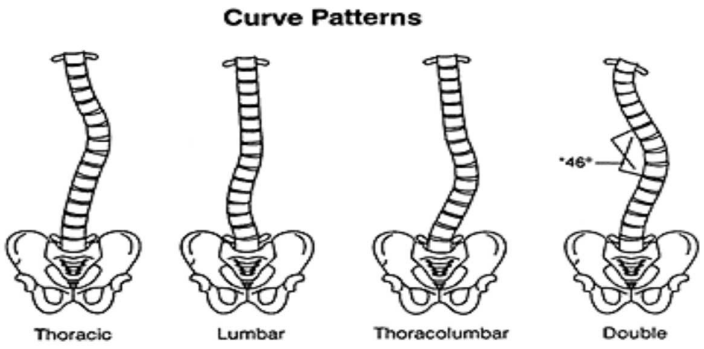

Figure 4.2 Curve patterns of scoliotic spine

4.3 Creating the spine curvature based on 2D X-ray images from scoliosis patients

In this section, capability of our method for creating a musculoskeletal model of the human body with different scoliosis curve patterns is evaluated. Based on the user's anthropometric

input, three default (pre-defined) multi-body spine models were initially generated in *LifeMOD*. These models were refined with creating 24 segments for the vertebrae, 24 joints representing intervertebral joint, spine ligaments, abdomen and lumbar muscles which mentioned in chapter 3. Since the motion capture has not been used in the simulation of this chapter, the intra abdominal pressure is added to each subject's model.

In the next step, the spine curvature was modified to the scoliotic curve pattern in the simulation model based on the X-ray images of the patient. Types of the curvatures used in these models have been described in Table 4.1. This table represents anthropometric data of three scoliosis patients with thoracolumbar and double scoliotic spine curvatures. All these subjects participated in the gait analysis test and also lateral bending, flexion and twisting tasks before doing the surgery and were supposed to do the post operation gait test after the surgery within 1 year. These tasks are the typical tasks used by clinicians to determine the severity of scoliosis condition and the ability enhancement of the patient movements after the surgery.

Table 4.1 Data on patients and scoliosis curve patterns

Parameters	**Patient**		
	PT1	PT2	PT3
Height (cm)	151	158	161
Weight (kg)	41	77	45.5
Sex	Female	Male	Female
Age at the time of experiment (years)	15	14.5	15.5
Scoliosis curve pattern	Thoracolumbar (towards right)	Thoracolumbar (towards left)	Double

For each subject the X-ray images in erect posture in frontal and sagittal planes were used in this study. The position and orientation of each vertebra was obtained based on the measurement that had been done in Computerized Patient Support System (CPSS).

The X-ray image and other clinical information of the subjects (required for this study) has been acquired from a 24-hr available online database developed by National Healthcare group. This is a password protected data base containing surgical operating notes, X-ray images, CT scan, and MRI, and other laboratory results of the patients. This system is designed to provide efficient access of the doctors to the patient information. In order to

protect the confidentiality of the patients, this system is protected with individually assigned passwords for doctors.

Figure 4.3 shows the procedure to determine and mark the center of mass (COM) of each vertebra measured in the X-ray images. The limitation of this study is that the exact position and orientation of the COM of the vertebrae cannot be found by the software and it has to be done manually by the user. Therefore the measurement may vary from person to person or time to time. The obtained model can be validated by comparing its results with those of the *in vivo* experiments (in similar conditions) and then can be reliably used for further studies.

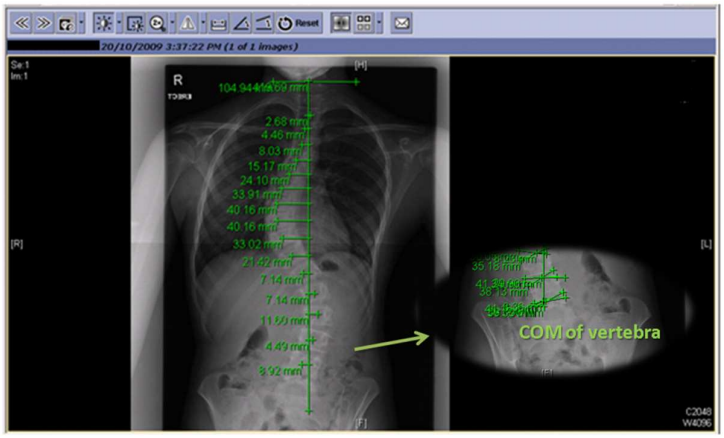

Figure 4.3 Location of the COM of the vertebrae in X-ray image

PT1: Spine with thoracolumbar curve

The first scoliosis subject who participated in this study had thoracolumbar scoliosis with convexity to the right at the thoracic region. Although the curvature was very obvious on frontal X-ray image of her back, this patient has no pain during her daily activity. In order to create the multi-body model of the deformed (scoliosis) spine, the position and orientation of each vertebra was found from the X-ray images in sagittal and frontal planes and the spine curvature is created based on Cartesian data. Based on these data, the vertebrae in the default 3D model were relocated. Figure 4.4 shows the X-ray image and 3D model of this subject in erect posture.

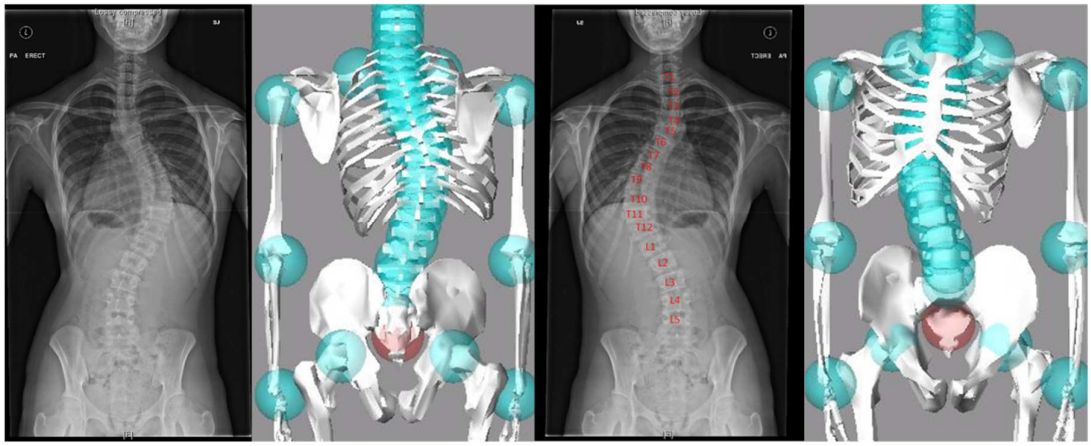

Figure 4.4 Front and back view of X-ray images and 3D model of PT1 in erect posture

PT2: Spine with thoracic curve

The second scoliosis subject who participated in this study had thoracolumbar scoliotic curve, starting from T7 and ending with L3, with convexity to the left at the thoracic region of his spine. The curvature was very obvious on his back. He was leaning to the left side during walking. Based on the X-ray images in two planes, the position and orientation of each vertebra was found to relocate the vertebrae in 3D model. Figure 4.5 shows the X-ray image and 3D model of this subject in the erect posture. This subject participated in the post operation experiment as well. Comparison between dynamic behavior of this subject before surgery and one year after surgery is studied in chapter 5.

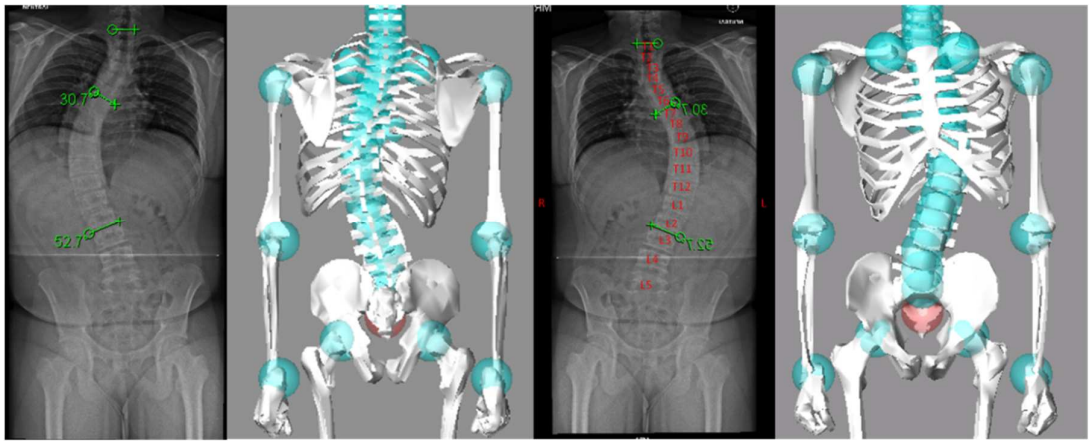

Figure 4.5 PT2's spine curvature in x-ray image and simulation model in front and back view

PT3: Spine with double curve

The third scoliosis subject who participates in this study had double scoliotic curve with convexity to the right at the thoracic region and to the left at the lumbar region. The curvature was not very obvious on her back. The position and orientation of each vertebra was found based on the X-ray images to relocate the vertebrae in 3D model. Figure 4.6 shows the X-ray image and 3D model of this subject in erect posture.

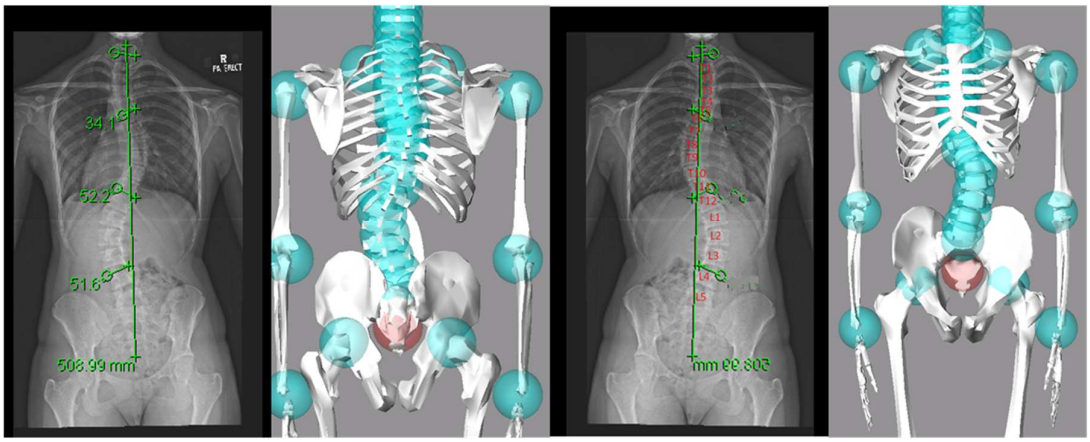

Figure 4.6 PT3's spine curvature in X-ray image and simulation model in front and back view

4.4 Spine Stability analysis for three scoliosis models

The stability of the spine is defined as the ability of retrieving its original position after being subjected to a perturbation, excessive force or deformity and if the spine cannot regain its original (e.g. upright) position, it is called instable spine. For example very fast and sudden motions or very severe external forces may deform the spine beyond its healthy range of motion in such a way that the spine is not able to return to its normal healthy orientation. These kinds of instabilities are usually followed by severe injuries. An equilibrium condition of the spine is of a critical role to determine its stability.

One of the important factors which can affect the range of stability of the spine is the response time of reaching stability. This response time is a function of physiological conditions of the body and can be different among different people. For example, the stability time of an athlete can be much shorter than that of a patient with back pain or scoliosis deformity. This can be explained in the light of muscle performance. While in the first case muscle are strong, and perform uniformly (in both sides) to respond against the

deformity of external force, in the latter case the muscles are fatigued, deformed and became asymmetric (to compensate the spine disorder) and may not be able to react rapidly to restore the initial position.

In this chapter, effect of spine deformity on the stability conditions of the three scoliosis models (which were generated earlier in this chapter) in upright standing posture has been studied. A pre-default multi-body spine model was initially generated depending on the user's anthropometric input. The process of discretizing spine, adding ligaments, lumbar muscles and abdomen muscles was done as explained in chapter 3. The curvature of the spine was created in the spine by displacing the vertebrae in the frontal plane to create the desirable Cobb angle. The detailed model was put in the upright standing posture. Then the inverse simulation without the gravity force was run such that the model can record muscle contractions which are required to maintain upright posture. After that the boundary conditions such as ground contact was added to the model. As explained in the previous chapter, at the beginning of the simulation (i.e. the inverse dynamic step), the history of the segments displacements and contraction of the muscles is recorded in the PID-servo controller. This information later will be used to recreate the recorded motion by updating the muscle contractions (in this example the recorded motion is just a static upright standing posture). In the final step, the effect of gravity and boundary conditions (contact force, etc.) were included in the model and the forward dynamic step was run.

By running the similar simulation procedure for all the models (with different scoliosis curves), the models obtained a new equilibrium state after a few seconds. From the results obtained, PT1 model became stable after 2.5 second, PT2 model became stable after 2 second and PT3 model became stable after 1.9 second. Figure 4.7 shows the velocity of the head of these three patients' model during the simulation time.

After reaching the equilibrium state, the joint force in the lumbar region for PT1 and PT2 increases from T12 to S1 and lumbosacral joint has the highest joint force value and thoracolumbar joint has the lowest joint force value; however in PT3 due to the double curve and change of the direction of the curve near thoracolumbar joint, the joint force increased and after L5/S1 and L4/L5 joints had the greatest joint force value. The joint force in all models varies from 60% to 120% of the of body weight which is in good agreement with relative intradiscal pressures measured *in vivo* (Nachemson 1981, Wilke, Neef et al. 1999, Wilke, Neef et al. 2001).

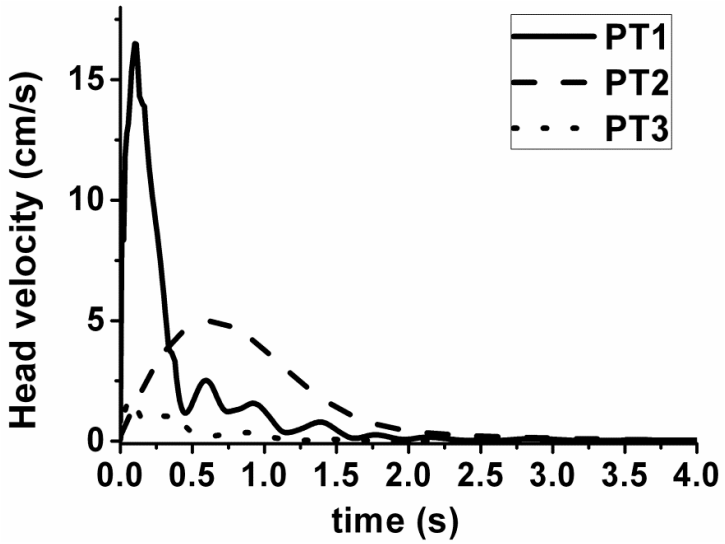

Figure 4.7 Head velocity (cm/s) of three models during stability simulation

4.5 Investigating the Lateral and Anterior/Posterior (A/P) motion of normal and scoliosis models using forward dynamics

In this section, three hypothetical scoliosis models with different Cobb angles of 38°±2, 52°±2 and 62°±2 were created in thoracic region (towards left) to investigate the stability of the model in forward dynamic analysis. One normal subject with a healthy spine was also built as a control model. In this section, effect of asymmetry on the scoliotic spine in terms of force and momentum in the joints was studied.

A pre-default multi-body spine model was initially generated in *LifeMOD* depending on the user's anthropometric input. The model used in this study was a male model of 178 cm height, 70 kg weight and 24 years old created from the GeBod anthropometric database (Cheng, Obergefell et al. 1994, Cheng, Obergefell et al. 1996). The process of discretizing spine, adding ligaments, lumbar muscles and abdomen muscles was done and the curvature of the spine was created in the thoracic region by proper displacing the vertebrae in the frontal plane to create the desirable Cobb angle. In this model, the apex is located on T7 and the curvature starts from T4 and ends with T10. Figure 4.8 shows all segments of 24 vertebrae in the cervical, thoracic and lumbar regions after discretizing the scoliosis spine with a 38° Cobb angle.

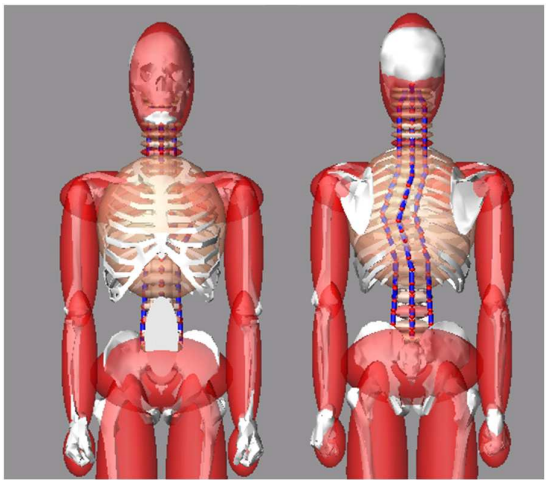

Figure 4.8 Anterior and posterior view of the complete discretized scoliosis spine model

Hereafter, the scoliosis models with Cobb angle of 38°, 52° and 62° are referred to as case I, case II and case III, respectively. Figure 4.9 shows the posterior view of four (three scoliosis and one normal) simulated models. In this figure, to make the curvature more obvious the muscle set of thoracic part and cervical part were hidden.

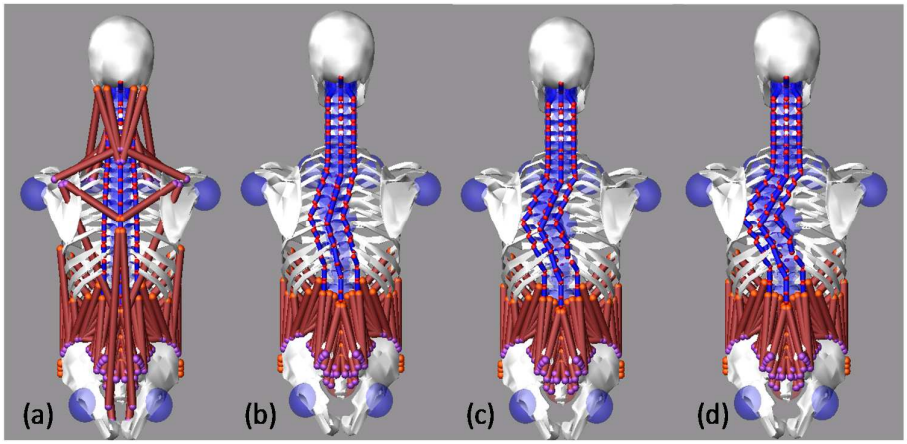

Figure 4.9 Posterior view (a)Normal model (b)Scoliosis model with 38° Cobb angle (c) Scoliosis model with 52° Cobb angle (d) Scoliosis model with 62° Cobb angle

4.5.1 Evaluation of the stability of the models

To evaluate the stability performance of the developed model, a single shear force was applied to the same vertebrae in all models. Magnitude and direction of the force, as well as the position at which the force is applied was selected in accordance with the previous work of other researchers (Tho 2010) for comparison purposes. A comparison between the

results of the current work with those of the other researchers enables us to evaluate the performance of the developed model. The maximum momentum by which this simulation model can successfully pass the inverse dynamic simulation analysis is 240 Nm on lumbosacral joint (McGill 1987, McGlashen 1987). To obtain this moment, an external A/P force of 1260 N must be applied on the T7 vertebra in our model. Corresponding to this force, axial and shear forces obtained from the normal model were 4582 N and 625 N, respectively which are in the same range of the forces reported in reference (Zee, Hansen et al. 2007). This is also in agreement with the results presented by McGill et al. (McGill and Norman 1986) who found axial forces in the range of 3929–4688 N and shear forces up to 650 N. Therefore, in this study, the A/P shear force of 1260 N was used for the simulation. According to the findings of previous researches (Tho 2010), it is known that the maximum lateral shear force which can be endured by a certain vertebra of the normal spine is 650N. Therefore, we selected a lateral shear force 600 N to be imposed on T7 in the scoliosis models in our second experiment to investigate the dynamic behaviour of spine under these static forces in all four models.

4.5.2 Body segment motion of the scoliotic patient under external 1260 N A/P and 600 N lateral shear forces applied on T7

One good measure to validate the performance and accuracy of the developed model is to evaluate its stability. Similar to a real human body, after imposing an external force or applying a motion agent, the model is expected to obtain a new equilibrium state. In this section of our study, while the model is in an standing position, a 1260 N horizontal external force from posterior to anterior in the sagittal plane in first simulation and 600 N lateral shear force from right to left in the frontal plane in second simulation were applied to the T7 of scoliotic spine. The force and torque distribution of the lumbo-sacral joints of the scoliosis models were compared with those of the normal one. It is noteworthy that in these simulations lower torso is fixed to the ground.

After applying the external force and passing a transition state, the head stabilizes in 2s in two simulations. Figure 4.10 shows the normal model and the scoliosis model with Cobb angle of 38°. This behaviour was exploited to evaluate the stability of the generated spine models in this work. After equilibrium analysis, contact constraint (e.g. ground contact constraints) was added to the simulation and inverse dynamic was performed for each simulation model. The process entails updating the joints to include the proportional-

differential (PD) controllers or "trained joints" and the muscles to include the proportional-integral-differential (PID) controllers or "trained muscles". In reality, in the case of an external shock (force or displacement), the nervous system fires with a certain time delay to trigger the muscles to prevent the segments from displacements or deformations beyond their anatomical range which otherwise may result in injury. In a mathematical human-body model, the effect of the nervous system to fire and react against an external shock can be modeled as feedback gains which can control the range of the motion of the segments and contractions of the muscles. With the trained joints and muscles based on the recorded motion from the inverse-dynamic analysis, the model is now ready for forward dynamic simulation. As such, the force and torque distribution of spine vertebrae can be obtained for further investigation.

Displacement of the head in frontal plane was found for all four models in the first and second simulations. In the normal model, since the spine has no asymmetry as shown in Figure 4.10, the head became stabilized in the sagittal plane and with almost zero lateral displacement (the head did not incline towards left or right). However, after stabilizing, the head in the scoliosis models inclined towards right. This behaviour can be directly attributed to the spine asymmetry in the scoliosis models. It is noteworthy that the equilibrium analysis was done for all simulations of this study as we did for the first experiment.

Position of the head of the scoliosis models with different Cobb angles after stabilization of the model is summarized in Figure 4.11 for the first simulation and in Figure 4.12 for the second one. Displacement of the head in the scoliosis models in sagittal and transverse planes is not very different from those of the normal model in first simulation (the difference does not exceed 4% as compared with the normal case); however, variation of the head displacement in the frontal plane in comparison with the normal case is considerable. Figure 4.11 shows the Variation of head lateral displacement of scoliosis models in frontal plane in the first simulation with respect to displacement of the normal model as the A/P external force is applied until it reaches a new equilibrium position. As can be seen, tendency of the head for leaning to the sides in the frontal plane increases by the severity of the scoliotic curvature (increases as the Cobb angle increases).

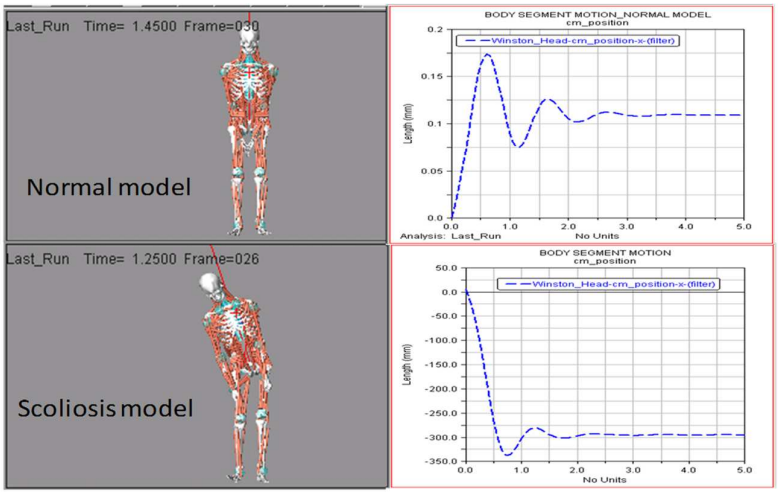

Figure 4.10 Stability test of normal and scoliosis simulated models

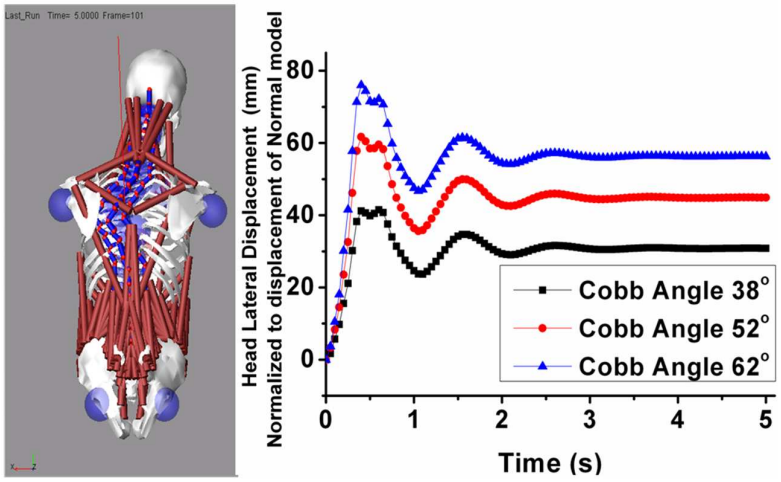

Figure 4.11 The variation of lateral head displacement of scoliosis models with respect to the normal model in first simulation

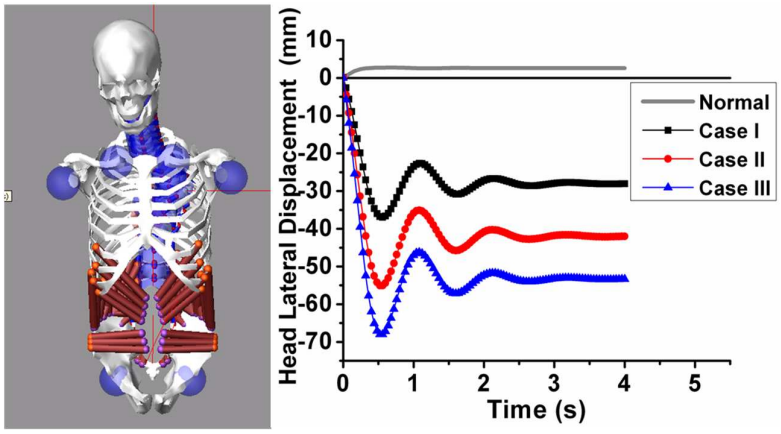

Figure 4.12 Head displacement of all simulated models in frontal plane after applying 600N lateral shear force on T7

4.5.3 Apply horizontal (A/P) force on T7 and study its effect on the lumbar joint force and torque

As mentioned in chapter 2, one of the main responsibilities of the spinal joints is to transfer the loads between vertebrae and also to enable the flexibility of the spine while maintaining its integrity. Among all these joints, the lumbar joints are of much more importance as they are supporting almost the whole weight of the trunk while providing an extensive range of the mobility for the trunk. Therefore, effect of any external shock/movement or movement (jumping, bending, and walking) can be clearly sensed in this joint. Because of its key biomechanical role, this joint is usually selected to monitor the effect of any boundary or loading conditions in biomechanical modeling of the spin (Panjabi 1990).

In this study, effect of the severity of the scoliosis (Cobb angle) on the loading condition of the lumbar joint will be studied. For this purpose, the models (one normal and three scoliosis models) are subjected to an external force, the resultant compression loads (normal to the vertebrae) and shear forces as well as the torques at the lumbar joints of the scoliosis models in equilibrium position were calculated and compared.

According to the obtained results, compression load in the scoliosis models is not considerably different from those in the normal model. The maximum difference was observed in the case of scoliosis model with maximum Cobb angle, which was only 3%. The difference was obtained by using equation 4.1. However, in the scoliosis cases, the lateral and the A/P shear forces increased by increasing the Cobb angle. Due to the regular spine symmetry in the normal model, the lateral shear force at the lumbar joints is almost zero. The maximum difference in A/P shear force was observed in the case of scoliosis model with maximum Cobb angle (62°) that happened at L3/L4 joints. This shear force was about 35% higher than that of the normal model in the same condition.

EQ 4.1 $$\left|\frac{F_{Scoliosis} - F_{Normal}}{F_{Normal}}\right| \times 100$$

Whilst scoliosis models differ significantly from normal models, they appear to follow the same trend regardless of scoliosis severity. The variation of the joint force value from throcolumbar joint to lumbosacral joint was obtained in this study. As shown in Figure 4.13 lateral shear force increased as the Cobb angle increase among the scoliosis models. In addition, the variations of lateral shear force in equilibrium position within the four models are depicted in this Figure. As can be seen in Figure 4.14, in the scoliosis models the pattern

is almost the same and the joint force increase as the Cobb angle increase in the scoliosis models.

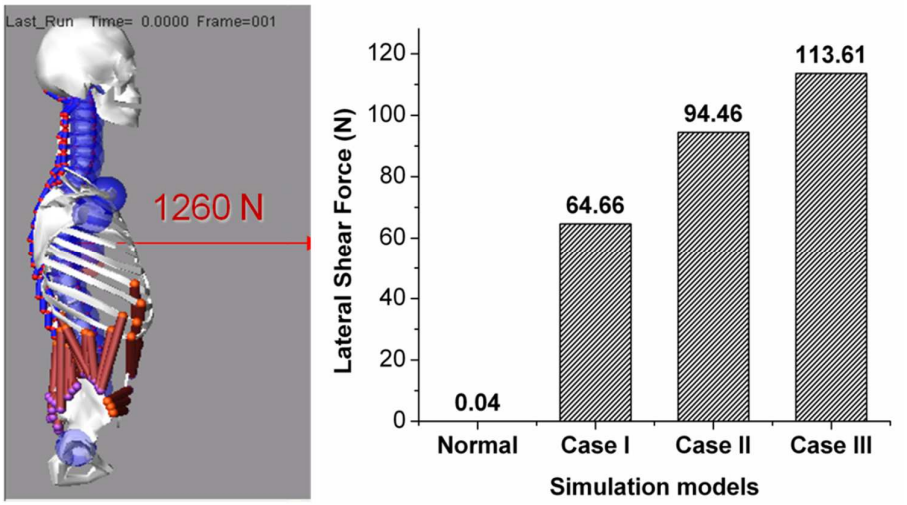

Figure 4.13 Lateral shear force in four simulated models

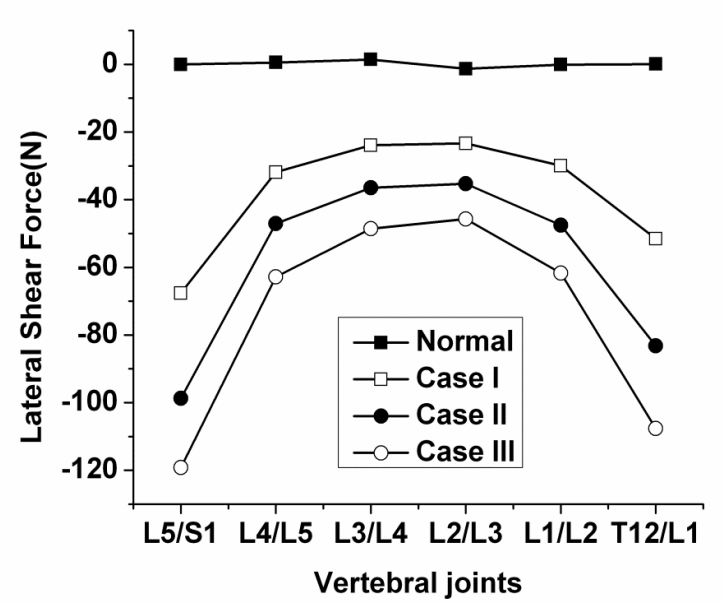

Figure 4.14 Lateral shear force pattern of the lumbar vertebral joints

Sagittal, lateral, and twisting torques were also compared in the same way among the models. Because of the symmetry of the spine in the normal model, lateral and twisting forces are near zero and only sagittal torque in lumbo-sacral joint is of a considerable value. However, in the scoliosis models, due to the asymmetric mass distribution of the model,

the magnitude of the other torques (lateral and twisting) are also considerable (4 to 16 Nm). The sagittal torque in the scoliosis models slightly increases by increasing the Cobb angle (2.6% for smallest Cobb angle and 6% for the largest Cobb in scoliosis with respect to that of the normal model). However, a remarkable difference in the lateral torque and twisting torque was observed between normal model and scoliosis models. Figure 4.15 shows lateral and twisting torques from throcolumbar to lumbosacral joints. As can be seen, in the scoliosis models the pattern is almost the same and the joint torque increase as the Cobb angle increase in the scoliosis models.

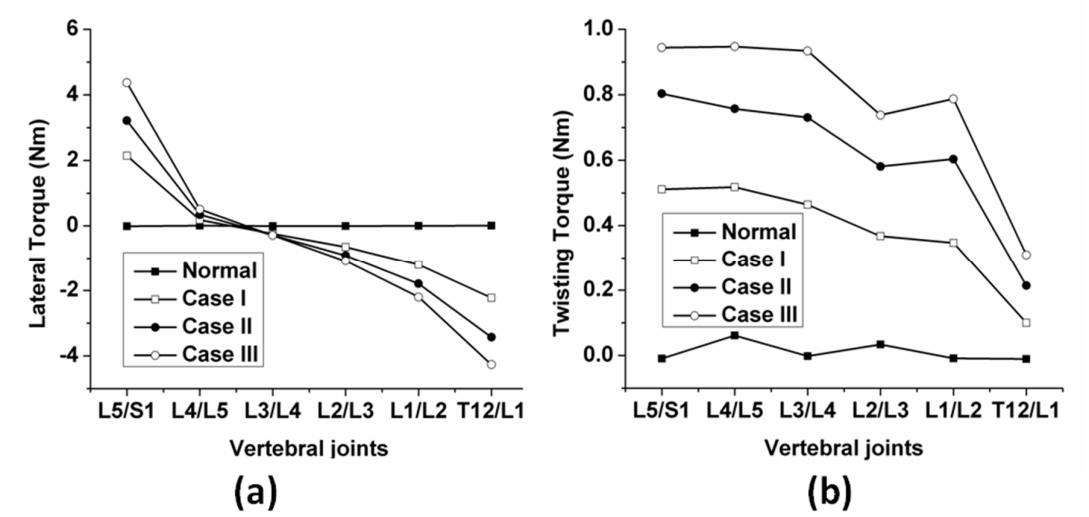

Figure 4.15 Joint torques in the lumbar region (a) Lateral torque (b) Twisting torque

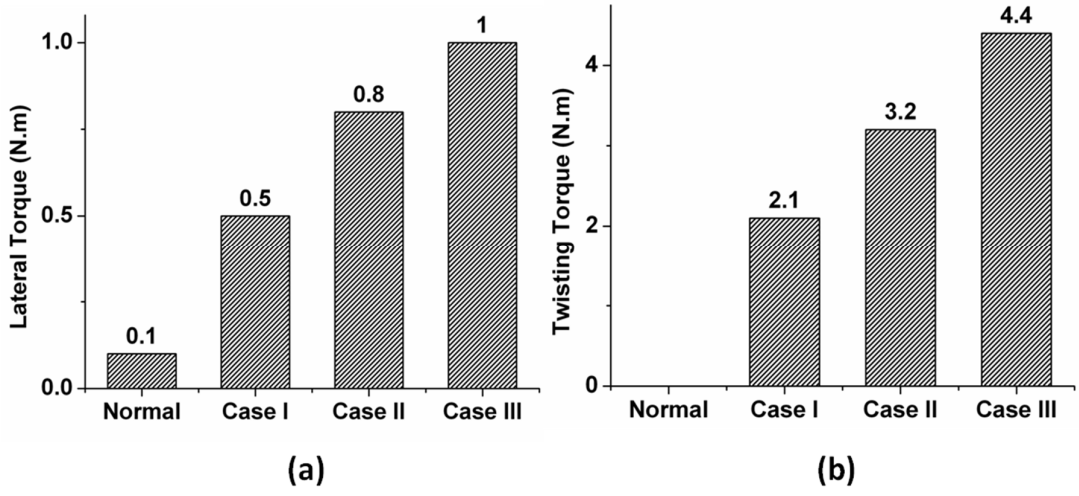

Figure 4.16 Joint torques within four simulated models (a) Lateral (b) Twisting

Lateral and twisting torques of the model with largest Cobb angle is 10 and 4 times higher than that of the normal one respectively (see Figure 4.16 (a) and (b)). As expected, since the spine of the normal model is symmetric, these torques are zero. However, in the other cases, by increasing the Cobb angle, they continuously increase.

4.5.4 Apply horizontal (lateral) force on T7 and study its effect on the lumbar joint force and torque

Compression load and shear forces as well as the torque at the lumbar joints of the scoliosis models in equilibrium position were also calculated and compared with those of the normal model in second simulation. The magnitude joint force for each vertebra includes compressive force, lateral shear force, and A/P shear force. As can be seen in Figure 4.17, magnitude forces in the scoliosis models are higher than those in the normal model and increase as the Cobb angle increases. The maximum difference was observed in the case of scoliosis model with maximum Cobb angle, which was 30% in compression load, 2% in A/P shear force and 3% in lateral shear force among the lumbar joints from those of the normal model.

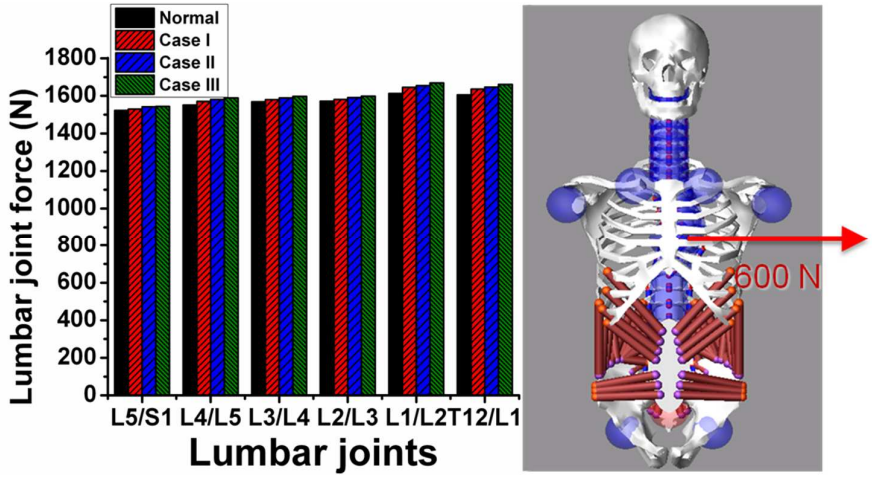

Figure 4.17 The lumbar joint forces in four simulated model

Sagittal, lateral, and twisting torques were also compared in the same way among the models in joints from throcolumbar to lumbosacral one. According to the results, twisting torque in the scoliosis models increase in lumbosacral and L4/L5 joints as the Cobb angle increases. However, the sagittal and lateral torques in the scoliosis models are not much

different from those of the normal one (less than 1% in sagittal and 5% in lateral torque. Generally the joint torque increases as the Cobb angle increases in the scoliosis models.

4.5.5 Nature of the mechanical loads on the spine

In Figure 4.18 the lumbar segment is shown under the loads from external force and upper body weight. Since the A/P external force is parallel to the normal vector of sagittal plane the momentum resulted from this force will have two components in transverse and frontal planes. Since in all simulations the applied force has the same magnitude, the magnitude of the resulted torque depends only on the length of the moment arm (MA) which has three components in three directions. However, only the component in lateral direction will change in the models. Therefore only twisting torque will increase as the distance increase or Cobb angle increase. Table 4.2 shows the magnitude of the external torque in transverse plane on the lumbar segment. This can explain why we have higher force and torque in the scoliosis model compare to the normal one and why increasing the Cobb angle results in increasing loads on the vertebrae. In other words, in the scoliosis models since the distance between the point at which the load is applied and CoM and Line of Gravity (LoG) of the body increases, the moment of the force and consequently the joint force increases. However the results values are different from the simulation results due to the different assumption. In this model, the lumbar region assumed to be one segment and the effect of muscle and ligaments are not considered.

In second simulation, the external lateral force is applied to CoM of T7. As can be seen in Figure 4.19, the external force and force moment will transfer from T7 to L1. Since the external force is in frontal plane and the MA has two components in sagittal planes, therefore the moment force will have only a component in transverse plane. Since the MA which produces the twisting torque is constant among the models, the external twisting torque does not change within the simulations. However the loads which are resultant of the gravity force, ground reaction forces, and forces generated by the ligaments and muscle contraction will change due to the asymmetry of the spine.

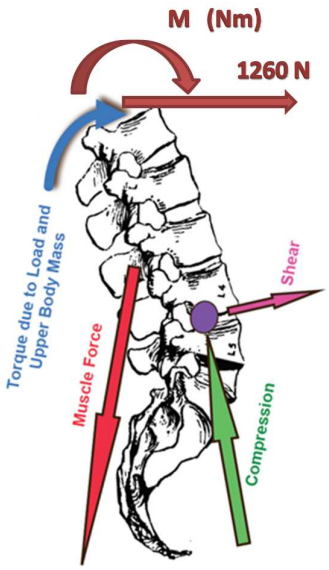

Figure 4.18 Force and torque diagram on the lumbar spine

Table 4.2 External torque on the lumbar region

Simulation model	Distance of CoM of T7 from Center line (mm)	Twisting Torque (Nm)
Normal	0	0
Scoliosis with 38	32	40.32
Scoliosis with 52	48	60.48
Scoliosis with 62	60	75.6

Figure 4.19 Free body of the lumbar spine diagram under external lateral force

Based on the results, the variation of the loads in first simulation was higher than the second one due to the external torque which varies in the first simulation.

4.6. Summary

In this chapter, common curve pattern of AIS scoliosis were discussed. Then the process of creating scoliosis spine model with different curve pattern based on X-ray images of the real subjects in *LifeMOD* was explained. The spine curvature in three scoliosis subjects has been created and analyzed. Using X-ray images the positions of each vertebra were found in two planes and the spine curvature is created based on Cartesian data. The spine stability of these models in upright standing posture was investigated.

Furthermore, three different scoliosis models with different Cobb angles were developed and analyzed for stability and also under static loads in sagittal and frontal planes. While the model is in a standing position, a horizontal force from posterior to anterior in the sagittal plane or a left to right shear force in coronal plane was applied to the T7 of scoliotic spine and the force and torque distribution of the lumbo-sacral joints of the scoliosis models in each case were compared with those of the normal one. The result of this study showed that the loads at the lumbosacral joint in the scoliosis models will increase by increasing the Cobb angle and these loads are considerably higher than the loads of normal subjects. This behaviour directly shows the effect of asymmetric mass distribution of the scoliosis model on the load distribution in the spine which may lead to a better understanding of corresponding back problems as well as improved treatment processes.

Chapter 5: Dynamic behaviour of the human body with scoliosis spine

5.1 Introduction

In the previous chapter, the process of modeling of scoliosis spine with different curve patterns based on X-ray images of the real subjects using *LifeMOD* and also stability analysis of these models in upright standing posture has been discussed. The main goal of this chapter is to study the effect of dynamic postures on the loading conditions of the intervertebral joints of human spine (normal and scoliosis) during the basic daily activities such as flexion, extension, lateral bending and rotation.

Knowledge of the movement of the whole spine is important for evaluating the clinical and pathologic conditions that may potentially produce unstable situations or permanent deformities such as disk degeneration. Among the different regions of the spine, the lumbar section provides the maximum load support and considerable movement. The functions of the lumbar spine are motion, support of body weight, and protection of nervous structures. Most of our daily activities consist of considerable amounts of forward/backward and lateral bending and torsion. The consequent spine deformities and the resultant forces have been considered as the main potential sources of disk degeneration and low-back pain (Hole 1981). This highlights the importance of having a clear understanding from the kinematic reaction of the lumbar spine to the physiological loads (due to daily spine deformities). For this reason, the dynamic load analysis of the human spine in this chapter is mainly focused on combined load effects in the lumbar spine region in different postures. Direct measurement of the loads (joint forces) in the spine is a very complicated process and is not possible unless by using *in-vivo* experiments. However the available data from these experiments are very limited for the subjects with scoliosis condition.

In most of the cases, the pressure of the intervertebral disks (intradiscal pressure: IDP) has been considered as a measure to study the effect of posture on load conditions between the vertebrae of the spine (Nachemson and Morris 1964, Nachemson 1966, Andersson, Örtengren et al. 1977, Nachemson 1981, Schultz, Andersson et al. 1982, Sato, Kikuchi et al. 1999, Wilke, Neef et al. 1999, Wilke, Neef et al. 2001). The pressure is usually measured by means of needle shape pressure transducers inserted into the disk in different postures such as sitting, bending, jumping, etc. (Nachemson and Morris 1964, Nachemson 1966,

Nachemson 1981). More advanced pressure sensors have been used to measure the vertical and horizontal pressures in the intervertebral disk (Sato, Kikuchi et al. 1999). In the recent years, implanted transducers together with telemetry techniques have been used to record the disk pressure during the daily activities (Wilke, Neef et al. 1999, Wilke, Neef et al. 2001). Although most of these methods have had major contributions to understanding the biomechanics of the spine and provided valuable data to validate the computational methods, they were only able to measure a portion of the spinal loads e.g. compression forces.

In spite of the complexity of these methods (in most of the cases these experiments were invasive), the disk pressure mainly reflects the effect of compression forces. On the other hand, it has been shown that the failure of the intervertebral disks (rupture of the disk fibers) is not only due to the compression forces but the combination of loads (tensile, shear and compression loads) (White and Panjabi 1990, Cholewicki, Crisco III et al. 1996). In other words, the risk of disk rupture increases when a combination of torsion, axial compression load, and bending is posed to the spine (Shirazi-Adl 1989).

However, as discussed in chapter two, direct measurement of the spinal loads is very difficult and in most of the cases is invasive and has to be done on cadaveric subjects. This has necessitated development of the computational methods and computer biomechanical models to estimate the spinal loads. The results of these experiment-based measurements provided valuable insight which can be used for validation of the simulation methods.

The main purpose of this chapter is to analyze the spinal load distribution in different body postures by means of a validated musculoskeletal model developed in *LifeMOD* biomechanical simulation package. In this work, the intervertebral loads between vertebrae of the lumbar region were estimated for four subjects with normal and scoliosis spines. In addition, the effect of the spine deformity in the load conditions of the spine in three basic bending tasks of flexion/extension, lateral flexion, and rotation (Figure 5.1) is investigated.

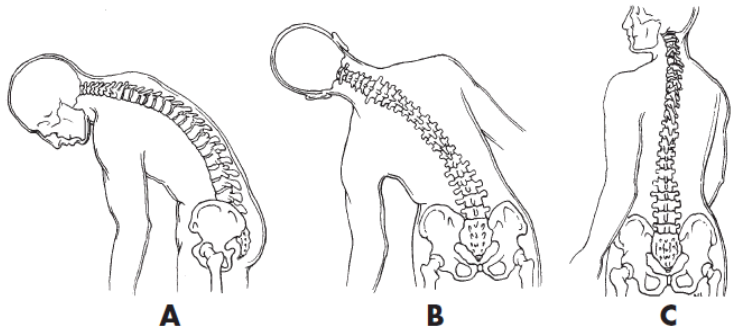

Figure 5.1 Basic spine bending tasks (a) Flexion in sagittal plane. (b) Lateral flexion in coronal plane. (c) Axial rotation in transverse plane (Pamela K. Levangie 2005)

Lateral bending, forward/backward bending and axial rotation are the most common assessment exercises which are carried out by surgeons to examine the ability of the patient to move in these directions before surgery. Motion capture experiments were used to record the deformity of the body in different exercises and to apply the recorded motions to the scoliotic and normal musculoskeletal models for load analysis.

In our experiments, two male subjects and two female subjects, one normal and one scoliosis in each group, with similar anthropometric data were asked to do the assessment exercises. Motion capture data of the subjects was obtained in each experiment. The motion capture results were used for training of the musculoskeletal multi-body model in forward and inverse dynamic simulations. Inverse dynamics simulation was performed to simulate the complicated multi-body motion of the spine in a given activity. In order to study the movement limitations of the scoliosis subjects, 3D musculoskeletal models of the two healthy subjects (both male and female), were created as the reference. These models were used to compare the motion of the scoliosis and normal subjects performing the same motion activities. The flexibility of the spine and ribcage was compared among the healthy and scoliosis female subjects with similar anthropometric data in the lateral bending exercise. The musculo-skeletal model was used to analyze combined loadings acting on the intervertebral joint between vertebrae during these exercises. The mobility of the ribcage, joint angles and joint force were analyzed in the lumbar region using the developed simulation model. At the end of this chapter, the behaviour of one of the scoliosis models that underwent the surgery was compared with its behaviour before the surgery.

5.2 Musculo-skeletal human-body modeling in dynamic exercises, lateral bending, flexion and axial rotation

Flexibility of the spine is determined by the capability of the spine to bend sideways (lateral bending), forward/backward (sagittal bending), and to rotate (twist in transverse plane). In order to function safely, the range of deformation (motion) is limited by biomechanical constraints (beyond which the subject may feel pain or permanent damage). Bending (forward/backward or lateral) applies both compressive and tensile stress (forces) on the spine. For example in lateral bending to left, the right half of the disk (fibers of the disk) is compressed and the left half is under tension (Lundon and Bolton 2001). Lateral bending of the spine is limited by the tensile force of the intertransverse ligament (on the convex side of the spine). These forces confine the range of motion and maintain the stability of the spine (see Figure 5.2).

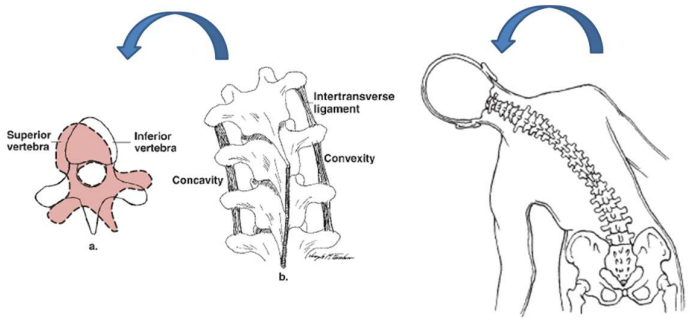

Figure 5.2 Lateral flexion task (Pamela K. Levangie 2005)

In the same manner, in flexion, the posteriori components of the spine (muscles and ligaments of the convex side of the spine, and anterior side of the disk) are stretched and the anterior half of the disk is compressed (see Figure 5.3).

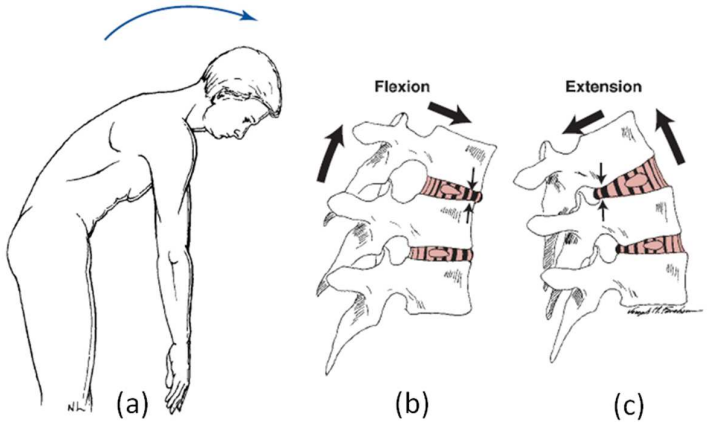

Figure 5.3 Spine in flexion (a) Flexion posture (b) Vertebra in flexion (c) Vertebra in extension (Pamela K. Levangie 2005)

Rotation is basically defined as the twisting (rotating) of the spine around its vertical axis. Among the basic spine deformities, rotation is more critical as it is associated with most of the back injuries. Because of the way that the vertebrae are articulated together, rotation of the spine is always accompanies with a secondary lateral bending of the spine to one side. The internal and external oblique abdominal muscles are the main muscles driving the rotation motion of the spine. This motion is constrained by so called "spine torsional stiffness". Intertransverse ligaments (see Figure 5.4), the outer layers of the vertebral bodies, and intervertebral disks, as well as the way that the vertebrae are articulated at the facet joints are the main factors contributing in the spine torsional stiffness (Klein and Hukins 1983). While the torsional stiffness of the joints of upper thoracic region (from T1 to T6) is almost similar, it increases in the region between T7/T8 to L3/L4 joints.

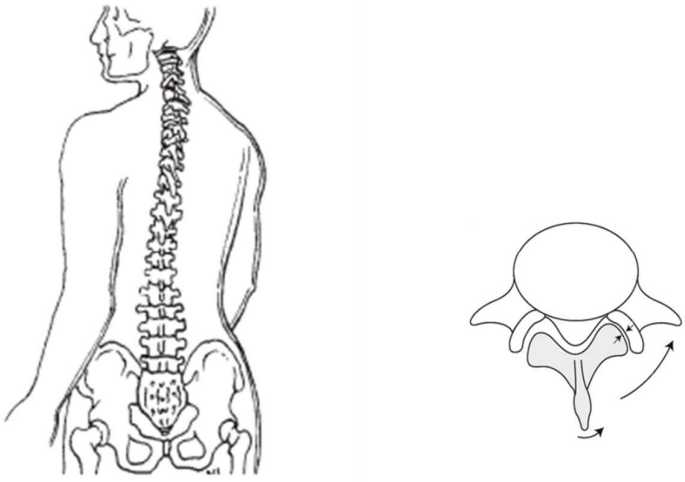

Figure 5.4 Spine in axial rotation (a) Axial rotation Posture (b) Vertebrae rotates toward the right (Pamela K. Levangie 2005)

5.2.1 Description of the human subjects studied in this work

Two normal subjects, one male and one female, and two scoliosis subjects, one female with thoracolumbar scoliosis spine with convexity to the right side and one male with thoracolumbar scoliosis spine with convexity to the left side participated in this study. The anthropometric data of the four subjects are shown in Table 5.1. In this table the scoliosis subjects (patients) are referred to as PT1 and PT2. Subjects gave informed consent to participate in this experiment, which was approved by *The University NHG Domain*

Specific Review Board (DSRB). Subjects performed three sets of tasks: (1) dynamic lateral bending; (2) dynamic bending forward and (3) dynamic axial rotation. For patient 2 (PT2) data is not available for axial rotation task. These are typical tasks used by clinicians to determine the severity of scoliosis condition. Three trials of each task were performed and the best trial in which most of the markers were visible was chosen to drive the musculoskeletal model.

Table 5.1 The anthropometric data of two subjects used in the experiments

Subject	Gender (f/m)	Age (years)	Height (cm)	Weight (kg)
Normal	F	24	157	49
PT1	F	15	151	41
Normal	M	26	178	70
PT2_before surgery	M	14	158	77
PT2_after surgery	M	15	165	84

5.2.2 Experimental procedure

In this study, the subjects were asked to perform lateral bending, bending forward and backward and axial twisting tasks in a serial manner, starting with upright posture, then bending/twisting, going back to upright standing, bending/twisting and going back to upright posture again. Three independent trials of each task were conducted to obtain the dynamic motion capture data for each subject.

Plug-in Gait modeling in the Vicon MX system generated the human body modeled segments according to the anthropometric input and the virtual marker trajectories which indicate kinematic and kinetic quantities, such as angles, moments etc. In order to capture the deformity (asymmetry) of the spine in thoracic region of the subject with scoliosis condition, in addition to the marker on T10 (in the plug in gait model) two more markers were attached to T1 and T6. To capture the effect of the curvature of the lumbar region two more markers have been attached to L1 and L5. In addition, to capture the hump two markers are attached to right and left side of the rib cage. Disregarding these changes, the rest of the Plug-in-Gait model remain the same as the conventional one. The output angles for thorax in the sagittal plane for bending forward and in frontal plane for lateral bending were measured and calculated by comparing the relative orientations of two related segments in the plug-in gait model. Figure 5.5 shows the subject during the motion capture

experiments in order to obtain the dynamic motion data, including upright standing, left and right lateral bending, twisting and forward and backward bending postures.

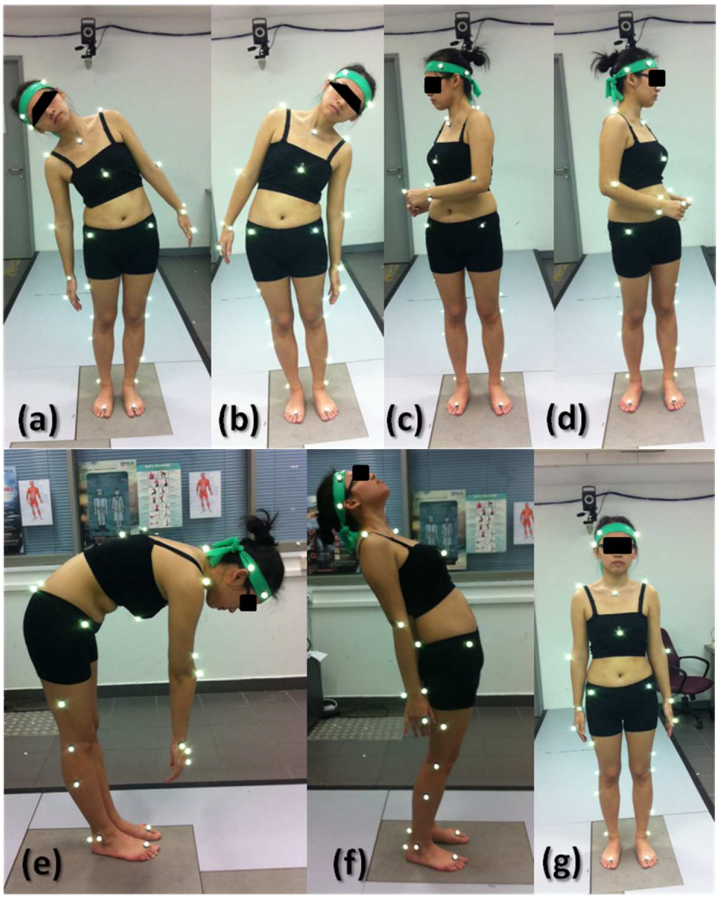

Figure 5.5 Different postures (a) Right lateral bending (b) Left lateral bending (c) Right axial rotation (d) Left axial rotation (e) Bending forward (f) Bending backward (g) Upright sitting posture

After conducting the experiment in gait lab and processing the motion data, an SLF file which is exported from *Nexus* was used to create the human body model from the measurements and to create motion from recorded motion data. This file contains information about the subject name, gender, age, height, weight and the motion trajectory data. *LifeMOD* uses this information to extract body segment measurements and mass properties from its internal anthropometric database. After building the musculoskeletal model, the motion agents of the subjects were added to the model to drive the muscles. In the *LifeMOD* model, during the simulations the markers were attached to the skin; therefore we can use the markers' trajectory without any compensation to drive the musculoskeletal

model in *LifeMOD*. For this model, passive joints were created for the inverse-dynamics simulation. These joints were used in an inverse dynamics analysis to record the joint angulations while the model was being manipulated by motion agents. The motion agents were later removed and replaced with servo actuator (torque generators) for the "trained" phase. The results may vary with change of the physical conditions of the subject. A possible explanation is that in these experiments, the subjects were asked to bend as much as possible (to stop the activity before they feel pain). Conducting *in-vivo* experiments to measure the intradiscal pressure, many researcher have demonstrated that the intradiscal pressure may vary among the subjects with the same anthropometric data (McGlashen 1987, Sato K 1999). To produce smooth response for both of the inverse-dynamics and forward-dynamics simulations, an equilibrium simulation was initially performed. This is a dynamics analysis which holds the positions of the data-driven motion agents fixed, while finding the minimum energy configuration in the springs of the motion agents.

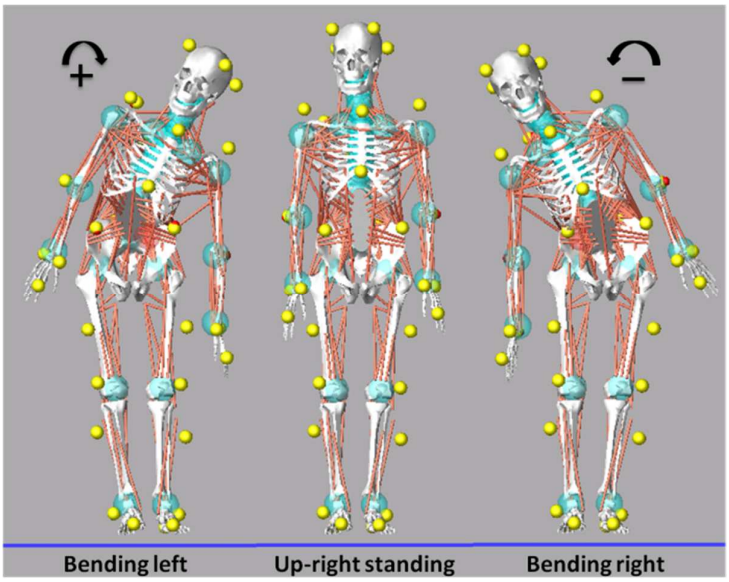

Figure 5.6 Musculoskeletal body model trained by motion capture data in inverse dynamic analysis

Figure 5.6 shows the model in lateral bending experiments after equilibrium analysis in which the markers are attached to the model. The stiffness and damping values of the connecting elements between motion agents in *LifeMOD* and imported motion agents from Vicon in equilibrium and inverse dynamics analysis were obtained in such a way that the compression load in the lumbar joints in upright standing is in the acceptable range of 0.8 to 1.2 times of the subject body weight (Nachemson 1966, Khoo, Goh et al. 1995).

After equilibrium analysis, the contact constraint was added to the simulation model and the inverse dynamics simulation was performed for each model. The joint angle histories recorded from the inverse-dynamics simulation were used later in a PD controller to produce torques to recreate the motion histories. During this analysis the muscle contraction histories were recorded as well. The process entails removing of the motion agents and updating the joints to include the proportional-differential (PD) controllers or "trained" joints and the muscles to include the proportional-integral-differential (PID) controllers or "trained" muscles. With the trained joints and muscles (based on the recorded motion from the inverse-dynamics analysis), the model is now ready for forward dynamics simulation. Using this approach, three bending motion activities in normal and scoliosis models were simulated and the force distribution of the scoliosis and normal models at the lumbar joints were compared together. In addition, activities of the back, abdomen and neck muscle groups of the scoliosis and the normal models in lateral bending motion were compared.

5.3 Results and discussion

5.3.1 Lateral bending

5.3.1.1 Investigating the mobility of the scoliosis spine

Differences between simulated and experimental data were determined for maximum angle of left and right bending in order to assess how well the simulation tracked the experimental data. From the obtained motion capture results, the bending angle in the normal case was at least 20 degree greater than that of the scoliosis case. In other words, rib or spine flexibility in the normal case is higher than the one with scoliosis. This confirms that the scoliosis subject experiences less mobility as compared to the normal one (Mahaudens, Banse et al. 2009). Figure 5.7(a) shows the thorax angle in lateral bending motion for normal and scoliosis female subjects which were obtained from Mocap data. The results of angular displacement of the ribs in scoliosis and normal models were also in agreement with the previous findings which predicted less flexibility of the scoliotic spine as compared to the normal one. Figure 5.7(b) shows the thorax angle in lateral bending motion for normal and scoliosis female subjects which were obtained from computational model. As depicted in this figure, the findings from computational modeling can be validated by comparing the results with those obtained from Mocap experiments. The variation between the angles obtained from computational model and those of Mocap data is in the range of

±1 degree which lies within an acceptable range (Goodvin, Park et al. 2006). The thorax angles follow the same trend in left and right side for both models. Results obtained from four healthy subjects shows that the bending degree in left and right bending are not the same for all subjects and the thorax angles in the right side bending is about seven degrees greater than that in the left side bending. This behaviour can be attributed to the difference between the strength of muscles in the left and right sides.

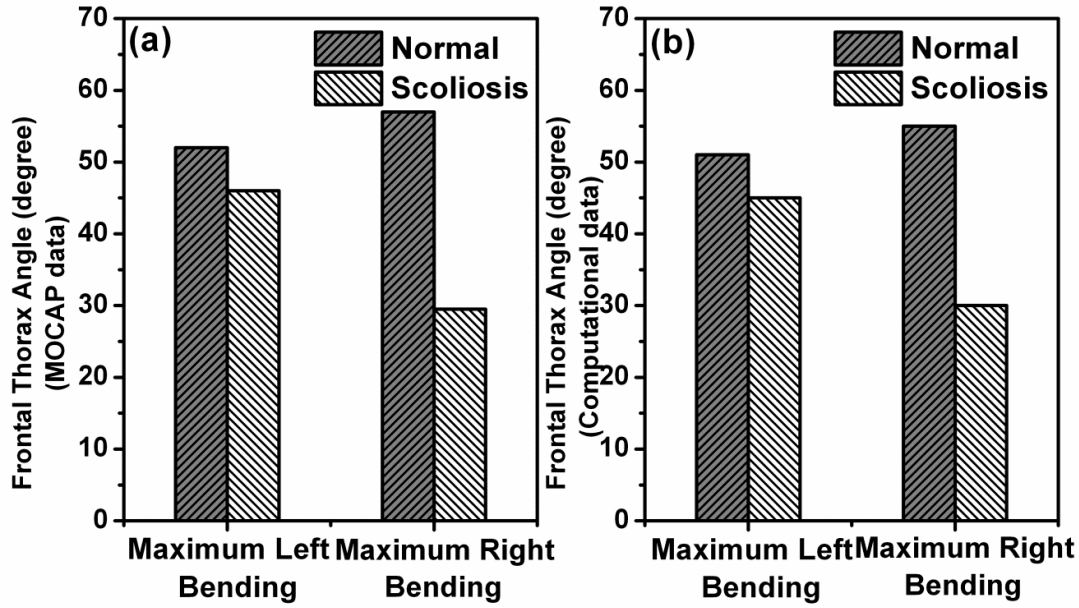

Figure 5.7 Thorax angle in frontal plane (a) data from the motion capturing data, (b) data from computational analysis

5.3.1.2 Evaluation of the muscle activity in lateral bending motion

The muscle strength is defined as the maximum force that a muscle can generated. The muscle activity represents the percentage of the maximum force that the muscle is producing. This activity can be assumed as a constant for the whole muscles which are considered in the model. Therefore, the muscle activity is defined as a value between 0 and 1.

When the load exceeds the strength of the muscles in the model, the inverse dynamic analysis returns to the maximum muscle activation value of 1. If the muscle configuration is insufficient to balance the load even with overloading of the muscles, the inverse dynamic analysis will fail. This means that omission of some muscles in the model may

lead to inability to complete the analysis, even when these muscles can be presumed not to carry loads that are important to the overall balance of the spine.

According to the simulation results, the muscle activation values in the scoliosis model are higher than that of the normal one in both female and male subjects. The effect of posture on the muscle activity was more pronounced for abdominal and erector spinae muscle groups. In this exercise, muscle activation of the neck, back and abdomen groups were obtained. Figure 5.8 shows the back view of these three muscle groups.

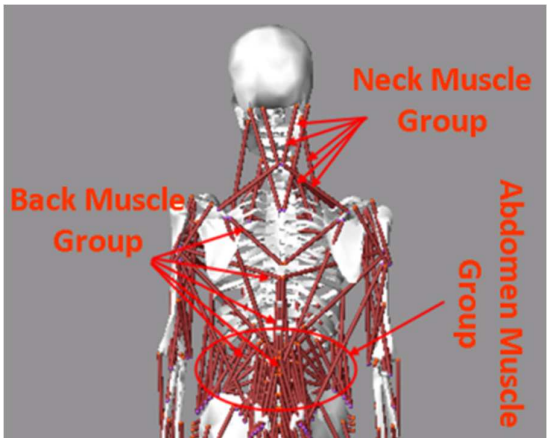

Figure 5.8 Back view of the neck, back and abdomen muscle groups

These muscle groups consist of the muscle sets that are depicted in Table 5.2. According to the results, in the scoliosis model, the activity of abdomen and neck muscle groups in the left and right bending are higher than those of the normal model.

For the female scoliosis model (PT1) in which the apex of the spine curvature was toward the right side of the center line, the muscle activity in the right side was higher than that of the normal subject. On the other hand, the muscle activity in the left side was less than that of the normal subject. Similarly, in the male scoliosis model with the apex of the spine curvature on the left side, the muscle activity in the left side was higher than that of the normal one and the muscle activity in the right side was lower than that of the normal one. In other words, this trend was observed that the activities of the back muscles of the side at which the apex is located is always higher than the muscles of the opposite side and also is higher than the activities of the muscles of the normal case. This behaviour can be attributed to imbalance mass distribution of the body in the scoliosis spine (mass distribution is more towards the apex) and also due to the change of the spine lateral stiffness because of the scoliosis deformation. Based on the obtained results, for the scoliosis cases, the bending

stiffness of the spine to bend to the convex side of the spine has increased which poses a higher muscle activity to bend the spine to the convex side (the side at which the apex is located).

Table 5.2 Abdomen, back and neck muscle groups

Abdomen muscle group	Back muscle group	Neck muscle group
Rectus abdominis	Erector spinae	Scalenus Anterior
		Scalenus Posterior
Obliquus Exenus abdominal	Qudratus Lumborum	Scalenus Medius
		Splenius Cervicis
Obliquus Internus abdominal	Multifidus	Splenius Capitis
	Psoas Major	Sternocleidomastioeus

The results imply that due to the asymmetry of the spine, the muscle activation in the scoliosis model is much higher than that of the normal one, although there appears to be little difference between right and left bending.

5.3.1.3 Comparison of the force distribution in the lumbar region of the normal and scoliosis models

The joint forces were obtained for four models and three trials for each model during the simulation. The pattern of the joint force in all three trials of each model was very similar but the values were slightly different. For example, the duration of each step in the trials was not exactly the same which could slightly influence the results.

Low-back pain is one of the most common musculoskeletal problems which frequently occur at the lumbar region. In the lumbar region, lumbosacral junction (L5/S1) is the most prone joint to back injuries. The main reason is that this region and particularly this joint are subjected to a great amount of joint forces (as a reaction to the body weight and tension of muscles and ligaments).

This was the motivation to study the combined loadings in the lumbar joints and more specifically in the lumbosacral (L5/S1) and L4/L5 joints in this part of the work. Figure 5.9(a)-(c) shows the average compressive load, lateral shear force, antero-posterior (A/P)

shear force and magnitude of force on the lumbosacral and L4/L5 joints during the simulation for normal and scoliosis female models.

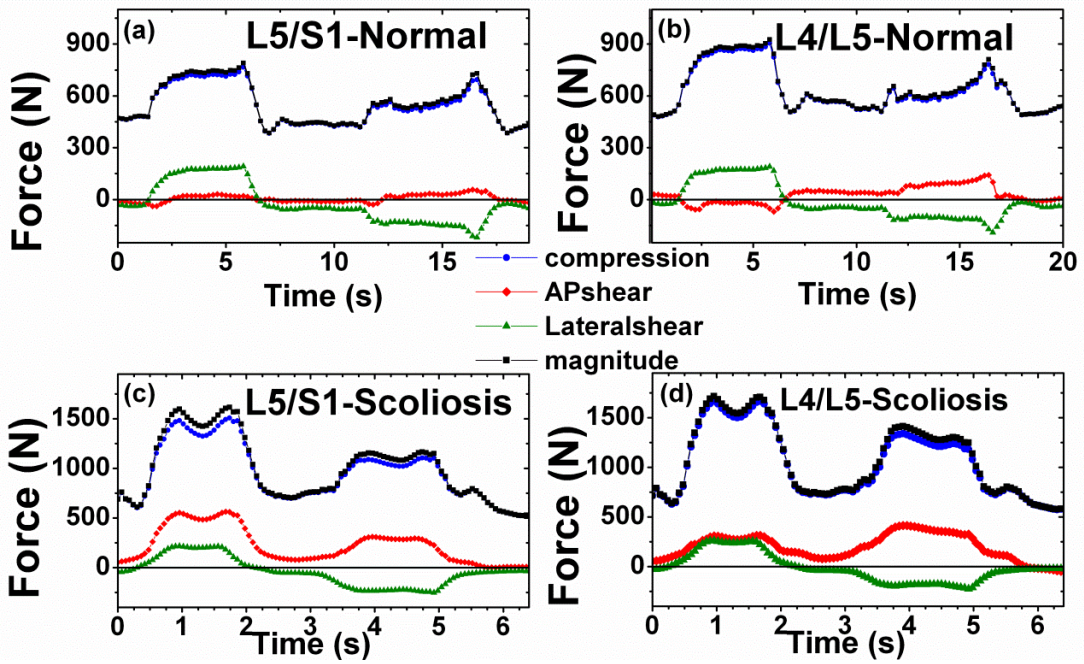

Figure 5.9 Average joint forces: in the normal female model at (a) L4/L5 joint and (b) lumbosacral joint; in the scoliosis female model at (c) L4/L5 joint and (b) lumbosacral joint

As can be seen in Figure 5.9, the maximum joint force on lumbosacral joint and L4/L5 joint in the normal female model in the left bending is around 700±50 N and 800±50 N and in right bending 600±50 N and 650±50 N respectively. It seems that, the muscles in the left side of the normal subject are stronger than the right side and can reduce the force on the vertebrae in the right bending as compared to the left bending.

In the scoliosis female model, the maximum lumbosacral joint force in left bending is 1400±50 N and significantly higher than the joint force in the right bending, which is 1050±50 N. Furthermore, the joint force in the left and right bending in L4/L5 joint is 1550±50 N and 1300±50 N, respectively. Simulation results indicate an error of less than 1° in joint angle which is acceptable.

These findings can be explained with the help from X-ray images of the patient in the left and right bending postures (see Figure 5.10). As can be seen in the left bending, the mass distribution from the line of gravity (LoG) is larger than the one in right bending posture. Gravitational vector which is also known as line of gravity (LoG) is a downward vector

(perpendicular to the earth surface) in the direction of the gravity force acting on the body. In the upright position of the normal spine, this line lays on the spine axis. However, deformity of the spine results in an offset between the spine axis and the LoG which consequently imposes a momentum on the spinal joints. The first tendency of this moment is to make the spine unstable. In order to maintain the stability of the spine, the muscles and ligaments have to apply forces (higher tension and muscle activities) to the spine to cancel this moment. This results in more energy consumption and higher compressive loads on the spinal joints (Pamela K. Levangie 2005).

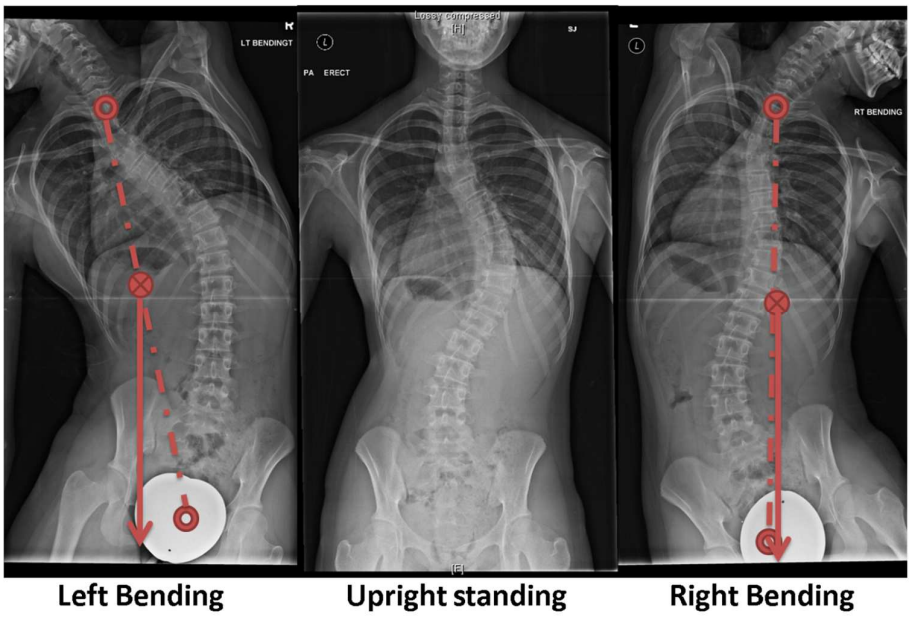

Figure 5.10 X-ray images of the scoliosis female subject in bending right and left postures

The joint forces for each model include compressive force, lateral shear force, and A/P shear force. The variation of magnitude forces at the lumbar region (average of the force over time) normalized by body weight in upright standing, right and left bending postures are shown in Figure 5.11 and the average joint forces (normalized by body weight) at the lumbar joints in the normal model in left bending, standing and right bending are summarized in Table 5.3.

In addition to the gravitational moments which result in increased muscular activities and tension of the ligaments, generally, any asymmetric body deformation may disrupt the optimum body alignment and interrupt the performance of the muscles and ligaments. The main consequent of such condition is abnormal weight bearing distribution which results

in abnormal compressive force on one side and excessive tensile force on the other side of the joints (Pamela K. Levangie 2005).

Table 5.3 Average joint force values in the lumbar joints in the female normal model

Joint force /body weight		L5/S1	L4/L5	L3/L4	L2/L3	L1/L2
Female (49×9.81)	Left bending	1.54	1.84	1.79	1.51	1.45
	Upright standing	0.92	1.19	1.08	0.89	1.07
	Right bending	1.28	1.44	1.45	1.47	1.68
Male (68×9.81)	Left bending	2.34	2.42	2.68	1.79	1.74
	Upright standing	0.92	1.04	0.94	1.15	0.99
	Right bending	1.32	1.39	1.81	1.74	2.11

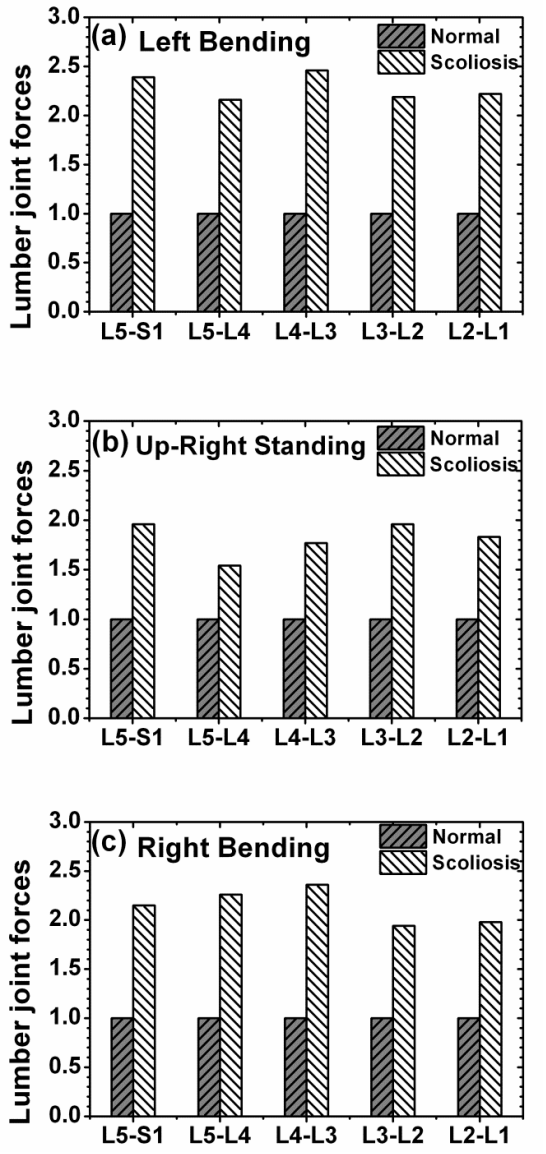

Figure 5.11 The variation of lumbar joint forces in (a) left bending (b) upright standing and (c) right bending in scoliosis respect to the normal female models

Joint forces of the lumbar region of the male subjects were calculated in a similar manner (see Figure 5.12). As can be seen the joint force in scoliosis subject is generally higher than those of the normal one.

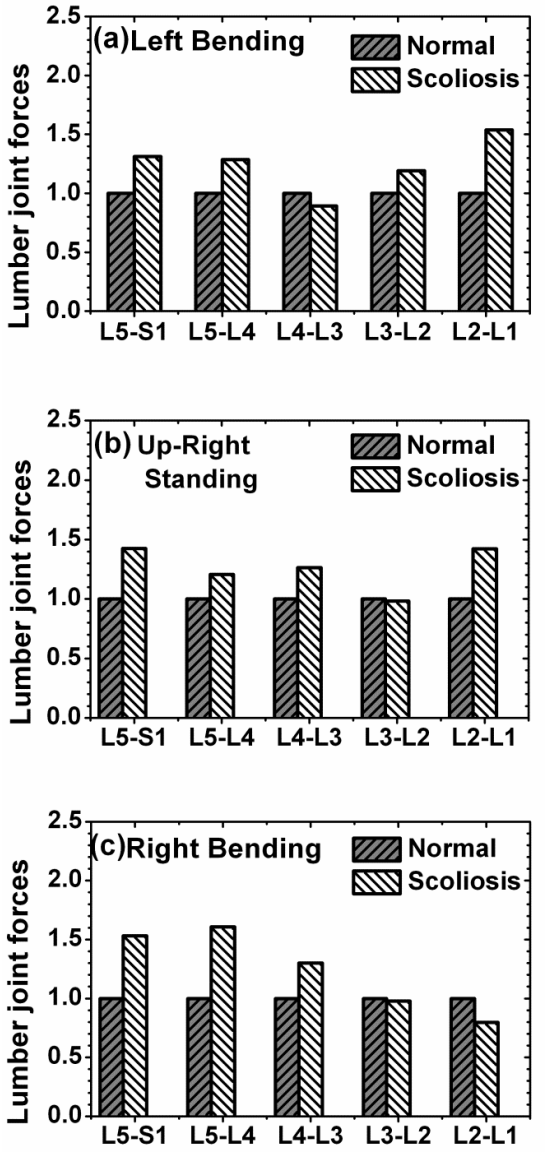

Figure 5.12 The variation of lumbar joint forces in (a) left bending (b) upright standing and (c) right bending in scoliosis respect to the normal male models

The results indicate that the magnitudes of the forces in the scoliosis models are significantly higher than those of normal ones. According to the results, in left and right bending the magnitudes of the lumbar joint forces in the scoliosis model are between 2 to 2.5 times of those of the normal model in female subjects. However this value changes between 1 to 1.5 for the male subjects. This can be explained by looking at the X-ray images of the male subject in lateral bending which is shown in Figure 5.13. As can be seen in this figure, the distance between LoG and centerline is very little and therefore the

gravitational moments are not considerable. In addition, in standing posture the ratio is between 1.5 to 1.9 times for the female models and 1 to 1.4 for male subjects.

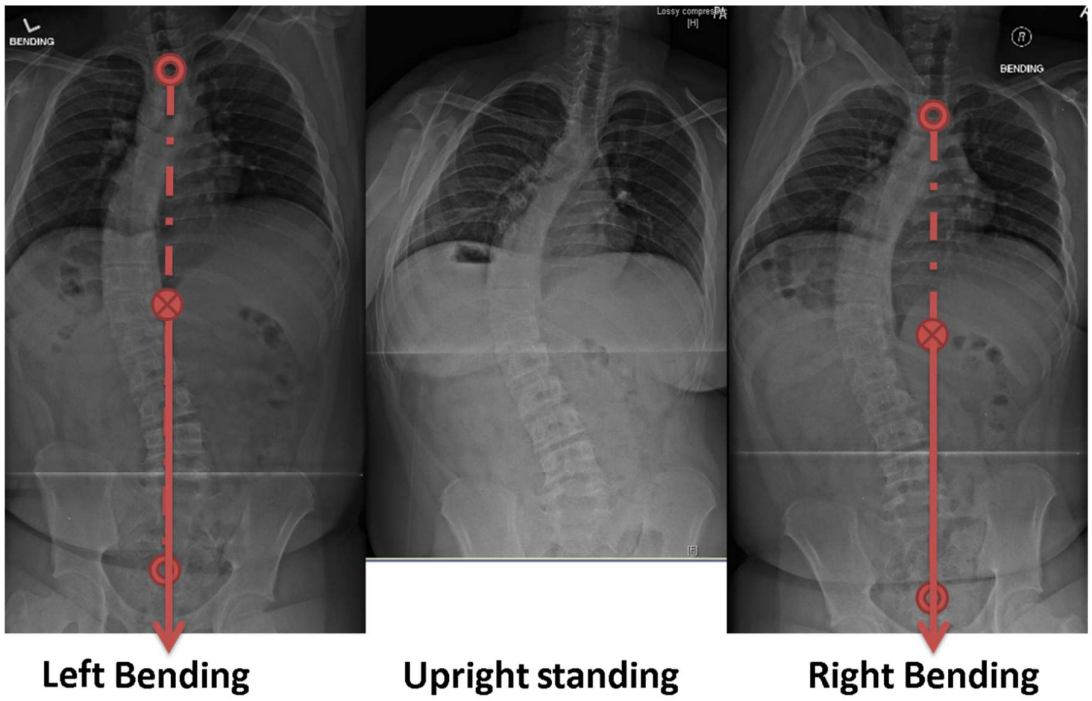

Figure 5.13 X-ray images of the scoliosis male subject in upright standing, bending right and left postures

The upright body position imposes a considerable spinal load due to the weight of the upper body segments. During the change of position, the magnitude of this load dramatically increases (Rohlmann, Petersen et al. 2012). It has been shown that dynamic posture changes impose much higher spinal loads (compression, anterior/posterior and lateral shear forces) as compared to the static positions (Marras and Granata 1997).

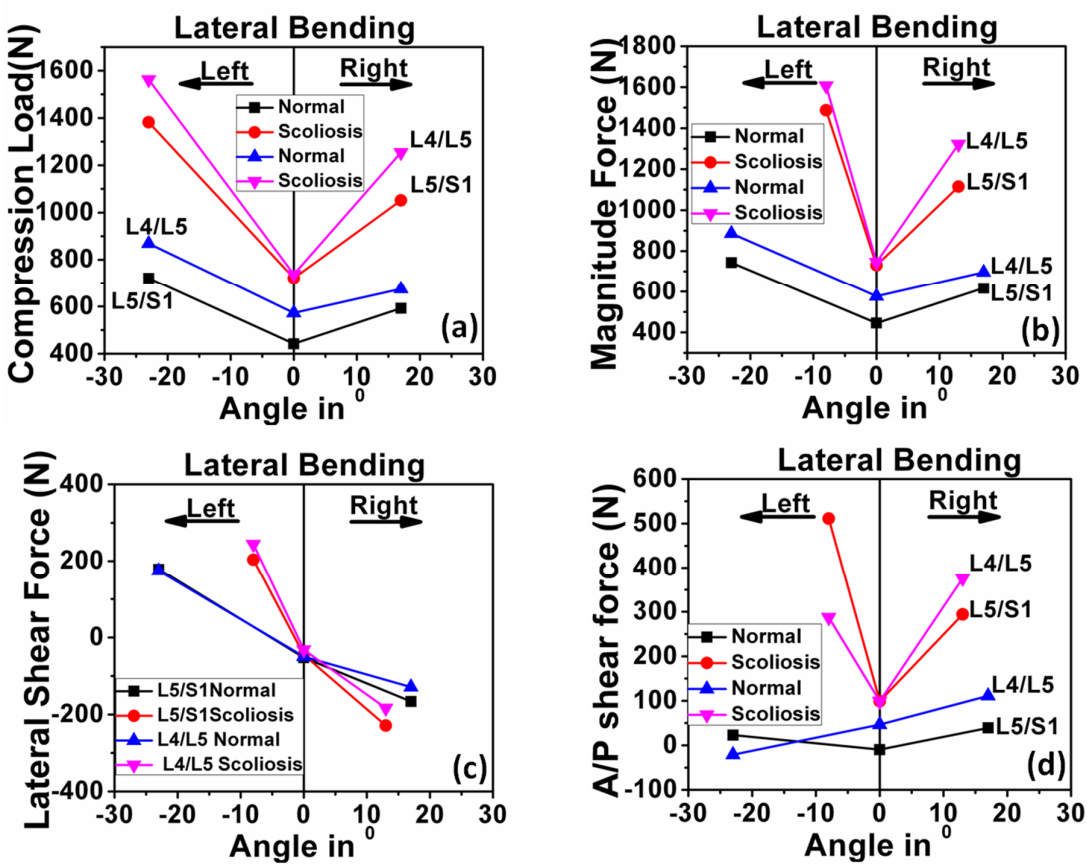

Figure 5.14 Comparison between joint forces in normal and scoliosis female models at L4/L5 and lumbosacral joints (a) Compression load (b) magnitude force (c) lateral shear force and (d) anterior posterior shear force

Figure 5.14 shows the forces in lumbosacral and L4/L5 vertebral joints in the maximum left and right bending and the upright standing postures. From the results, the compression load at lumbosacral and L4/L5 joints in the normal model is around 1±0.1 in upright standing, 1.6±0.1 in left bending, and 1.3±0.1 times of weight of the subject in right bending postures. However in the scoliosis model, the value is 1.8±0.01, 3.6±0.2 and 2.8±0.2 for upright standing, left and right bending postures respectively. Since the motion is in the coronal plane, the lateral shear forces in both models are considerable and close to each other. Similar results can be obtained for male subjects. Figure 5.15 shows the comparison between compression loads in normal and scoliosis male models at L4/L5 and lumbosacral joints.

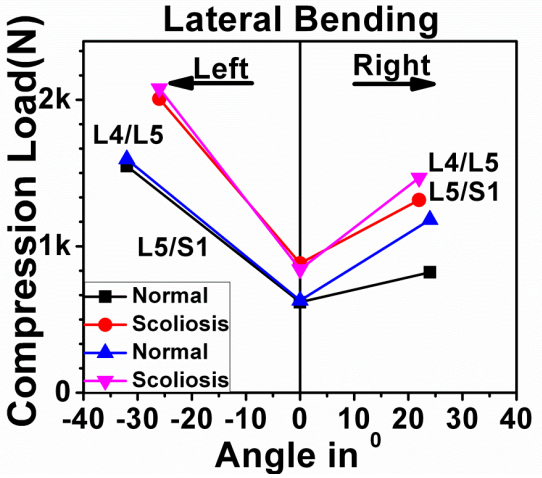

Figure 5.15 Comparison between joint forces in normal and scoliosis male models at L4/L5 and lumbosacral joints

Figure 5.16 shows the normalized lumbar joint force in lateral bending exercise in normal and scoliosis models. According to this figure the bending angle in scoliosis model is smaller while the joint force is considerably higher.

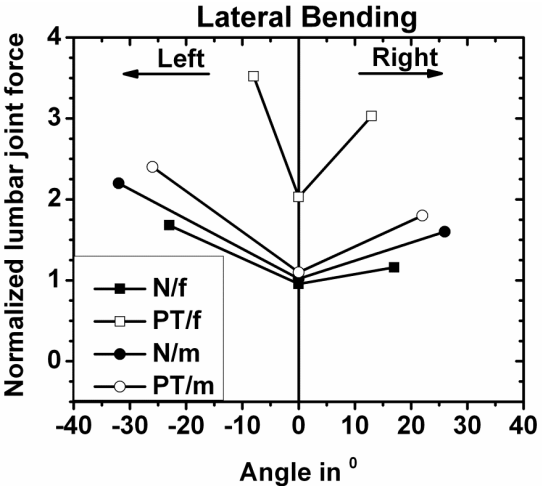

Figure 5.16 Normalized lumbar joint force in normal and scoliosis models (N, PT, f and m represent normal, scoliosis, female and male subjects respectively)

5.3.2 Bending forward/backward

In this experiment, the flexion and extension are quantified by measuring the angle between the thoracolumbar junction and the sacrum in sagittal plane. Flexion is represented by positive values and extension is represented by negative values. (See Figure 5.17)

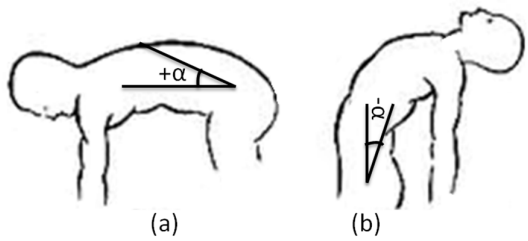

Figure 5.17 Angles in flexion and extension (a) positive in flexion (b) negative in extension

The compression load and shear forces were obtained from the simulation for normal and scoliosis subjects in this exercise. Since the markers on the chest in forward bending cannot be exposed in some frames due to the clothing of the female subjects, to find the position of the markers during flexion, we used some assumption and interpolation points (the position of the lost markers were interpolated based on the methods explained in section 3.8.2). Therefore, the error in flexion is expected to be higher than lateral bending exercise and is about 1.5 degree in joint measurement compare to the 0.2 degree in lateral bending exercise. Figure 5.18 shows the normal subject, model in *Nexus* and model in *LifeMOD* in flexion and extension postures.

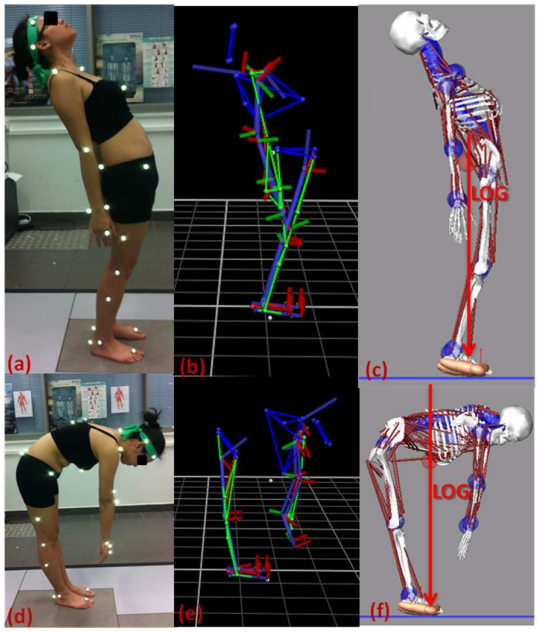

Figure 5.18 (a) Subject (b) Simulation model in Nexus (c) Simulation model in LifeMOD in maximum extension posture (d) Subject (e) Simulation model in Nexus (f) Simulation model in LifeMOD in maximum flexion posture.

As can be seen in Figure 5.18, while in upright standing posture the center of mass of the body lies on the spinal joint axes, in flexion and extension postures it lies anterior and posterior to the spinal joint axes respectively. Similar to the lateral bending, in flexion/extension activity, increasing the distance between LoG and the vertical axis of the spine increases the imbalance mass torque which imposes higher ligamentous tension and muscle activity to retain the body stability. It has to be mentioned that in these experiments, the subjects were not instructed how to perform the activities. Therefore, the subjects performed the activities in the way that they were used to do in their daily life. This causes appreciable variations in patterns of the subjects' activities.

Figure 5.19 shows comparison of the magnitude force on the lumbar joints in maximum flexion, upright standing and maximum extension postures in scoliosis and normal female and male subjects, respectively. The magnitude of the lumbar joint forces normalized by the body weight of the normal subjects was shown in Table 5.4. According to the results, in flexion, compression load and lateral shear forces on the lumbar joints in the scoliosis model are greater and the A/P shear forces are smaller than the normal one. However, in extension, all forces are slightly higher in the normal model as compared to the scoliosis model.

Table 5.4 Joint force on the lumbar region in normal subject

		Joint force /weight				
		L5/S1	L4/L5	L3/L4	L2/L3	L1/L1
Female (49×9.81)	Flexion	2.19	4.31	3.36	2.48	3.03
	Upright standing	1.24	1.74	1.34	1.17	1.55
	Extension	0.95	1.00	1.06	1.06	1.17
Male (68×9.81)	Flexion	3.87	4.62	4.12	3.65	3.41
	Upright standing	0.94	1.00	1.12	1.13	0.96
	Extension	1.6	1.71	1.83	1.74	1.61

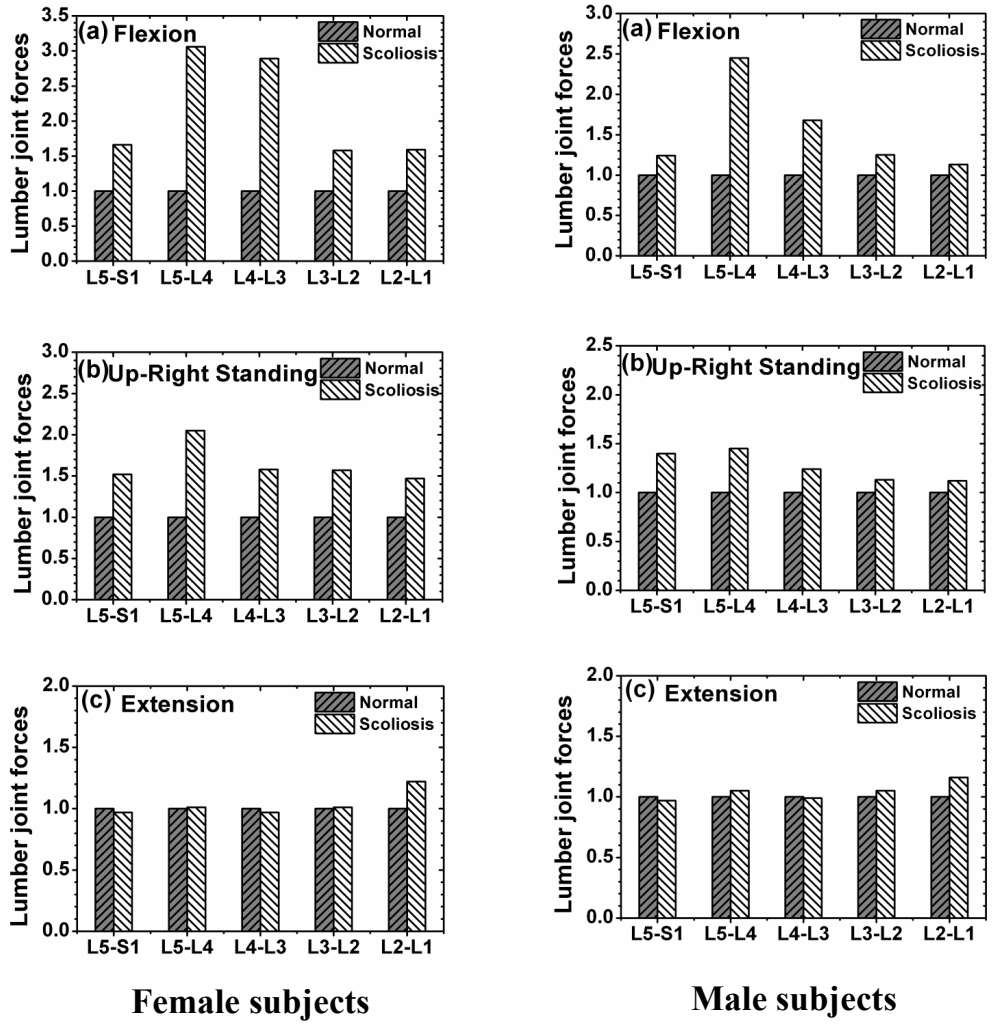

Figure 5.19 The variation of lumbar joint forces in (a) flexion (b) upright standing and (c) extension in scoliosis respect to the normal model (in female and male subjects)

It is found from Figure 5.19 and Table 5.4 that the vertebral combined loadings in both normal and scoliosis increase in forward bending and standing postures. Generally, the magnitude of the combined loadings on the vertebral joints in the scoliosis model is higher than the ones in the normal model during the whole motion.

It is obvious that the maximum compression force is imposed on the spine at maximum flexion angle. In a similar manner, the maximum joint force occurs at the maximum extension (backward bending) angle. Similar to the lateral bending, in flexion/extension activity, increasing the distance between LoG and the vertical axis of the spine increases the torque resulted from the mass imbalance of the spine. This torque consequently imposes higher ligamentous tension and muscle activity to retain the body stability.

Monitoring the loads of the lumbar joint in the bending motion (forward to backward bending), it was understood that that the minimum joint force takes place at the extension angle of -8° and -5° for normal female and male subjects respectively. However, for scoliosis female subject, the minimum value of the lumbar joint force is at maximum extension at the angle of -25° (see Figure 5.20). This result clearly shows the effect of spine deformity on the loading conditions of the spine in dynamic motion of the body.

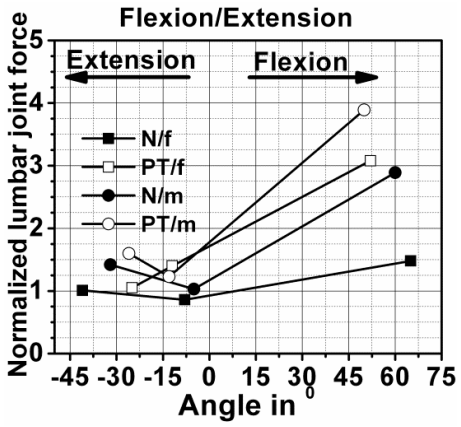

Figure 5.20 Normalized lumbar joint force to the subject's weight in maximum flexion and extension of normal and scoliosis models

5.3.3 Axial Rotation

In this section, the subjects were asked to perform axial rotation exercise while standing. This experiment was only performed for the female subjects. The simulation models of *Nexus* and *LifeMOD* in three postures of maximum left and right rotation as well as upright standing are depicted in Figure 5.21.

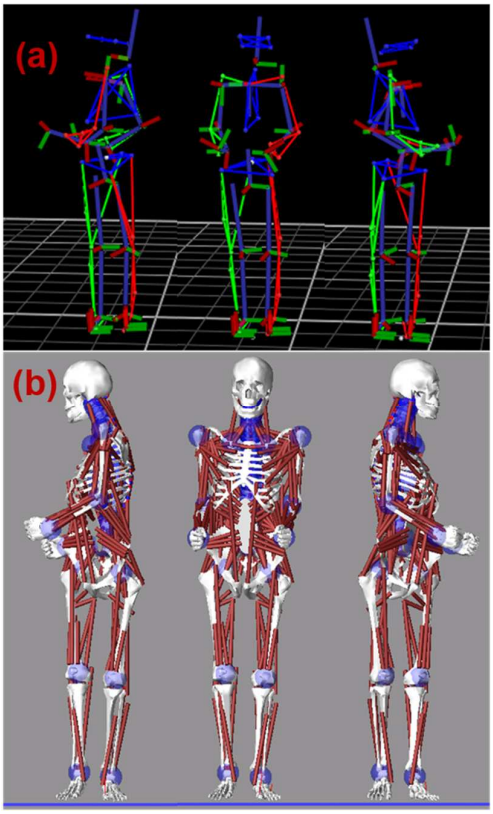

Figure 5.21 (a) Simulation model in *Nexus* (b) Simulation model in *LifeMOD* in maximum left rotation posture, maximum right rotation posture and upright standing posture.

The magnitude of the lumbar joint forces normalized by subject's weight in the normal model was shown in Table 5.5. Figure 5.22 shows the magnitude force on the lumbar joints at maximum left rotation, upright standing and maximum right rotation postures in scoliosis subjects and compares them to those of normal spine (the magnitude of each force is normalized based on the load of the same joint in the normal case). According to the results, in rotation exercise, the force magnitude at the lumbar joint in the scoliosis model is higher than the normal one.

Table 5.5 Magnitude joint force in lumbar joints in the normal model

	Joint force /weight (49×9.81 N)				
	L5/S1	L4/L5	L3/L4	L2/L3	L1/L1
Left rotation	0.92	0.97	1.10	1.03	1.05
Upright standing	1.15	1.16	1.30	1.10	1.20
Right rotation	0.90	1.10	1.28	1.05	1.25

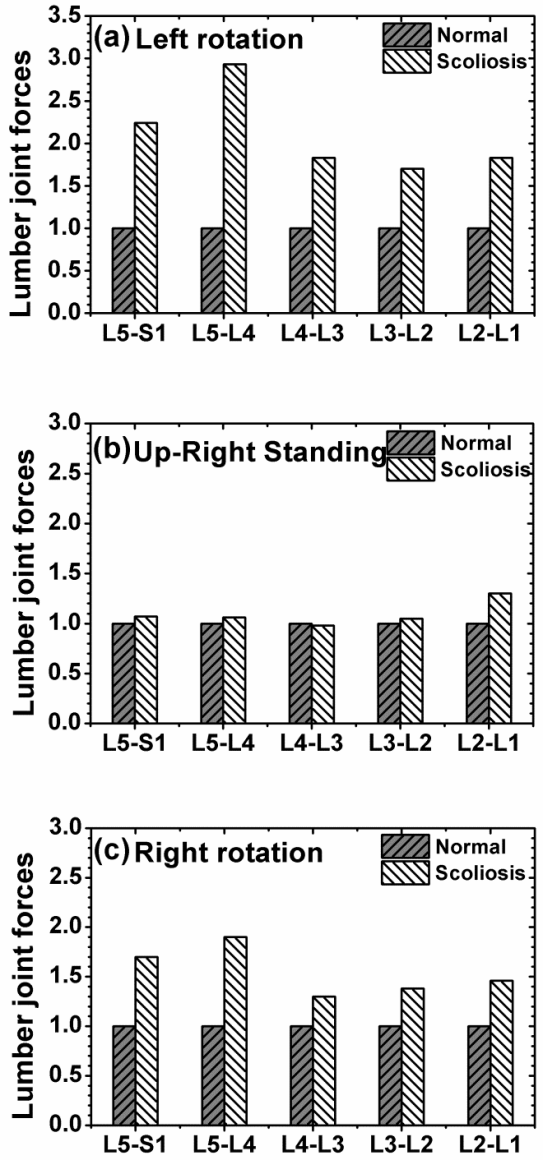

Figure 5.22 The variation of lumbar joint forces in (a) Left rotation (b) upright standing and (c) Right rotation in scoliosis respect to the normal model

5.3.4 Discussion

Any possible movement of the spine is a combination of the flexion and extension, lateral bending, and rotation motions. During the flexion/extension no torsional or lateral force is imposed to the spine. However, there is no pure rotation or pure lateral flexion and in each case any of the other basic motions has to take place (White and Panjabi 1990, Cholewicki,

Crisco III et al. 1996). This coupled motion results in a combined force condition. This necessitates developing a simulation model capable of incorporating the effect of different motion modes and measuring combined loading on the spine. The main goal of this chapter was to develop a simulation human body model with scoliosis spine condition to study the combination of dynamic loadings due to the regular basic daily activities i.e. flexion and extension, lateral flexion, and rotation.

A magnitude force (compression load and shear forces) between 0.8 and 1.7 times of body weight for normal subjects and 1.3 to 3.2 times of the body weight for scoliosis subjects was obtained from the simulation results for the lumbar joints. These values were in the range of compression forces of moderate loading conditions reported in the literature (Wilke, Neef et al. 1999, Arjmand, Gagnon et al. 2009, Rohlmann, Zander et al. 2009).

Based on the analysis performed with the use of inverse and forward dynamics simulations, flexion, extension, lateral bending and axial rotation impose different loads (different magnitude) on a certain intervertebral (L5/S1) joint. According to the results, joint forces in these four postures were between 90 to150 percent of the body weight for normal model and between 95 to 320 percent of the body weight of the scoliosis model. Figures 5.23 to 5.25 indicate that in flexion, lateral bending and axial rotation, the joint force increases in the scoliosis female models as compared to the normal one. However, in extension posture, L5/S1 joint force of the scoliosis model is smaller than that of the normal model. The values are normalized by joint force values of normal and scoliosis models in up-right standing phase. As can be seen in these figures, in most of the non-standing postures (forward and lateral bending and rotation), which are all very common postures in the daily life, lumbar intervertebral joints experience much higher forces as compared to the upright standing. This increase is more pronounced in the scoliosis cases implying that in a similar daily activity, the patient with scoliosis spine has to spend more energy (muscle activity) to maintain its position and may experience more pain due to fatigue of the muscles. In addition, since the value of the intervertebral joint forces represent the amount of load on the intervertebral disk, a higher amount of load increases the risk of disk deformation/regeneration or rupture in the scoliosis case which is the main source of back injury in both normal and scoliosis cases.

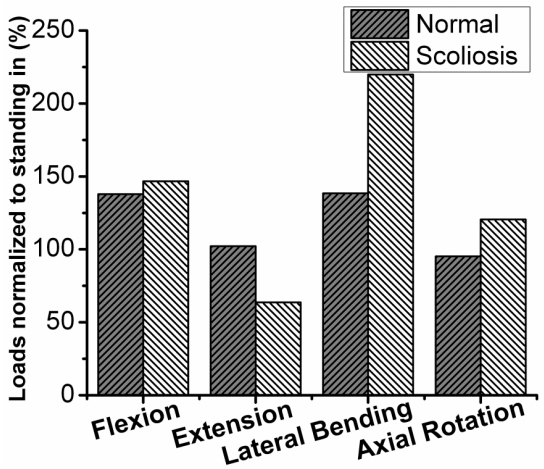

Figure 5.23 Loads normalized by standing in normal and scoliosis female models at L5/S1 joint

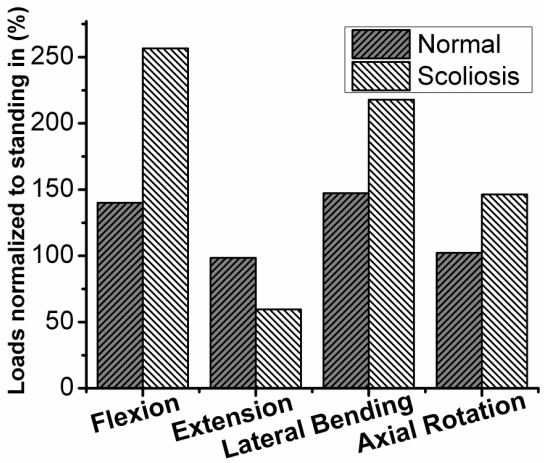

Figure 5.24 Loads normalized by standing in normal and scoliosis female models at L4/L5 joint

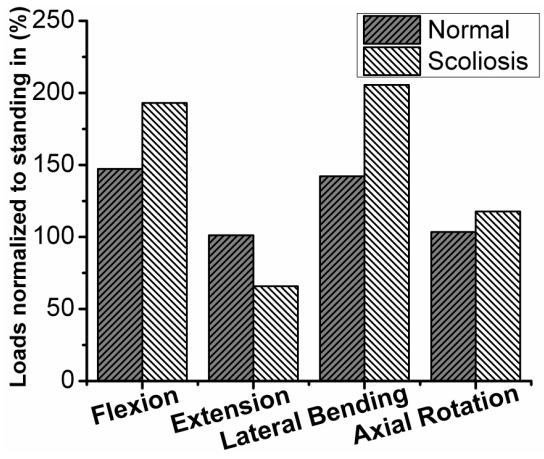

Figure 5.25 Loads normalized by standing in normal and scoliosis female models at 5 lumbar joints

This study is able to help the users (orthopedic surgeons, physiotherapists, etc.) to gain a better insight into the spinal load conditions of the subjects with scoliosis conditions in different postures. The method presented in this chapter can be used to determine (estimate) the load conditions of any other joint(s) of the spine.

5.4. Investigating the effect of corrective spine surgery on dynamic behaviour of the spine after surgery

By acquiring the motion data of the patient performing the same test exercises (movement tasks) before and after the surgery, the effect of the correction surgery on the biomechanical factors such as range of motion, joint forces, and muscle activation can be investigated. For this purpose, the motion results and X-ray images of the patient (PT2 as described in table 5.1) before and after the surgery was used to construct the multi-body model in *LifeMOD*. The subject was also asked to perform the basic movement exercises to record his body motion using the motion capture technique.

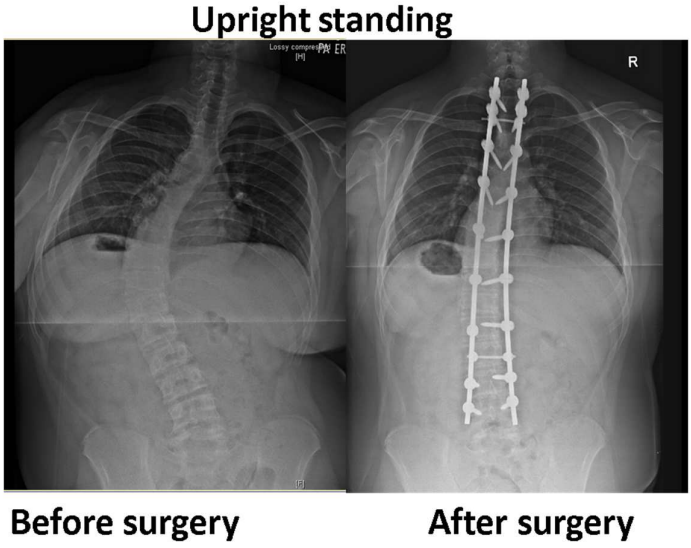

Figure 5.26 X-ray image of PT2 with scoliosis spine before and after instrumentation surgery. The convexity of the spine was to left side.

One year after the surgery, the scoliosis patient was asked to return to the clinic for follow up checkups. In this session, X-ray imaging and gait analysis motion capture analysis for the similar basic motion activities were acquired again. X-ray images of the subject before and after the surgery are shown in Figure 5.26. These results were analyzed to assess spine

curvature, lumbar joint forces and movement of the patient after the surgery. In this section, the main work was focused on analyzing the output of the surgery process by modeling the spine in the virtual environment and finding the reaction forces in the lumbar region and also the flexibility of the body after the surgery. The simulation results were compared to those obtained before doing the surgery.

Similar to the previous cases, the amplitude of the lumbar joints forces was studied before and after the surgical treatment. Figure 5.27 shows the lumbar joint force values for scoliosis male subject before and after the surgery in the left/right (lateral) bending exercise. These values have been normalized based on the body weight of the subject before and after the surgery.

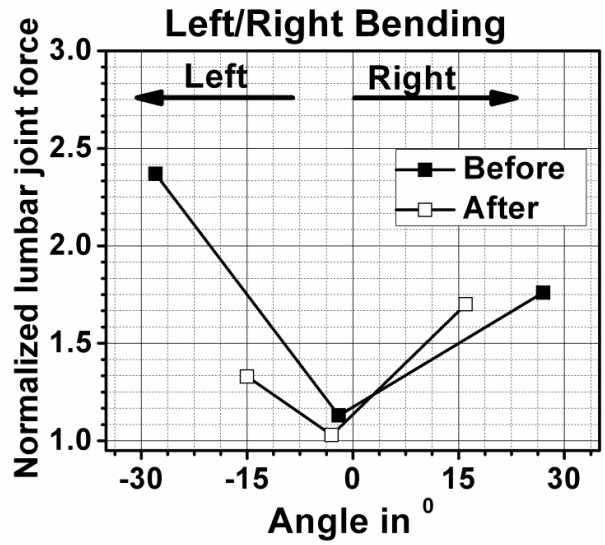

Figure 5.27 Joint forces in lumbar region of the patient doing the left/right lateral bending before and after surgery.

The effect of the instrumentation for correction of the spine curvature can be observed from two points of view. As can be seen in Figure 5.27, instrumentation has decreased the lateral bending range of the motion of the subject to about half of the range before the surgery. This behaviour can be directly attributed to the addition of the rigid implants which has connected the vertebrae together and reduced the general motion flexibility of the spine. From joint force point of view, the magnitude of the joint force in the right side bending task has not changed. However, the joint force in the left bending (toward the convexity of the spine) has dramatically decreased after the surgery. This result clearly shows the corrective effect of the surgery to decrease the loads applied to the joints due to the

abnormal spine deformity. From this result, it can be inferred that while the patient may not feel any changes in the activities comprising right bending, now he feels a considerable change (more comfortable) in doing activities comprising left bending. In the past, an abnormal extra muscle contraction was needed to make the spine bend toward the convex side which could result in fatigue muscle pains. However, by correction of this deformity, these unwanted contraction forces are also relieved which results in less joint forces in the lumbar region (less potential back pain) and also makes the patient may feel more comfortable doing the right bending.

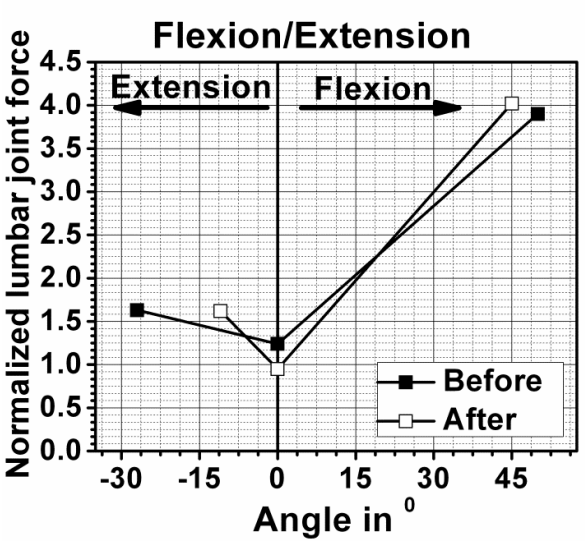

Figure 5.28 Joint forces in lumbar region of the patient doing the flexion/extension bending before and after surgery.

Similar analysis for the flexion/extension task before and after the instrumentation treatment was performed (Figure 5.28). In contrast to the lateral bending task in which the limitation of the lateral motion range was symmetric, in flexion/extension the correction surgery cause more limitation in the extension after the surgery. It can be inferred from this result that the instrumentation has increased the stiffness of the spine which consequently limits the magnitude of the extension. However, as can be seen in Figure 5.28, the effect of the surgery and correction of the scoliosis curve on the lumbar joint force in the forward bending is negligible. This difference can be explained in terms of the nature of forward and backward bending. In backward bending, the main source of movement is because of backward deflection of the spine. However, in forward bending, the major portion of the bending angle is because of pelvic flexion and contribution of the spine flexion is

secondary. Since the instrumentation is not directly affecting the pelvic joint, its effect on the range of forward bending is negligible.

5.5. Summary

A fully discretized bio-fidelity simulation model for analysis of scoliosis conditions in various patients was built. In this chapter the effect of thoracolumbar scoliosis condition on spinal angles, muscle activation and joint forces was investigated by the application of motion data capturing and virtual musculo-skeletal modeling in flexion, bending and axial rotating exercises. The scoliosis subjects who participated in this study had thoracolumbar scoliosis. A comparison between the obtained results from the scoliosis subjects and normal subject with the same anthropometric parameters, conducting the same tasks can be summarized as:

- Joint forces in the scoliosis subjects are greater than the normal one.
- Muscle activation in scoliosis subjects is higher than that of the normal one and it relates to the direction of curvature (convexity) of the spine
- The range of motion (bending angle) in scoliosis subjects is less than that of the normal ones

The results of this study showed that the mobility of the spine in the scoliosis model was less as compared to that of the normal model with the same anthropometric data. Furthermore, the resultant forces and moments at the lumbar joints in the scoliosis model are considerably higher than the loads of normal model in all bending exercises. This finding may lead to a better understanding of the corresponding pains during some activities in scoliosis subjects.

Finally the model was used to study the effect of corrective surgery (to improve the scoliosis deformity) on the lumbar joint force and range of motion. According to the simulation results, the instrumentation (corrective surgery) has limited the range of the motion of the spine in both of the forward and lateral bending activities. The effect of the instrumentation on the lumbosacral joint forces in the lateral and backward bending is more pronounced due to change of the spine stiffness. This effect is not considerable in the forward bending task because in this task the bending is mainly done through flexion of the pelvic joint rather than flexion of the spine. This model is versatile enough to study the response of the spine to these basic motions before and after the corrective surgery. This

simulation tool can potentially be used to predict the effect of the surgery by making a model of the spine based on the proposed corrective surgery plan. This enables the surgeon to gain better insight about the potential outcome of the surgery and allows him to refine/correct the surgery strategy to obtain the best results.

Chapter 6: Conclusion

Scoliosis is a complicated condition characterized by a lateral curvature of the spine and accompanied by rotation of the vertebrae about its axis. Although scoliosis can be treated by methods such as vertebral fusion and using surgical instrumentation, the biomechanical understanding of the surgeons about scoliosis condition is still limited, the treatment methods are not optimized and their outcomes cannot be predicted yet.

Most of the previous works in the field of biomechanics of the spine (and scoliotic spine) comprised of complicated reconstruction methods to develop a 3D model of the spine. In these methods, a complete new model had to be constructed for each specific patient which made it a very time consuming approach that cannot be used for a large group of patient with a similar general scoliotic conditions.

In relation to this background, the first goal of the current study was to develop and validate a high-fidelity personalized multibody simulation model of the human full body based on the specific parameters of the patient (subject). This model comprises of a fully discretized spine and is able to consider the abnormal spine deformities such as scoliosis and was developed using a combination of the results of motion capture analysis and X-ray images of the real subjects. *LifeMOD* software was used as the multibody simulation platform in this research work. The main use of this virtual musculoskeletal multibody model was to quantify various biomechanical (kinematical) aspects of the human spine such as spinal loads and joint forces which may not be easily (efficiently) calculated by *in-vivo* experiments. The spine model was validated by comparing the obtained simulation results with the experimental and simulation results carried out by the other researchers in the similar conditions.

The second goal of this work was to study the response of this model to the different static and dynamic loads at different landmarks and finally to simulate the effect of spine deformities (scoliosis condition) on the kinematic performance of the spine during the basic daily activates (movements).

Such models can be used by wheelchair designers or other seating systems to gain a better insight regarding the role of the spine deformity and its effect on interaction between the spine and the seating systems. Furthermore, these models can be combined with analysis tools to help surgeons to examine kinematic behaviors as well as force distributions around scoliotic spines and to optimize surgical plans (for minimum spine loads and movement limitations and maximum deformity correction) before spine correction operations.

Trajectories and forces can be computed for various postures and the models can be used to assist surgeons in pre-operative planning and post-operative treatments. In this chapter a summary of the findings and accomplishments of this work is presented, the strength and added values of the developed method are highlighted and the application as well as interpretation limitations of the models and their results are discussed. Finally, recommendations to address the limitations of this simulation method and also its implications for future research are personated.

6.1 Discussion of the model

6.1.1 Construction of the model and basic validation

LifeMOD software was used as the computational platform to develop the complete detailed spine model. In order to validate the developed model, its static and dynamic performance in certain loading conditions/activities was compared with those of the reliable spine models presented by previous researchers of this field. The accuracy and stability of the model was improved by adding and considering more details such as muscles, ligaments, abdominal pressure, etc. The final musculoskeletal multi body was capable of describing dynamic behaviour of the human subject with normal and scoliosis spine. The main advantage of this model is its capability to describe the mechanics of the whole spine by considering the effect of the entire human body without oversimplifying the properties of the anatomical features such as ligaments, vertebral joints, and muscles. Taking into account the anatomical/biomechanical details of the human body enables the model to adopt independent patient-specific parameters to increase the accuracy of the analysis.

6.1.2 Incorporating the scoliosis condition into the model

The developed detailed spine model is able to adopt different spine deformities such as scoliosis condition. This is because all components such as intervertebral disc, muscle and ligaments surrounding spine are taken into account and at the same time the whole spine can be analyzed. Two methods of reconstruction of the spine based on X-ray images of the subject and reconstruction based on the motion capture results were explained. In this study, the combination of both methods was used to develop the spine model with scoliosis condition. Stability of the model in up-right standing posture for three hypothetical scoliosis

models were tested successfully. Furthermore, effect of severity of the scoliosis condition (Cobb's angle) on the lumbar joint forces under A/P and lateral external forces was studied using the three scoliosis models hypothetically developed with left thoracic curvature. The obtained results showed that the loads at the lumbosacral joint in the scoliosis models will increase by increasing the Cobb angle and these loads are considerably higher than those of normal subjects.

6.1.3 Dynamic behaviour of the real normal and scoliosis subjects in basic motion tasks

One of the main goals of this study was to estimate the spinal joint loads in different postures. The novelty of this study was to investigate the compressive loads on intervertebral joints throughout the spine by the combination of motion capture results and musculoskeletal modeling. The motion data of subjects were applied to train musculoskeletal human-body models for the inverse and forward dynamic simulations in *LifeMOD*.

In the next step, this model together with motion capture analysis was used to investigate the dynamic behaviour of scoliosis spine during the basic daily activities (movements). The obtained results were compared with those of a healthy subject with similar anthropometric data. In this part of the study, the influence of basic daily activities such as bending and twisting while standing on the intervertebral joints and/or muscle forces of the healthy and scoliotic subjects were investigated. Biomedical questions about the spine loading conditions and range of motion for scoliosis patients in basic daily activities can be, and have been, answered in these simulations. According to the obtained results, in lateral bending toward the convex side of the scoliosis curve, the spine presents a higher stiffness. This result implied that in order to perform a similar bending with the same magnitude of deformation, the scoliosis spine has to tolerate a higher amount of force due to the muscle contraction as compared to the healthy spine. This can directly increase the spinal joint forces and result in lower back pain as well as the pain due to fatigue of the muscles.

Finally this model was used to study the effect of the corrective surgery (instrumentation) on the spinal loads and stiffness of the spine. The obtained results implied that the instrumentation of the spine confines the range of motion of the spine and this effect is more pronounced in the lateral bending as compared to flexion/extension. However, for both the lateral and forward/backward bending, it was concluded that the instrumentation

of the spine has reduced joint forces of the lumbar region which may help to increase the onset of muscle fatigue pains.

6.2 Model limitations and recommendations for the future research

In this work the effect of shape and deformation of the vertebrae was not taken into account in the modeling. In this model, each vertebra has been represented by an ellipsoid which only describe the mass distribution of the vertebrae (to find the CoM and mass inertia) has been considered and the actual shape and geometry of the vertebra was not considered.
The second limitation of the model is related to the validity of the loading condition on the intervertebral disc and facet joints. In our model the disk and facet joint together represented by a 3DOF joint which connect two vertebrae together which may result in different contact area and disc properties as compared to the real conditions.
Thirdly, in this work, GeBOD data base was used to develop the models. Therefore, two subjects with similar anthropometric parameters will have exactly similar models. However, it has to be noted that each human body is unique and the physical condition of the body may be different between two subjects of the same anthropometric data. It is noteworthy that among many anatomical and biomechanical parameters, in the existing model, parameters such as muscle and joint stiffness and damping values can be personalized based on experiment data of the subject (if available). *In-vivo* stiffness measurements are one of the most useful experiments to acquire such patient specific information.
Finally, in the existing model the mobility of the rib pairs is neglected and the ribcage is modeled as a single segment. The ribcage has a close interaction with the spine (one side of the ribs are connected to the vertebrae of the thoracic spin) and plays an important role in maintaining the stiffness and stability of the spine. In most of the scoliotic cases (especially in the severe cases), at least one curve is located in the thoracic region. Since each rib is connected to the sternum from one end and to corresponding vertebrae from the other end, the ribcage and sternum may undergo rotation and shape changes to maintain this constraint (connections).
In this study our focus was mainly on the dynamic behaviour of the spine with scoliosis condition rather than considering details of the spine curvature. In order to increase the accuracy of the modeling of the spine with scoliosis deformity, the ribcage needs to be discretized and each rib pair has to be connected to the sternum and vertebrae through

proper joint. Discretizing the ribcage and sternum was recommended to develop a more realistic model. In this PhD work, a preliminary attempt was done to discretize the rib cage. For this purpose, the ribcage and sternum of the subject were exported from *LifeMOD* to *3-matic* software. In *3-matic*, ribcage was discretized into 12 independent rib pairs and was exported as STL files (Figure 6.1 The discretized ribcage model) was imported back to the *LifeMOD* environment. Thereafter, the ribs were manually located in the appropriate positions to comply the scoliosis curve. Doing so, individual joints were created between each pair of ribs and the corresponding thoracic vertebra in one side and the sternum in the other side. Further study needs to be done to consider the ribcage as a refined segment in the existing multibody model.

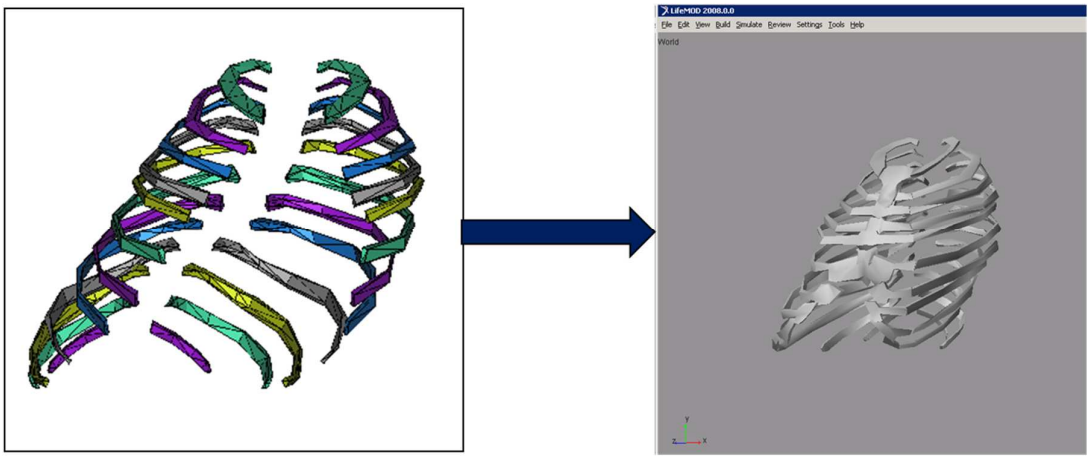

Figure 6.1 Discretized ribs and sternum of the real case

Based on the available motion capture data of the subject after the surgery, the simulation of the flexion/extension exercise was done and the results were compared to those of the model before the surgery (chapter 5). Another limitation of this work was that in the simulation model of the subject after the surgery, rods and screws were not modeled. As a topic for the future investigations, it is recommended to properly model these devises consider their mass and elasticity to study their effect on the vertebral joint forces and torques.

6.3 Global validation

The developed model and simulation method has been validated based on a limited number of *in-vivo* experiments and in simplified conditions. Although the preliminary results are

promising, in order to be served in clinical application, an extensive global validation is still necessary. However, validation of a multibody model in which every details of the spine (material and mechanical properties of the elements, geometry and subject dependencies) and its deformities have been taken into consideration is a huge project beyond research capabilities of only one research team. Full validation of such simulation model (similar to what we have developed in this work) requires a global research effort and world-wide availability of the model. This will allow other researchers to evaluate the simulation strength of the model in many different conditions and address its overlooked aspects.

In order to validate the spine biomechanical models, having access to a reliable experimental data base (as input parameters for comparison) is necessary. While biomechanical properties of the normal spine has been extensively evaluated (through *in-vivo* and *in-vitro* experiments) and classified in different data bases, very less material, mechanical, and *in-vivo* experimental results are available for scoliosis cases. This consequently poses limits on development and validation of the realistic multibody models to simulate the scoliosis spine. In order to address this limitation and to create a reliable biomechanical scoliosis data base, controlling and measuring the actual forces and movements of the spines is necessary.

So far, this particular research study has only been carried out on three scoliosis subjects with different levels of scoliosis curvatures. The current work is being continued by the other members of our research team in which more scoliosis subjects with different types of deformities are supposed to be involved. In the cases that proper experimental results are not available, simulation results obtained from the finite element methods can be used for comparison and evaluation purposes.

The current scoliotic model generally describes a specific patient that is favorable for the clinical applications in which patient specific results are required. This necessitates acquiring the specific biomaterial and biomechanical properties and geometry of the elements (segments) of the subject. In future improvements, *in-vivo* stiffness measurements can be used as an efficient and accurate method to measure important biomechanical parameters such as joint stiffness for each specific subject.

reference

. "Spinal curves." from http://www.nlm.nih.gov/medlineplus/ency/imagepages/19463.htm.
Abouhossein, A., B. Weisse and S. J. Ferguson (2011). "A multibody modelling approach to determine load sharing between passive elements of the lumbar spine." Computer Methods in Biomechanics and Biomedical Engineering **14**(06): 527-537.
Adams. "The Multibody Dynamics Simulation Solution." from http://www.mscsoftware.com/product/adams.
Adams, M. A. and P. Dolan (1995). "Recent advances in lumbar spinal mechanics and their clinical significance." Clinical Biomechanics **10**(1): 3-19.
Ahmed, A. M., A. Shirazi-Adl and S. C. Shrivastava (1986). "A finite element study of a lumbar motion segment subjected to pure sagittal plane moments." Journal of Biomechanics **19**(4): 331-350.
Andersson, G. B., R. Örtengren and A. Nachemson (1977). "Intradiskal pressure, intra-abdominal pressure and myoelectric back muscle activity related to posture and loading." Clinical Orthopaedics and Related Research **129**: 156-164.
Arjmand, N., D. Gagnon, A. Plamondon, A. Shirazi-Adl and C. Lariviere (2009). "Comparison of trunk muscle forces and spinal loads estimated by two biomechanical models." Clinical biomechanics (Bristol, Avon) **24**(7): 533-541.
Arjmand, N. and A. Shirazi-Adl (2006). "Role of intra-abdominal pressure in the unloading and stabilization of the human spine during static lifting tasks." European Spine Journal **15**(8): 1265-1275.
Aubin, C.-É., Y. Petit, I. A. F. Stokes, F. Poulin, M. Gardner-Morse and H. Labelle (2003). "Biomechanical Modeling of Posterior Instrumentation of the Scoliotic Spine." Computer Methods in Biomechanics and Biomedical Engineering **6**(1): 27 - 32.
Aubin, C. and H. Labelle (2004). "Patient-specific mechanical properties of a flexible multi-body model of the scoliotic spine." Medical and Biological Engineering and Computing **42**(1): 55-60.
Aubin, C. E., et al. (2003). "Biomechanical modeling of posterior instrumentation of the scoliotic spine." Comput Methods Biomech Biomed Engin **6**(1): 27-32.
Aubin, C. E., V. Goussev and Y. Petit (2004). "Biomechanical modelling of segmental instrumentation for surgical correction of 3D spinal deformities using Euler-Bernoulli thin-beam elastic deformation equations." Medical & Biological Engineering & Computing **42**(Copyright 2004, IEE): 216-221.
Bakker, E. W., A. P. Verhagen, E. van Trijffel, C. Lucas and B. W. Koes (2009). "Spinal mechanical load as a risk factor for low back pain: a systematic review of prospective cohort studies." Spine **34**(8): E281-E293.
Balan, A. O., L. Sigal and M. J. Black (2005). A quantitative evaluation of video-based 3D person tracking. Visual Surveillance and Performance Evaluation of Tracking and Surveillance, 2005. 2nd Joint IEEE International Workshop on, IEEE.
Belytschko, T., T. Andriacchi, A. Schultz and J. Galante (1973). "Analog studies of forces in the human spine: computational techniques." Journal of biomechanics **6**(4): 361-371.
Belytschko, T. B., R. F. Kulak, A. B. Schultz and J. O. Galante (1974). "Finite element stress analysis of an intervertebral disc." Journal of Biomechanics **7**(3): 277-285.
Berkson, M. H., A.L. Nachemson, and A.B. Schultz (1979). "Mechanical properties of human lumbar spine motion segments – part 2: responses in compression and shear; influence of gross morphology." Journal of Biomechanical Engineering **101**: 52-57.
Bogduk, N. (1980). "A reappraisal of the anatomy of the human lumbar erector spinae." Journal of Anatomy **131**(3): 525-540.
Bogduk, N., J. E. Macintosh and M. J. Pearcy (1992a). "A universal model of the lumbar back muscles in the upright position." Spine **17**(8): 897-913.

Bozic, K. J., J. H. Keyak, H. B. Skinner, H. U. Bueff and D. S. Bradford (1994). "Three-dimensional finite element modeling of a cervical vertebra: an investigation of burst fracture mechanism." Journal of Spinal Disorders **7**(2): 102-110.
Callaghan, J. P. and S. M. McGill (2001). "Low back joint loading and kinematics during standing and unsupported sitting." Ergonomics **44**(3): 280-294.
Cameron, J. and J. Lasenby (2005). A real-time sequential algorithm for human joint localization. ACM SIGGRAPH 2005 Posters, ACM.
Cavalloa, F., G. Megalia, S. Sinigagliaa, O. Toneta, P. Darioa and A. Pietrabissa (2007). "A step towards biomechanical analysis of surgeon's gesture on Adams-LifeMOD platform." International Journal of Computer Assisted Radiology and Surgery **2**(1): 160-180.
Chaffin, D. B. (1967). The Developement of a Prediction Model for the Metabolic Energy Expended During Arm Activities, University of Michigan.
Chaffin, D. B. (1969). "A computerized biomechanical model-development and use in studying gross body actions." Journal of Biomechanics **2**(4): 429-441.
Chaffin, D. B. (1969). "A computerized biomechanical model—development of and use in studying gross body actions." Journal of biomechanics **2**(4): 429-441.
Chen, C.-S., W.-J. Chen, C.-K. Cheng, S.-H. E. Jao, S.-C. Chueh and C.-C. Wang (2005). "Failure analysis of broken pedicle screws on spinal instrumentation." Medical engineering & physics **27**(6): 487-496.
Cheng, H., L. Obergefell and A. Rizer (1994). Generator of Body Data (GEBOD), Manual, DTIC Document.
Cheng, H., L. Obergefell and A. Rizer (1996). The development of the GEBOD program. Biomedical Engineering Conference, 1996., Proceedings of the 1996 Fifteenth Southern, IEEE.
Cheng, P.-T., C.-L. Chen, C.-M. Wang and C.-Y. Chung (2006). "Effect of neuromuscular electrical stimulation on cough capacity and pulmonary function in patients with acute cervical cord injury." Journal of Rehabilitation Medicine **38**(1): 32-36.
Chiropractic, S. (1997). Sofia Chiropractic. Auburn.
Cholewicki, J., J. J. Crisco III, T. R. Oxland, I. Yamamoto and M. M. Panjabi (1996). "Effects of posture and structure on three-dimensional coupled rotations in the lumbar spine: A biomechanical analysis." Spine **21**(21): 2421-2428.
Cholewicki, J., K. Juluru and S. M. McGill (1999). "Intra-abdominal pressure mechanism for stabilizing the lumbar spine." Journal of biomechanics **32**(1): 13-17.
Cholewicki, J., S. M. McGill and R. W. Norman (1995). "Comparison of muscle forces and joint load from an optimization and EMG assisted lumbar spine model: towards development of a hybrid approach." Journal of biomechanics **28**(3): 321-331.
Clin, J., C.-É. Aubin, S. Parent and H. Labelle (2011). "Biomechanical modeling of brace treatment of scoliosis: effects of gravitational loads." Medical & Biological Engineering & Computing **49**(7): 743-753.
Clin, J., C. E. Aubin and H. Labelle (2007). "Virtual prototyping of a brace design for the correction of scoliotic deformities." Med Biol Eng Comput **45**(5): 467-473.
Cobb, J. (1948). "Outline for the study of scoliosis." Instr Course Lect **5**: 261-275.
Cobb, J. (1948). "Outline for the study of scoliosis." Am Acad Orthop Surg Instr Course Lect **5**: 261-275.
Cotrel, Y., J. Dubousset and M. Guillaumat (1988). "New universal instrumentation in spinal surgery." Clinical Orthopaedics and Related Research **227**: 10-23.
d'Alembert, J. "1743, Traité de dynamique." David, Paris.
Daggfeldt, K. and A. Thorstensson (1997). "The role of intra-abdominal pressure in spinal unloading." Journal of biomechanics **30**(11): 1149-1155.
De-Jongh, C. U., A. H. Basson and C. Scheffer (2007). "Dynamic simulation of cervical spine following single-level cervical disc replacement." Proceedings of the 29th Annual International Conference of the IEEE EMBS: 4289-4292.

Desroches, G., C.-E. Aubin, D. J. Sucato and C.-H. Rivard (2007). "Simulation of an anterior spine instrumentation in adolescent idiopathic scoliosis using a flexible multi-body model." Medical & Biological Engineering & Computing **45**(8): 759-768.
Desroches, G., C. E. Aubin, D. J. Sucato and C. H. Rivard (2007). "Simulation of an anterior spine instrumentation in adolescent idiopathic scoliosis using a flexible multi-body model." Med Biol Eng Comput **45**(8): 759-768.
Diab, K. M., J. A. Sevastik, R. Hedlund and I. A. Suliman (1995). "Accuracy and applicability of measurement of the scoliotic angle at the frontal plane by Cobb's method, by Ferguson's method and by a new method." European Spine Journal **4**(5): 291-295.
Dickson, R. A. (2009). Spinal deformities, Springer.
Dlugosz, M. M., D. Panek, P. Maciejasz, W. Chwala and W. Alda (2012). "An improved kinematic model of the spine for three-dimensional motion analysis in the Vicon system." Studies in health technology and informatics **176**: 227-231.
Driscoll, M., C. E. Aubin, A. Moreau and S. Parent (2010). "Finite element comparison of different growth sparring instrumentation systems for the early treatment of idiopathic scoliosis." Stud Health Technol Inform **158**: 89-94.
Duke, K., et al. (2005). "Biomechanical simulations of scoliotic spine correction due to prone position and anaesthesia prior to surgical instrumentation." Clin Biomech (Bristol, Avon) **20**(9): 923-931.
Dwyer, A. F. (1973). "Experience of anterior correction of scoliosis." Clin Orthop Relat Res(93): 191-214.
Dwyer, A. F., N. C. Newton and A. A. Sherwood (1969). "An anterior approach to scoliosis. A preliminary report." Clin Orthop Relat Res **62**: 192-202.
Edidin, A. A., S. M. Kurtz and ebrary Inc. (2006). Spine technology handbook. Amsterdam ; Boston, Elsevier Academic Press**:** xiv, 535 p.
El-Rich, M., A. Shirazi-Adl and N. Arjmand (2004). "Muscle activity, internal loads, and stability of the human spine in standing postures: combined model and in vivo studies." Spine **29**(23): 2633-2642.
Euler, L. (1776). "Nova methods motum corporum rigidarum determinandi." Novi Commentarii Academiae
Scientiarum Petropolitanae **20**: 208**–**238.
Fagan, M. J., S. Julian and A. M. Mohsen (2002). "Finite element analysis in spine research." Journal of Engineering in medicine **216**(5): 281-298.
Ferguson, A. B. (1930). "The Study and Treatment of Scoliosis." Southern Medical Journal **23**(2): 116-120.
Fischer, O. (1906). "Einführung in die Mechanik lebender Mechanismen." Teubner, Leipzig.
Gait, P.-i. (2010). "Product Guide—Foundation Notes."
Garcia, T. and B. Ravani (2003). "A biomechanical evaluation of whiplash using a multi-body dynamic model." Journal of biomechanical engineering **125**(2): 254.
Gardner-Morse, M. and I. A. F. Stokes (1994). "Three-dimensional simulations of the scoliosis derotation maneuver with Cotrel-Dubousset instrumentation." Journal of Biomechanics **27**(2): 177-181.
Gignac, D., C.-É. Aubin, J. Dansereau and H. Labelle (2000). "Optimization method for 3D bracing correction of scoliosis using a finite element model." European Spine Journal **9**(3): 185-190.
Goel, V. K., and J. N. Weinstein. and B. R. C. Press. (1980). " Clinical Biomechanics of the Lumbar Spine."
Goel, V. K., H. Park and W. Z. Kong (1994). "Investigation of vibration characteristics of the ligamentous lumbar spine using the finite element approach." Journal of Biomechanical Engineering **116**(4): 377-383.
Goh, J., A. Thambyah and K. Bose (1998). "Effects of varying backpack loads on peak forces in the lumbosacral spine during walking." Clinical Biomechanics **13**(1): S26-S31.

Goodvin, C., E. J. Park, K. Huang and K. Sakaki (2006). "Development of a real-time three-dimensional spinal motion measurement system for clinical practice." Medical and Biological Engineering and Computing **44**(12): 1061-1075.
Gréalou, L., C. É. Aubin and H. Labelle (2002). "Rib cage surgery for the treatment of scoliosis: a biomechanical study of correction mechanisms." Journal of orthopaedic research **20**(5): 1121-1128.
Greaves, C. Y., M. S. Gadala and T. R. Oxland (2008). "A three-dimensional finite element model of the cervical spine with spinal cord: an investigation of three injury mechanisms." Annals of Biomedical Engineering **36**(3): 396-405.
Greenspan, A., J. W. Pugh, A. Norman and R. S. Norman (1978). "Scoliotic index: a comparative evaluation of methods for the measurement of scoliosis." Bull Hosp Joint Dis **39**(2): 117-125.
Hansen, L., M. De Zee, J. Rasmussen, T. B. Andersen, C. Wong and E. B. Simonsen (2006). "Anatomy and biomechanics of the back muscles in the lumbar spine with reference to biomechanical modeling." Spine **31**(17): 1888-1899.
Harrington, P. R. (1962). "Treatment of scoliosis. Correction and internal fixation by spine instrumentation." J Bone Joint Surg Am **44-A**: 591-610.
Hodges, P. W., A. G. Cresswell, K. Daggfeldt and A. Thorstensson (2001). "In vivo measurement of the effect of intra-abdominal pressure on the human spine." Journal of biomechanics **34**(3): 347-353.
Hole, J. W., Jr. . Ed. John Stout. (1981). Human Anatomy and Physiology. Dubuque, Iowa, Wm. C. Brown Company.
Hoogendoorn, W. E., M. N. van Poppel, P. M. Bongers, B. W. Koes and L. M. Bouter (1999). "Physical load during work and leisure time as risk factors for back pain." Scandinavian journal of work, environment & health: 387-403.
http://www.naturalheightgrowth.com/. "Natural Height Growth." from http://www.naturalheightgrowth.com/.
Huynh, K. T., I. Gibson, B. N. Jagdish and W. F. Lu (2013). "Development and validation of a discretised multi-body spine model in LifeMOD for biodynamic behaviour simulation." Comput Methods Biomech Biomed Engin.
James, J. (1951). "Two curve patterns in idiopathic structural scoliosis." Journal of Bone & Joint Surgery, British Volume **33**(3): 399-406.
Jerkovsky, W. (1978). "The structure of multibody dynamics equations." Journal of Guidance, Control, and Dynamics **1**(3): 173-182.
Kane, T. and D. Levinson Dynamics: theory and applications. 1985, McGraw-Hill, New York.
Kane, T. and M. Scher (1969). "A dynamical explanation of the falling cat phenomenon." International Journal of Solids and Structures **5**(7): 663-666.
Kane, W. J. (1977). "Scoliosis prevalence: a call for a statement of terms." Clinical Orthopaedics and Related Research(126): 43.
Kapandji, I. A. and L. H. Honore (1981). The physiology of the joints: annotated diagrams of the mechanics of the human joints. Edinburgh, Churchill Livingstone.
Keim, H. A. (1982). Scoliosis, Springer.
Khoo, B., J. Goh and K. Bose (1995). "A biomechanical model to determine lumbosacral loads during single stance phase in normal gait." Medical engineering & physics **17**(1): 27-35.
Kim, S. M., I. C. Yang and M. P. Lee (2007). "Cervical spine injury analysis regarding frontal and side impacts of wheelchair occupant in vehicle by LifeMOD." IFMBE Proceedings **14**: 2521-2524.
King, H. A., J. H. Moe, D. S. Bradford and R. B. Winter (1983). "The selection of fusion levels in thoracic idiopathic scoliosis." J Bone Joint Surg Am **65**(9): 1302-1313.
Klein, J. and D. Hukins (1983). "Functional differentiation in the spinal column." Engineering in Medicine **12**(2): 83-85.

Klein, P., C. Broers, V. Feipel, P. Salvia, B. Van Geyt, P. Dugailly and M. Rooze (2003). "Global 3D head–trunk kinematics during cervical spine manipulation at different levels." Clinical Biomechanics **18**(9): 827-831.
Kumaresan, S., N. Yoganandan and F. A. Pintar (1999). "Finite element analysis of the cervical spine: a material property sensitivity study." Clinical Biomechanics **14**(1): 41-53.
Kurtz, S. M. and A. Edidin (2006). Spine technology handbook, Academic Press.
Lafage, V., et al. (2004). "3D finite element simulation of Cotrel-Dubousset correction." Comput Aided Surg **9**(1-2): 17-25.
Lagrange, J. L. (1853). Mécanique analytique, Mallet-Bachelier.
Lalonde, N. M., I. Villemure, R. Pannetier, S. Parent and C. E. Aubin (2010). "Biomechanical modeling of the lateral decubitus posture during corrective scoliosis surgery." Clinical biomechanics (Bristol, Avon) **25**(6): 510-516.
Lee, R. Y., J. Laprade and E. H. Fung (2003). "A real-time gyroscopic system for three-dimensional measurement of lumbar spine motion." Med Eng Phys **25**(10): 817-824.
Lenke, L. G., R. R. Betz, J. Harms, K. H. Bridwell, D. H. Clements, T. G. Lowe and K. Blanke (2001). "Adolescent idiopathic scoliosis a new classification to determine extent of spinal arthrodesis." The Journal of Bone & Joint Surgery **83**(8): 1169-1181.
LifeMOD. "LifeMOD Biomechanics Modeler." from http://www.lifemodeler.com/.
Lundon, K. and K. Bolton (2001). "Structure and function of the lumbar intervertebral disk in health, aging, and pathologic conditions." The Journal of orthopaedic and sports physical therapy **31**(6): 291.
Machida, M. (1999). "Cause of idiopathic scoliosis." Spine **24**(24): 2576.
Macintosh, J. E. and N. Bogduk (1986). "The morphology of the human lumbar multifidus." Clinical Biomechanics **1**(4): 196-204.
Macintosh, J. E. and N. Bogduk (1987). "Volvo award in basic science: the morphology of the lumbar erector spinae." Spine **12**(7): 658-668.
Macintosh, J. E., N. Bogduk and M. J. Pearcy (1993). "The effects of flexion on the geometry and actions of the lumbar erector spinae." Spine **18**(7): 884-893.
Mahaudens, P., X. Banse, M. Mousny and C. Detrembleur (2009). "Gait in adolescent idiopathic scoliosis: kinematics and electromyographic analysis." European spine journal : official publication of the European Spine Society, the European Spinal Deformity Society, and the European Section of the Cervical Spine Research Society **18**(4): 512-521.
Małgorzata Syczewska, A. Ł., Beata Górak, Graff, Krzysztof (2007). "Changes in gait pattern in patients with scoliosis Zmiany stereotypu chodu u pacjentów z bocznym skrzywieniem kręgosłupa." **10**(4): 12-21.
Marras, W. and K. Granata (1997). "Spine loading during trunk lateral bending motions." Journal of biomechanics **30**(7): 697-703.
Marras, W. S., S. A. Lavender, S. E. Leurgans, F. A. FATHALLAH, S. A. FERGUSON, W. GARY ALLREAD and S. L. RAJULU (1995). "Biomechanical risk factors for occupationally related low back disorders." Ergonomics **38**(2): 377-410.
Maruyama, T. (2008). "Bracing adolescent idiopathic scoliosis: a systematic review of the literature of effective conservative treatment looking for end results 5 years after weaning." Disability & Rehabilitation **30**(10): 786-791.
Maurel, N., F. Lavaste and W. Skalli (1997). "A three-dimensional parameterized finite element model of the lower cervical spine: study of the influence of the posterior articular facets." Journal of Biomechanics **30**(9): 921-931.
McGill, S. M. and R. W. Norman (1986). "Partitioning of the L4-L5 dynamic moment into disc, ligamentous, and muscular components during lifting." Spine **11**(7): 666-678.
McGill, S. M., Norman, R.W. (1987). "Effects of an anatomically detailed erector spinae model on L4/L5 disc compression and shear." Journal of Biomechanics **20**(6): 591-600.

McGlashen, K. M., et al. (1987). " Load displacement behavior of the human lumbo-sacral joint." Journal of Orthopedic Research **5(4)**: 488-496.
McNamara, J. E., B. Feng, K. Johnson, S. Gu, M. A. Gennert and M. A. King (2007). Motion capture of chest and abdominal markers using a flexible multi-camera motion-tracking system for correcting motion-induced artifacts in cardiac SPECT. Nuclear Science Symposium Conference Record, 2007. NSS'07. IEEE, IEEE.
Moroney, S. P., et al. (1988). "Load-displacement properties of lower cervical spine motion segments." Journal of Biomechanics **21(9)**: 769-779.
Mutluay, F., R. Demir, S. Ozyilmaz, A. Caglar, A. Altintas and H. Gurses (2007). "Breathing-enhanced upper extremity exercises for patients with multiple sclerosis." Clinical rehabilitation **21**(7): 595-602.
Nachemson, A. (1966). "The load on lumbar disks in different positions of the body." Clinical Orthopaedics and Related Research **45**: 107-122.
Nachemson, A. (1976). "The lumbar spine: an orthopaedic challenge." Spine **1**(1): 59-69.
Nachemson, A. and G. Elfstrom (1970). "Intravital dynamic pressure measurements in lumbar discs." Scand J Rehabil Med **1**: 1-40.
Nachemson, A. and J. M. Morris (1964). "In vivo measurements of intradiscal pressure discometry, a method for the determination of pressure in the lower lumbar discs." The Journal of Bone and Joint Surgery (American) **46**(5): 1077-1092.
Nachemson, A. L. (1981). "Disc pressure measurements." Spine **6**(1): 93.
Natarajan, R. N., J. R. Williams, S. A. Lavender and G. B. J. Andersson (2007). "Poro-elastic finite element model to predict the failure progression in a lumbar disc due to cyclic loading." Computers & Structures **85**(11-14): 1142-1151.
Ng, H. W. and E. C. Teo (2005). "Development and validation of a C0-C7 FE complex for biomechanical study." Journal of Biomechanics **127**(5): 729-735.
Olszewski, A. D., M. J. Yaszemski and A. A. White III (1996). "The anatomy of the human lumbar ligamentum flavum: new observations and their surgical importance." Spine **21**(20): 2307-2312.
Pamela K. Levangie, C. C. N. (2005). Joint Structure and Function: A Comprehensive Analysis F A Davis Co.
Panjabi, A. A. W. a. M. M., Ed. (1990). Clinical Biomechanics of the Spine. Philadelphia, Lippincott Williams & Wilkins.
Panjabi, M. M., R.A. Brand, and A.A. White (1976). "Mechanical properties of the human thoracic spine as shown by three-dimensional load-displacement curves." Journal of Bone and Joint Surgery **58(5)**: 642-652.
Pankoke, S., B. Buck and H. P. Woelfel (1998). "Dynamic FE model of sitting man adjustable to body height, body mass and posture used for calculating internal forces in the lumbar vertebral disks." Journal of Sound and Vibration **215**(4): 827-839.
Parnianpour, M., M. Nordin, N. Kahanvitz and V. Frankel (1988). "1988 Volvo Award in Biomechanics: The Triaxial Coupling of Torque Generation of Trunk Muscles during Isometric Exertions and the Effect of Fatiguing Isoinertial Movements on the Motor Output and Movement Patterns." Spine **13**(9): 982-992.
Patias, P., T. B. Grivas, A. Kaspiris, C. Aggouris and E. Drakoutos (2010). "A review of the trunk surface metrics used as Scoliosis and other deformities evaluation indices." Scoliosis **5**(1): 12.
Perie, D., C. E. Aubin, Y. Petit, H. Labelle and J. Dansereau (2004). "Personalized biomechanical simulations of orthotic treatment in idiopathic scoliosis." Clin Biomech (Bristol, Avon) **19**(2): 190-195.
Perie, D., et al. (2004). "Personalized biomechanical simulations of orthotic treatment in idiopathic scoliosis." **19**(2): 190-195.
Petit, Y., C.-E. Aubin and H. Labelle (2004). "Patient-specific mechanical properties of a flexible multi-body model of the scoliotic spine." Medical and Biological Engineering and Computing **42**(Compendex): 55-60.

Pintar, F. A., N. Yoganandan, T. Myers, A. Elhagediab and A. Sances Jr (1992). "Biomechanical properties of human lumbar spine ligaments." Journal of biomechanics **25**(11): 1351-1356.
Poulin, F., C. Aubin, I. Stokes, M. Gardner-Morse and H. Labelle (1998). [Biomechanical modeling of instrumentation for the scoliotic spine using flexible elements: a feasibility study]. Annales de chirurgie.
Ringer, M. and J. Lasenby (2002). A procedure for automatically estimating model parameters in optical motion capture. In British Machine Vision Conference, Citeseer.
Roberson, R. E. and R. Schwertassek (1988). Dynamics of multibody systems, Springer-Verlag Berlin.
Robitaille, M., C. É. Aubin and H. Labelle (2009). "Effects of alternative instrumentation strategies in adolescent idiopathic scoliosis: a biomechanical analysis." Journal of orthopaedic research **27**(1): 104-113.
Rohlmann, A., G. Bergmann and F. Graichen (1999). "Loads on internal spinal fixators measured in different body positions." European Spine Journal **8**(5): 354-359.
Rohlmann, A., U. Gabel, F. Graichen, A. Bender and G. Bergmann (2007). "An instrumented implant for vertebral body replacement that measures loads in the anterior spinal column." Medical engineering & physics **29**(5): 580-585.
Rohlmann, A., F. Graichen, U. Weber and G. Bergmann (2000). "Monitoring in vivo implant loads with a telemeterized internal spinal fixation device." Spine **25**(23): 2981-2986.
Rohlmann, A., R. Petersen, V. Schwachmeyer, F. Graichen and G. Bergmann (2012). "Spinal loads during position changes." Clinical Biomechanics.
Rohlmann, A., T. Zander, N. Burra and G. Bergmann (2008). "Flexible non-fusion scoliosis correction systems reduce intervertebral rotation less than rigid implants and allow growth of the spine: a finite element analysis of different features of orthobiom™." European Spine Journal **17**(2): 217-223.
Rohlmann, A., T. Zander, M. Rao and G. Bergmann (2009). "Applying a follower load delivers realistic results for simulating standing." Journal of biomechanics **42**(10): 1520-1526.
Ryan, S. D. and L. P. Fried (1997). "The impact of kyphosis on daily functioning." Journal of the American Geriatrics Society **45**(12): 1479.
Sato, K., S. Kikuchi and T. Yonezawa (1999). "In vivo intradiscal pressure measurement in healthy individuals and in patients with ongoing back problems." Spine **24**(23): 2468.
Sato K, K. S., Y Yonezawa T (1999). "In vivo intradiscal pressure measurement in healthy individuals and in patients with ongoing back problems." spine **24(23)**: 2468-2474.
Schiehlen, W. (1997). "Multibody system dynamics: roots and perspectives." Multibody system dynamics **1**(2): 149-188.
Schmidt, H., F. Heuer, L. Claes and H. J. Wilke (2008). "The relation between the instantaneous center of rotation and facet joint forces – A finite element analysis." Clinical Biomechanics **23**(3): 270-278.
Schultz, A., G. Andersson, R. Ortengren, K. Haderspeck and A. Nachemson (1982). "Loads on the lumbar spine. Validation of a biomechanical analysis by measurements of intradiscal pressures and myoelectric signals." The Journal of bone and joint surgery. American volume **64**(5): 713.
Schultz, A., T. Belytschko, T. Andriacchi and J. Galante (1973). "Analog studies of forces in the human spine: mechanical properties and motion segment behavior." Journal of biomechanics **6**(4): 373-383.
Schultz, A. B., et al. (1979). "Mechanical properties of human lumbar spine motion segments-part 1: responses in flexion, extension, lateral bending and torsion." Journal of Biomechanical Engineering **101**: 46-52.
Schultz, A. B. and C. Hirsch (1973). "Mechanical analysis of Harrington rod correction of idiopathic scoliosis." The Journal of Bone and Joint Surgery (American) **55**(5): 983-992.
Schultz, A. B. and C. Hirsch (1974). "Mechanical analysis of techniques for improved correction of idiopathic scoliosis." Clinical Orthopaedics and Related Research **100**: 66-73.

Schultz, A. B. a. J. A. A.-M., Ed. (1991). Biomechanics of the human spine, in Basic orthopaedic biomechanics. New York, Raven Press.
Seidel, H., B. Hinz and R. Bluthner (2001). "Application of finite element models to predict forces acting on the lumbar spine during whole-body vibration." Clinical Biomechanics **16**(1): S57-S63.
Serway, R. A. and J. W. Jewett Jr (2009). Physics for scientists and engineers, Brooks/Cole Publishing Company.
Shirazi-Adl, A. (1989). "Strain in fibers of a lumbar disc. Analysis of the role of lifting in producing disc prolapse." Spine **14**(1): 96.
Shirazi-Adl, A., M. El-Rich, D. Pop and M. Parnianpour (2005). "Spinal muscle forces, internal loads and stability in standing under various postures and loads—application of kinematics-based algorithm." European Spine Journal **14**(4): 381-392.
Silaghi, M.-C., R. Plänkers, R. Boulic, P. Fua and D. Thalmann (1998). "Local and global skeleton fitting techniques for optical motion capture." Modelling and Motion Capture Techniques for Virtual Environments: 26-40.
Sponseller, P. D. (2011). "Bracing for adolescent idiopathic scoliosis in practice today." Journal of Pediatric Orthopaedics **31**: S53.
Stokes, I. A. (1994). "Three-dimensional terminology of spinal deformity. A report presented to the Scoliosis Research Society by the Scoliosis Research Society Working Group on 3-D terminology of spinal deformity." Spine (Phila Pa 1976) **19**(2): 236-248.
Stokes, I. a. and M. Gardner-Morse (1991). "Analysis of the interaction between vertebral lateral deviation and axial rotation in scoliosis." Journal of biomechanics **24**(8): 753-759.
Stokes, I. A. and M. Gardner-Morse (1995). "Lumbar spine maximum efforts and muscle recruitment patterns predicted by a model with multijoint muscles and joints with stiffness." Journal of Biomechanics **28**(2): 173-186.
Stokes, I. A. and M. Gardner-Morse (1999). "Quantitative anatomy of the lumbar musculature." Journal of biomechanics **32**(3): 311-316.
Stokes, I. A. and M. Gardner-Morse (2004). "Muscle activation strategies and symmetry of spinal loading in the lumbar spine with scoliosis." Spine **29**(19): 2103.
Stokes, I. A. and J. P. Laible (1990). "Three-dimensional osseo-ligamentous model of the thorax representing initiation of scoliosis by asymmetric growth." Journal of biomechanics **23**(6): 589-595.
Syczewska, M., K. Graff, M. Kalinowska, E. Szczerbik and J. Domaniecki (2012). "Influence of the structural deformity of the spine on the gait pathology in scoliotic patients." Gait & posture **35**(2): 209-213.
syndrome Homocystinuria, E.-D. S. M. (2001). "Adolescent idiopathic scoliosis: review and current concepts." Am Fam Physician **64**(1): 111-117.
Tay, S. K., I. Gibson and B. N. Jagdish (2009). Detailed spine modeling with LifeMOD. 3rd International Convention on Rehabilitation Engineering and Assistive Technology, ICREATE '09, April 22, 2009 - April 26, 2009, Singapore, Association for Computing Machinery.
Teo, E. C. and H. W. Ng (2001). "First cervical vertebra (atlas) fracture mechanism studies using finite element method." Journal of Biomechanics **34**(1): 13-21.
Tho, H. K. (2010). Haptically Integrated Biodynamic Simulation of a Detailed Spine Model. Ph.D, National University of Singapore.
Van-Dieen, J. H. (1997). "Are recruitment patterns of the trunk musculature compatible with a synergy based on the maximization of endurance?" Journal of Biomechanics **30**(11): 1095-1100.
Vanderby Jr, R., M. Daniele, A. Patwardhan and W. Bunch (1986). "A method for the identification of in-vivo segmental stiffness properties of the spine." Journal of biomechanical engineering **108**(4): 312.
VICON. "Motion Capture Systems from Vicon." from www.vicon.com/.
Villafranca, I. F., M. M. Ballasteros, S. P. Applegate, R. H. Rivera, J. M. Clarke, J. Clarke, P. Makovicky, V. H. R. Rosales, O. Carranza and D. Prothero (2000). "SIXTIETH ANNUAL MEETING

SOCIETY OF VERTEBRATE PALEONTOLOGY FIESTA AMERICANA REFORMA HOTEL MEXICO CITY, MEXICO OCTOBER 25-28, 2000."
Viviani, G., D. Ghista, P. Lozada, K. Subbaraj and G. Barnes (1986). "Biomechanical analysis and simulation of scoliosis surgical correction." Clinical Orthopaedics and Related Research(208): 40.
Vrtovec, T., F. Pernuš and B. Likar (2009). "A review of methods for quantitative evaluation of spinal curvature." European Spine Journal **18**(5): 593-607.
Vukobratovic, M., A. Frank and D. Juricic (1970). "On the stability of biped locomotion." Biomedical Engineering, IEEE Transactions on(1): 25-36.
Wang, Z., Z. Liu and C. Wang (2008). "[Development of the personalized finite element model of the adolescent idiopathic scoliosis and its significance]." Sheng Wu Yi Xue Gong Cheng Xue Za Zhi **25**(5): 1084-1088.
Weinstein, S. L. (1986). "Idiopathic scoliosis: natural history." Spine **11**(8): 780-783.
Weinstein, S. L., L. A. Dolan, J. C. Cheng, A. Danielsson and J. A. Morcuende (2008). "Adolescent idiopathic scoliosis." The Lancet **371**(9623): 1527-1537.
Weiss, H.-R., S. Bess, M. S. Wong, V. Patel, D. Goodall and E. Burger (2008). "Adolescent idiopathic scoliosis-to operate or not? A debate article." Patient Saf Surg **2**(1): 25.
White, A. A. and M. M. Panjabi (1990). Clinical biomechanics of the spine, Lippincott Philadelphia.
Wilke, H.-J., P. Neef, B. Hinz, H. Seidel and L. Claes (2001). "Intradiscal pressure together with anthropometric data-a data set for the validation of models." Clinical biomechanics (Bristol, Avon) **16**: 111-126.
Wilke, H. J., P. Neef, M. Caimi, T. Hoogland and L. Claes (1999). "New in vivo measurements of pressures in the intervertebral disc in daily life." Spine **24**(8): 755.
Wilke, H. J., P. Neef, M. Caimi, T. Hoogland and L. E. Claes (1999). "New in vivo measurements of pressures in the intervertebral disc in daily life." Spine **24**(8): 755-762.
Wilke, H. J., P. Neef, B. Hinz, H. Seidel and L. Claes (2001). "Intradiscal pressure together with anthropometric data-a data set for the validation of models." Clinical Biomechanics **16**: S111-S126.
Wilke HJ, N. P., Caimi M, Hoogland T, Claes LE. . , ; (1999). "New in vivo measurements of pressures in the intervertebral disc in daily life." spine **24(8)**: 755-762.
Woltring, H. J. (1986). "A FORTRAN package for generalized, cross-validatory spline smoothing and differentiation." Advances in Engineering Software (1978) **8**(2): 104-113.
Wooley, P. H., M. J. Grimm and E. L. Radin (2005). "The structure and function of joints." Arthritis and Allied Conditions. A Textbook of Rheumatology, Lippincott Williams & Wilkins, Philadelphia: 149-173.
Yoganandan, N., S. Kumaresan, L. Voo, F. A. Pintar and S. J. Larson (1996). "Finite element modeling of the C4-C6 cervical spine unit." Medical Engineering Physics **18**(7): 569-574.
Yoganandan, N., S. Kumaresan, and F.A. Pintar (2001). "Biomechanics of the cervical spine-Part 2: Cervical spine soft tissue responses and biomechanical modeling." Clinical Biomechanics **16(1)**: 1-27.
Zander, T., A. Rohlmann, C. Klockner and G. Bergmann (2002). "Comparison of the mechanical behavior of the lumbar spine following mono-and bisegmental stabilization." Clinical Biomechanics **17**(6): 439-445.
Zee, M. D., L. Hansen, C. Wong, J. Rasmussen and E. Simonsen (2007). "A generic detailed rigid-body lumbar spine model." Journal of Biomechanics **40**(6): 1219-1227.
Zheng, Y., M. Nixon and R. Allen (2003). "Lumbar spine visualisation based on kinematic analysis from videofluoroscopic imaging." Medical engineering & physics **25**(3): 171-179.
Zielke, K. (1982). "[Ventral derotation spondylodesis. Results of treatment of cases of idiopathic lumbar scoliosis (author's (author's transl)]." Z Orthop Ihre Grenzgeb **120**(3): 320-329.

Appendix

STEP-BY-STEP GUIDELINE FOR DEVELOPING A DETAILED SPINE MODEL IN LIFEMOD

In this section developing a detailed spine model was explained step by step using ADAMS/View commands. For each step, based on the information of the model and the maneuver, the script may change. There is one main file which read all command files. Each step has a command file separately which save as a command file in the same folder as the main file is. Having main file, user need to run this file only and it automatically read the other command files. For reading command file, user can choose "read command file" from Tools or F2 as a shortcut key.

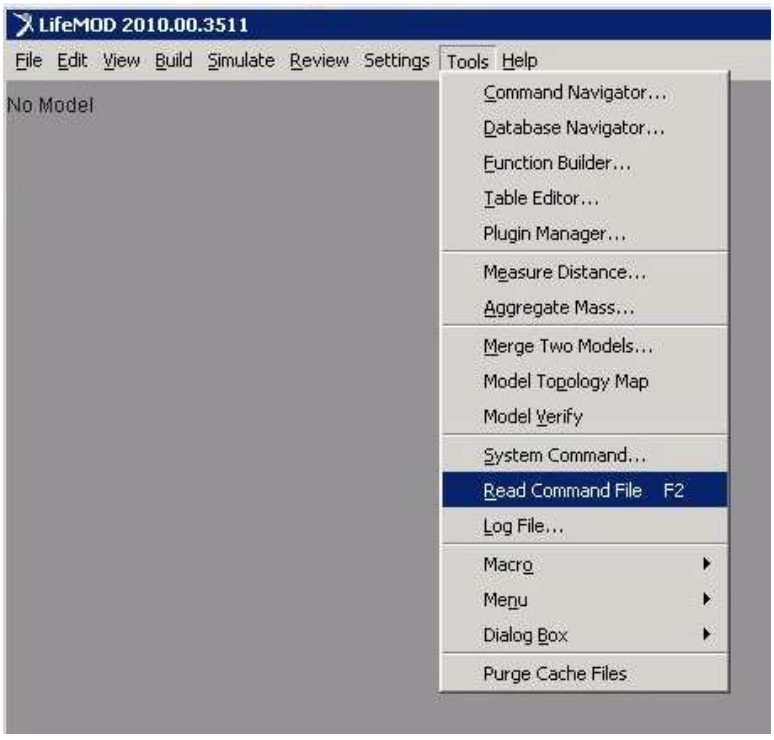

Figure 1: read command file

The main script file is shown below.

*!!********** Detailed spine model **********

!!===1. Creating body by running the Vicon slf file or existing data base in Life MOD ====*

file command read file="base segment.cmd"

!!======== 2. Creating base joints (excluding the spinal part) ==========
file command read file="base joints.cmd"

!!======== 3. Creating base muscle (using legacy 17 set muscle sets) ==========
file command read file="base muscle.cmd"

!!= 4. Creating individual vertebrae and related marker for following creation of individual joints =
file command read file="detailed spine-segments.cmd"

!!========== 5.Reassign muscles ======
file command read file="ReassignMuscles.cmd"

!!========= 6.Create Ligaments========
file command read file=" ligaments.cmd"

!!==== == 7.connect the vertebrae by creating joints =======
file command read file="detailed spine-joints.cmd"

!!======= ======= 8.CreateLumberMuscles==========
file command read file="erector spinae.cmd"
file command read file="psoas major muscle.cmd"

!!============== 9.CreateAbdominalMuscles =======
file command read file="Rectus sheath.cmd"
file command read file="abdominal muscle.cmd"
file command read file="QLM.cmd"
file command read file="MM.cmd"

!!============== 10.CreateIDP in passive models =======
file command read file="Create IDP.cmd"

!!======= ======11.Editing the MOT agents =========

file command read file="modifyMOTagents.cmd"

By using this script file (main command) and the other 10 files which were used in the above script, the detailed spine model was developed. It is important to put all the script files in the folder which the model will be saved on it. After this the model is ready for equilibrium analysis. Now each step will be explained in detail as follow:

Step 1: Generating the Body Segments

Generating the body Segments by running the Vicon slf file

In this phase, an SLF file is used to create the human body motion from recorded motion data. The body segments are created using the parameters which were measured and stored in the SLF file. This file contains information on the subject name, gender, age, height and weight. Figure 2 shows an example of SLF file. Motion capture data consists of two blocks, a marker set and a motion data block. The marker set block indicates which marker location has available data. The ordering in the motion data block is dictated by the order of the marker locations in the marker set block. First LifeMOD™ uses this information to extract body segment measurements and mass properties from the internal anthropometric database. The motion data (MOCAP) for the specific maneuver is imported into the model and used to drive the motion agents created on the model. Select Use PARTIAL Data Set if some part of data is unusable or the most accurate for the simulation and FULL Data Set if the whole data set is useable. The SLF file should be in the same folder as command files are in.

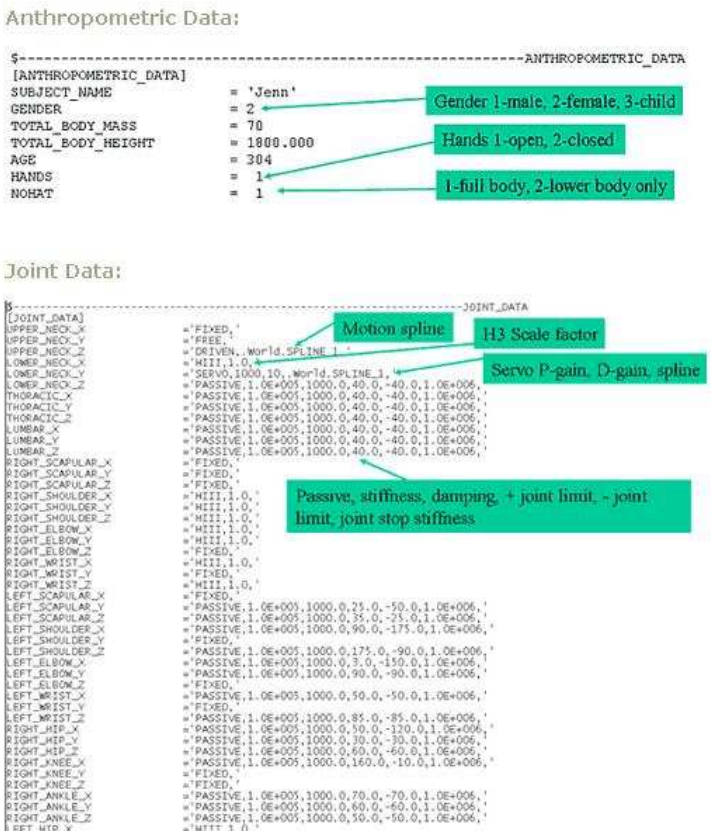

Figure 2: SLF file

!!==========="base segment.cmd" ==========

!!========== ========"full data set" ==========

LM Import filename=" Sanditi-cal13-twisting.slf" bodyname=Sanditi body=on joint=off posture=off motion=on grx=off window=full refM=yes

!!==========="partial data set" ==========

LM Import filename=" Sanditi-cal13-twisting.slf" bodyname=Sanditi body=on joint=off posture=off motion=on grx=off window=partial start=2.55 end=16.11 refM=yes

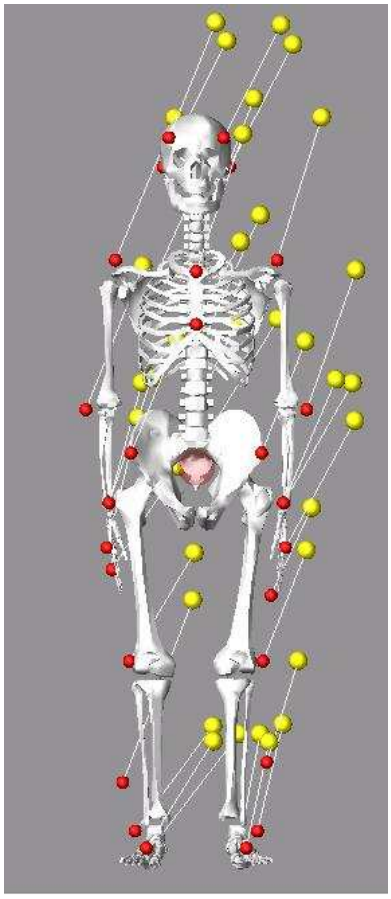

Figure 3: The resulting model with the body and motion data installed.

Generating the Body Segments by database of Life MOD

There are three data base in Life MOD to use for creating segments, GeBOD, PeopleSize and US Army - Natick anthropometric database. In some simulation of this study, the body is created using GeBod database. The body segment will be generated based on the age, weight, height and gender.

!!=========='BODY MATRIX DATA GENERATED FROM GEBOD DATABASE'========

LM Panel Body Gebod &

bod_name=Sanditi &

model_name='World' &

bod_gender=1 & (1 for male and 2 for female)

bod_ht=1778 &

bod_wt=70 &

bod_age=288 &

hands=2 & (1 for open hands and 2 for close hands)

nohat=1 & (body configuration :1 for full body and 2 for lower body)

units=mmks

LM Panel Body Create &

model_name='World' &

bod_name=Winston &

color=red &

units=mmks &

nohat=1

Step2: Generating base body Joints excluding spinal joints

For this model passive joints will be created for the inverse-dynamics simulation. The passive joint consists of a tri-axis hinge joint (3 DOF) which includes angulation stops, stiffness and damping torques. This type of joint is used primarily to stabilize the body during the inverse-dynamics simulation. They are later removed and replaced with Servo-type torque generators for the "trained" phase. The parameters of the passive joints can be included in the SLF file as well. To modify stiffness and damping ratio of each joint set, simply change the values in the command file. Copy the command for the right side as well.

!!========================= == 2. Joint ==================

LM joint build section=Lleg action=create &

dofType='passive','passive','passive','passive','fixed','fixed','passive','passive','passive' &

stiffness=*'100000','100000','100000','100000','','','100000','100000','100000'* &

damping=*'10000','10000','10000','10000','','','10000','10000','10000'* &

posLimit=*'50','30','60','160','','','70','60','50'* &

negLimit=*'120','30','60','10','','','70','60','50'* &

bump=*'3.3895448708E+009','3.3895448708E+009','3.3895448708E+009','3.3895448708E+009','','','3.3895448708E+009','3.3895448708E+009','3.3895448708E+009'* &

t1='on' t2='on' t3='on'

LM joint build section=Larm action=create &

dofType=*"fixed","passive","passive","passive","fixed","passive","passive","passive","fixed","passive","fixed","passive"* &

stiffness=*"","100000","100000","100000","","100000","100000","100000","","100000","","100000"* &

damping=*"","10000","10000","10000","","10000","10000","10000","","10000","","10000"* &

posLimit=*"","25","35","90","","175","3","90","","50","","85"* &

negLimit=*"","50","25","175","","90","150","90","","50","","85"* &

bump=*"","3.3895448708E+009","3.3895448708E+009","3.3895448708E+009","","3.3895448708E+009","3.3895448708E+009","3.3895448708E+009","","3.3895448708E+009","","3.3895448708E+009"*

Step3: Creating base Muscle set

Standard muscle sets are generated from LifeMOD database of muscles. These muscles are to be trained in an inverse-dynamics simulation. The recording elements in the muscles record the contraction history of the muscle when the model is driven by the motion agents. They then serve as actuators for the forward-dynamics simulations. The muscle actuators are programmed not to exceed the physiological limits of the individual muscle.

!!========== = 3. Creating muscle ==========

LM Tissue Create Section &

model = .World &

type = record &

```
  sections  = Rarm,Larm,Rleg,Lleg,Trunk            &
  stiffness = 0.4448221615                  &
  damping   = 1.75E-002                     &
  preload   = 0.4448221615                    &
  tone      = 1.0
```

Step4: Creating individual vertebrae and related markers for following creation of individual joints

Individual segments for the Neck (C1 – C7), Upper Torso (T1– T12) and Central Torso (L1 – L5), corresponding to the cervical, thoracic and lumbar regions are created. The centre of mass location of an individual segment is estimated and mass properties are determined via ellipsoid volume approximation and default human tissue density. The existing shell geometry is used for visualization. The Ribs and Sternum, which also belong to the default upper torso segment, are also re-created. The script below should be modified for other vertebrae from C2 to L5 and also Ribs and Sternum.

```
!!===============4. Refining spine segments into 24 individual segments==========
LM Gui Dialog Display topLevel=segments subLevel="create_set"
LM Gui Dialog Display topLevel=segments subLevel=create_one
LM status text='CREATING PART REPRESENTATION'
LM Panel Body Single &
  segment="C1" &
  cm_location=0.0, 576.0, -24.0 &
  cm_orientation=0,0,0 &
   mp_method=ellip &
  use_human_density=on &
  ellipx=100 &
  ellipy=25 &
  ellipz=100 &
  create=yes &
  shells=exist &
  shell_entity=.World.Sanditi_Neck.Skel_atlas
marker create marker=.World.Sanditi_C1.m1 loc=0.0, 584.0, -16.0 ori=0,0,0 rel=.World
LM status text='CREATING PART REPRESENTATION'
```

Note: Since the default spine model in Life Mod has only 3 segments and this version is compatible with the Vicon exported file (SLF), the motion data of Neck Upper_Torso and Centeral_Torso will have problem if we delete these parts. Therefore we keep the original segments and only rename them and change the properties of them to meet our requirements. In this study, Centeral_Torso with L3, neck with C7 and Upper_Torso renamed with T10. The reason is because two markers which were represent neck and upper_torso were attached to C7 and T10 in plug in gait set.

```
!!============4.1 Modify Neck, Upper_Torso and Central_Torso===============
!automatically update neck, uppertorso and lower torso to fit with C7 ,T10 and L3
entity modify entity = .World.Sanditi_Neck new = .World.Sanditi_C7
marker modify marker_name = .World.Sanditi_C7.cm location = 0.0, 456.0, -26.0
marker modify marker_name = .World.Sanditi_C7.gmE  location = 0.0, 456.0, -26.0 orientation = 0.0, 0.0, 0.0
geometry modify shape ellipsoid  &
  ellipsoid_name = .World.Sanditi_C7.Ellipsoid  &
  x_scale_factor = 100  &
  y_scale_factor = 25  &
  z_scale_factor = 100
entity attributes &
 entity_name = .World.Sanditi_C7.Ellipsoid &
 type_filter = Ellipsoid &
 color = .colors.PEACH
```

Step5: Reassign muscle attachments

The muscles are attached to the respective bones based on geometric landmarks on the bone graphics. With the new vertebra segments created, the muscle attachments to the original segment must be reassigned to be more specific to the new vertebra segments. The physical attachment locations will remain the same. All muscles associated with the refined spine must be re-assigned. The reassigning command shows as below. The blue parts can change based on the Table 1. This command will repeat for right and left side, for attachment 1 and 2 for all muscles.

```
!!============== ======= 5. Reassign muscles    ======================

!------Reassign Muscle Attachments (all for left and right side)
```

LM Muscle Attachment Modify attachment=.World.Sanditi_ScalPos_Rtiss_1.attachment_1
segment=.World.Sanditi_C5

Table 1. Attachment locations of neck and trunk muscle set

Index	Muscle	Attach proximal (attachment_1)	Attach distal (attachment_2)
1	Rectus abdominis	Sternum	Pelvis
2	Obliquus externus	Ribs	Pelvis
3	Scalenus medius	C5	Ribs
4	Scalenus anterior	C5	Ribs
5	Sternocleidomastiodeus	Head	Scapula
6	Erector spinae 1	T7	Pelvis
7	Erector spinae 2	L2	Pelvis
8	Erector spinae 3	T7	L2
9	Scalenus posterior	C5	Ribs
10	Splenius cervicis	Head	C7
11	Splenius capitis	Head	T1
12	Trapezius 1	C7	Scapula
13	Trapezius 2	T6	Scapula
14	Trapezius 3	L2	Scapula
15	Trapezius 4	C6	Scapula
16	Pectoralis Major1	Ribs	Scapula
17	Pectoralis Major2	Ribs	Scapula
18	Pectoralis Major3	Ribs	Scapula
19	pectoralis minor_1	Ribs	Scapula
20	pectoralis minor_2	Ribs	Scapula
21	pectoralis minor_3	Ribs	Scapula
22	LatissimusDorsi1	T7	Upper_arm
23	LatissimusDorsi2	Upper_arm	L1
24	Psoas Major	L3	Upper_leg
25	subclavious	Sternum	Scapula

Step6: Create spinal ligamentous

Ligaments are passive spring/dampers and are not included in the generic full body tissue set. Between every two vertebra, six ligaments (interspinous, ligementum flavum, anterior/posterior longitudinal and joint capsule) are created, with user defined stiffness, damping and preload. The purpose of ligaments is to guide segment motion and contribute to spinal stability. Set the stiffness according to Tables 2 and 3 and the damping is 10% of the stiffness value. For the present model, cervical stiffness values are also used for the thoracic region.

```
!!============================ 6.Create Ligaments====================
LM Gui Dialog Display topLevel=muscles subLevel="create_one"
LM Gui Dialog Display topLevel=muscles subLevel=create_one
!-----creat the Flaval Ligaments
LM Panel Tissue Single &
    action=create &
    model=.World &
    type=ligament &
    Vgroup=3 &
    f_muscle='NStiss_49' &
    f_part1=.World.Sanditi_Head &
    f_part2=.World.Sanditi_C1 &
    f_location1=0.0, 582.0, -56.0 &
    f_location2=0.0, 576.0, -40.0 &
   f_stiff=23.3 &
   f_damp=2.33 &
   f_preload=0.0 &
```

Table 2: Stiffness properties of cervical spine ligaments (N/mm)

Cervical spine region	Interspinous ligament (ISL)	Ligament flavum (LF)	Anterior longitudinal ligament (ALL)	Posterior longitudinal ligament (PLL)	Joint capsule (JC)
Stiffness	7	23.3	17	24.2	32.5

Table 3: Stiffness properties of lumbar spine ligaments (N/mm)

Lumbar spine region	Interspinous ligament (ISL)	Ligament flavum (LF)	Anterior longitudinal ligament (ALL)	Posterior longitudinal ligament (PLL)	Joint capsule (JC)
Stiffness	11.5	27.2	33	20.4	33.9

Note: for thoracic spine ligaments, stiffness properties are mean values of those in the cervical and lumbar spine regions.

Step7: Generating the Spinal Joints

It is necessary to create individual non-standard joints between each newly created vertebra. The spinal joints are modeled as torsional springs and the passive 3 DOF jointed action can be defined with user-specified stiffness, damping, angular limits and limit stiffness values. These values can be referenced in Table 4 and 5. In this step, 24 joints representing intervertebral disc generated as a connector between each two vertebrae.

Table 4: Average torsional stiffness values for adult human spines (N.mm/deg)

Spinal level	Flexion/Extension	Lateral bending	Axial rotation
Occ-C1	40/20	90	60
C1-C2	60/50	90	70
C2-C7	400/700	700	1200
T1-T12	2700/3300	3000	2600
L1-L5	1400/2900	1600	6900
L5-S1	2100/3000	3600	4600

Table 5: Average segmental ranges of motion at each spine level (degree)

Spinal level	Flexion	Extension	Lateral bending	Torsion
Occ-C1	13	13	8	0
C1-C2	10	9	0	47
C2-C3	8	3	10	9
C3-C4	7	9	11	11
C4-C5	10	8	13	12
C5-C6	10	11	15	10
C6-C7	13	5	12	9
C7-T1	6	4	14	8
T1-T2	5	3	2	9
T2-T3	4	4	3	8
T3-T4	5	5	4	8
T4-T5	4	4	2	8
T5-T6	5	5	2	8
T6-T7	5	5	3	8
T7-T8	5	5	2	8
T8-T9	4	4	2	7
T9-T10		3	2	4
T10-T11	4	4	3	2
T11-T12	4	4	3	2
T12-L1	5	5	3	2
L1-L2	8	5	6	1
L2-L3	10	3	6	1
L3-L4	12	1	6	2
L4-L5	13	2	3	2
L5-S1	9	5	1	1

```
!!====================7. Creating  joints ==================
LM joint build section=single action=create prefix=NSjoint_5  inboard=.World.Sanditi_C1
outboard=.World.Sanditi_Head axis=.World.Sanditi_C1.m1  &
  dofType='passive','passive','passive'  &
  stiffness='30','60','90' &
  damping='3','6','9' &
  posLimit='13','0','8' &
  negLimit='13','0','8' &
  bump='1e6','1e6','1e6'
```

Step8: Create lumbar back muscles

In this section, four lumbar muscle sets were implemented to the model, Multifidus, erector spinae , psoas major and quadratus lumborum muscles. Attachment points and mechanical properties of each muscle will change based on the anthropometric data of the subject.

```
!!====================8. Creating lumbar back muscles  =================
LM Panel Tissue Single &
    action=create &
    model=.World &
    type=recording &
    Vgroup=3 &
    f_muscle='NStiss_231' &
    f_part1=.World.Sanditi_L1 &
    f_part2=.World.Sanditi_Lower_Torso &
    f_location1=-33.0, 194.5, -47.0 &
    f_location2=-50.0, 58.5, -47.0&
   f_preload=0 &
   f_Sigmax=0.7  &
   f_Tcsa=107  &
```

Step9: Create Abdomen muscles

Two abdominal muscles are included in the model: obliquus externus and obliquus internus. Modeling of these muscles requires the definition of an artificial segment with a zero mass and inertia. This artificial segment mimics the function of the rectus sheath on which the abdominal muscles can attach.

!!==========9.1 Creating rectus sheath ==========

```
material create  &
     material_name = .World.Rectus_Material  &
     youngs_modulus = 1E-008  &
     poissons_ratio = 1E-003  &
     density = 1.0E-007 &

LM status text='CREATING PART REPRESENTATION'
LM Panel Body Single &
 segment="Rectus_Sheath" &
 cm_location=0,0,0 &
 cm_orientation=0,0,0 &
  mp_method=material &
material=.World.Rectus_Material &
 shells=parasolid &
 geo_type=other &
 parasolid=":/location of the rectus sheath file" &
 parasolid_type=ASCII &
```

!!========== 9.2 Creating Abdomen muscles ==========

```
LM Panel Tissue Single &
     action=create &
     model=.World &
     type=recording &
     Vgroup=3 &
     f_muscle='NStiss_281' &
     f_part1=.World.Sanditi_Ribs &
     f_part2=.World.Sanditi_Lower_Torso &
     f_location1=-61.0, 200.0, -48.0 &
     f_location2=-110.0, 119.0, 0.0 &
    f_preload=0 &
```

```
f_Sigmax=0.7  &
f_Tcsa=397.4  &
```

Step10: Create Intra Abdominal Pressure

IAP is created only for passive simulation and when the motion data is absent. The stiffness value of the bushing element will change based on the anthropometric data of the subject.

```
!!==================== 10. CREATE BUSHING ==================
  marker create marker=.World. Sanditi _Ribs.MARKER_3001 &
  adams_id=3001 &
  location=0.0, 63.0, -9.0 &
  orientation=326.1830483667, 1.4168571039, 33.610633754
  marker create marker=.World. Sanditi _Lower_Torso.MARKER_3002 &
  adams_id=3002 &
  location=0.0, 63.0, -9.0 &
  orientation=326.1830483667, 1.4168571039, 33.610633754
  force create element_like bushing &
 bushing_name=.World.BUSHING_1 &
 adams_id=1 &
 i_marker_name=.World. Sanditi _Ribs.MARKER_3001 &
 j_marker_name=.World. Sanditi _Lower_Torso.MARKER_3002 &
 stiffness=(122.668(newton/mm)),(89.76(newton/mm)),(122.668(newton/mm)) &
 damping=(2.0E-002(newton-sec/mm)),(2.0E-002(newton-sec/mm)),(2.0E-002(newton-sec/mm)) &
 tstiffness=(6602.329(newton-mm/deg)),(9022.888(newton-mm/deg)),(6602.329(newton-mm/deg)) &
 tdamping=(3.490658504(newton-mm-sec/deg)),(3.490658504(newton-mm-sec/deg)),    (3.490658504(newton
mm-sec/deg)) &
```

Step11: Modify motion agents

Three of red markers in LifeMOD are belonging to Upper_Torso, one on T10, two on sternum and one on the right scapula. After refining Thoracic segment (upper_torso) these markers should be renamed to the appropriate segment. The script for renaming

MOTagent_9 is shown as below. Repeat this for MOTagent_7 and MOTagent_8 according to Table6.

```
!!==================== 11. Modify motion agents ==================
group modify group=SELECT_LIST obj=.World.Sanditi_T10.E_Sanditi_MOTagent_9
expand_groups=no
mdi modify_macro

entity modify entity=.World.Sanditi_T10.Sanditi_MOTagent_9
new_entity=.World.Sanditi_Right_Scapula.Sanditi_MOTagent_9

geometry modify shape ellipsoid  &
  ellipsoid_name = .World.Sanditi_Right_Scapula.E_Sanditi_MOTagent_9  &
  center_marker = .World.Sanditi_Right_Scapula.Sanditi_MOTagent_9  &
  x_scale_factor = 26.67  &
  y_scale_factor = 26.67  &
  z_scale_factor = 26.67
```

Table 6:Modify motion agents

	entity modify entity	*new_entity*
MOTagent_7	*.World.Sanditi_T10.Sanditi_MOTagent_7*	*.World.Sanditi_Sternum.Sanditi_MOTagent_7*
MOTagent_8	*.World.Sanditi_T10.Sanditi_MOTagent_8*	*.World.Sanditi_Sternum.Sanditi_MOTagent_8*

Step12: Running an equilibrium analysis

The equilibrium analysis consists of three steps:

I. In order to fit the model to the data positions, an equilibrium analysis must be performed. This is a dynamics analysis which holds the positions of the data-driven motion agents (yellow balls) fixed, while finding the minimum energy configuration

in the springs of the motion agents. The motion agents with the higher weights will have more influence on the model and the initial configuration. (see Figure 4.a)

II. Update model posture with equilibrium results.(see Figure 4.b)

III. Synchronize body marker locations with data locations to be equivalent with the data source (see Figure 4. c).

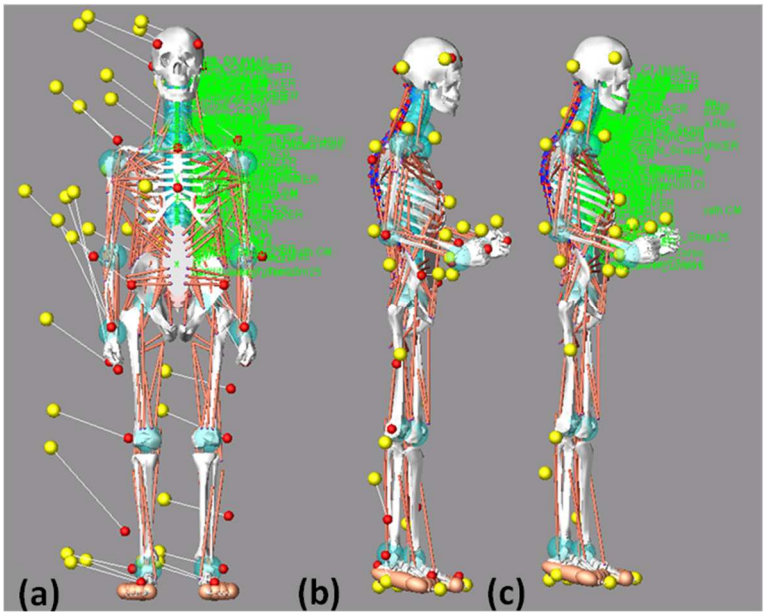

Figure 4: Data locations when agents first created (left), after moving into center of data cloud (center) and after equilibrium simulation (right)

The weights and the global scale factors on the motion agents can be adjusted in parameters section from the main menu based on the maneuver. The ultimate goal after modeling is to minimize the error. By tuning parameters during modeling we can achieve the minimum error. Increasing the global scale factors means that we increase the accuracy of the model to following the same motion as the subject had done in reality. But it can increase the joint force. In the other hand with less stiffness of motion agents, the forces go down, but the error will increase between the red and yellow balls. Ideally we want the forces in the MAs to be high enough that the kinematic errors are acceptably small in the motion. For accurate joint forces, we need to tune these parameters such that the model represents a real human by comparing the joint force results to the literature.

Step13: Create Foot-Floor contacts

Create the ground marker and foot-floor ellipsoids contact using the following ADAMS/View commands.

```
!!====================Create Foot-Floor contact ==================
marker create marker=.World.ground.flr loc=0.0, -766.0, 0.0 ori=0,-90,0 rel=.World
LM Panel Contact Set &
 type=ellipsoid &
 segment_head=off &
 segment_neck=off &
 segment_upper_torso=off &
 segment_central_torso=off &
 segment_lower_torso=off &
 segment_Right_Scapula=off &
 segment_right_upper_arm=off &
 segment_right_lower_arm=off &
 segment_right_hand=off &
 segment_Left_Scapula=off &
 segment_left_upper_arm=off &
 segment_left_lower_arm=off &
 segment_left_hand=off &
 segment_right_upper_leg=off &
 segment_right_lower_leg=off &
 segment_right_foot=off &
 segment_left_upper_leg=off &
 segment_left_lower_leg=off &
 segment_left_foot=off  &
 segment_right_foot_multiple=on &
 segment_left_foot_multiple=on &
 con_marker=.World.ground.flr &
 con_plane=on &
 con_thick=10 &
 con_color=blue &
```

con_x=10000 &
con_y=10000 &
con_stiff=200 &
con_exp=1.5 &
con_damp=2 &
con_depth=1 &
fric_static=1.0 &
fric_velocity =1 &
t_1vec=on &
t_simple=on &

Step14: Running the Inverse-Dynamics Simulation

From this simulation, it can be seen that the human model will track the motion data. Discrepancies between the recorded motion history and the performance of the model can be witnessed by observing the Motion Agents during animation. A yellow sphere will track the motion exactly; a red sphere is rigidly attached to the body segment. When a discrepancy between the data and the kinematics restraints in the model occur there will be a separation of these two spheres (the bushing uniting the two parts extends). This flexibility allows the Motion Agents to become "motion influencers" rather that motion governors. This allows for errors in data, measurement and collection. As a product of the inverse-dynamics simulation or the "training" phase, the rotations of the joints are recorded to be used in the following forward-dynamics simulation.

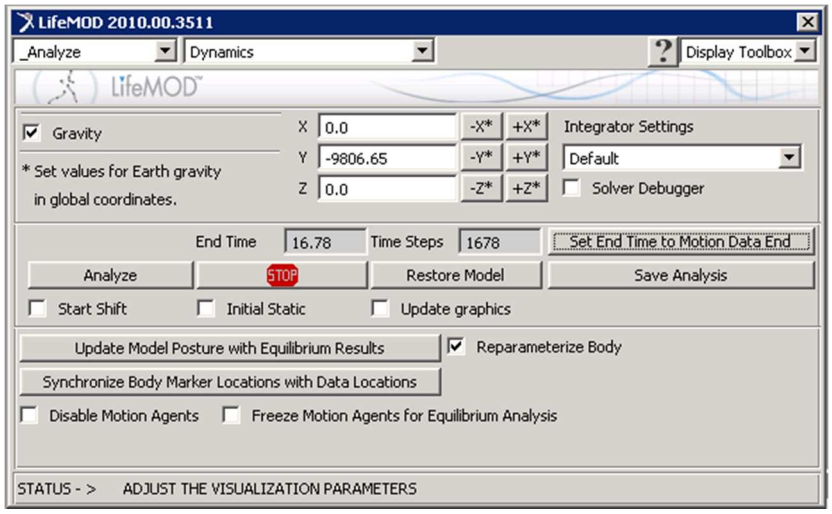

Figure 5: Inverse dynamic step

Step15: Preparing the Model for the Forward Dynamics Simulation

After the inverse-dynamics simulation is performed the joint angulation histories are now recorded for each joint. In this section, trained elements or PD-Servo controllers are exchanged for the passive learning elements on the joints.

The motion agents are removed from the model and a "Tracker Agent" is installed. The tracker agent is a motion agent located at the center of the pelvis which provides force-stabilization for the forward-dynamics simulation. During the inverse-dynamics simulation the location and orientation of the frame of the tracker agent is recorded (it is not generating a force during the inverse-dynamics simulation). The location and orientation information may then be used to drive the tracker agent in the forward-dynamics simulation. Usually various degrees-of freedom are specified as "free" to allow for proper dynamical interaction.

Install Trained DRIVER rotational joint elements

Select "Install Trained Driver Rotational Joint Elements." Enter 1e5 and 1e3 for the servo proportional and derivative gain respectively. Select APPLY to update the joints.

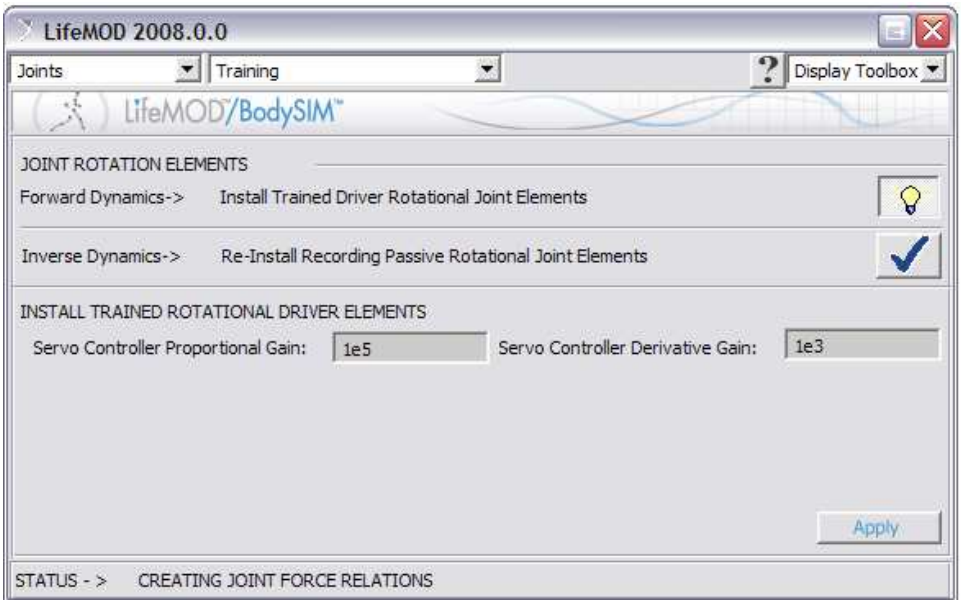

Figure 6. Panel to install PD-Servo controller ("trained" elements) on the joints for forward dynamic simulation

Create the tracking agent

A tracking agent is a motion agent used during a forward-dynamics simulation. It is used to guide the model by applying small spring forces via the connector bushing to account for various minor instabilities in the model. Instabilities could occur due to mathematical round-off error, model imbalance, etc. See Figure A7 for the location of the tracking agent. In this study, the freedom in the direction normal to the floor would be specified as free, to allow for proper ground reaction force generation between the feet and the steps.

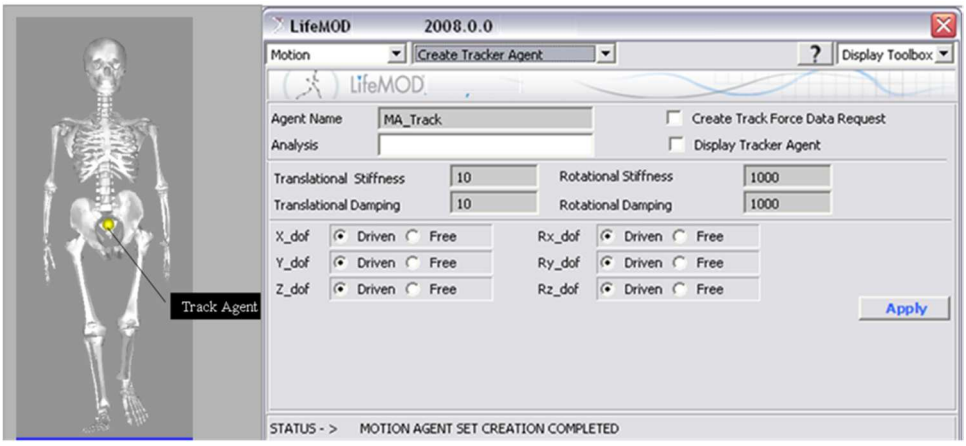

Figure 7. Panel to create the tracker agent

Install Trained DRIVER rotational joint elements

With the muscle contraction history recorded from the inverse-dynamics simulation, it is now used in linear PD-Servo formulation to produce a force to recreate the motion history. The process entails deactivating the Motion Agents and updating the muscles. Select SOFT TISSUES on the sub-menu and TRAINING on the panel. Select "Install Trained Closed-loop Contractile Elements on Muscles"

Specify 1e8 as the proportional gain, 1e6 as the integral gain, and 1e4 as the derivative gain. These values control how well the PID-servo actuators will track the desired contraction at each time step in the analysis. Note that the individual muscle will not produce a force greater than the physiological cross section area (pCSA) times the maximum tissue stress. Select APPLY to update the muscles.

Step 16: Running the Forward-Dynamics Simulation

With the joint formulated to include PD-servo controllers based on motion recorded from the inverse-dynamics analysis and the foot-floor contact forces installed, the model is now ready for a forward dynamics simulation. Be sure to disable the motion agents.

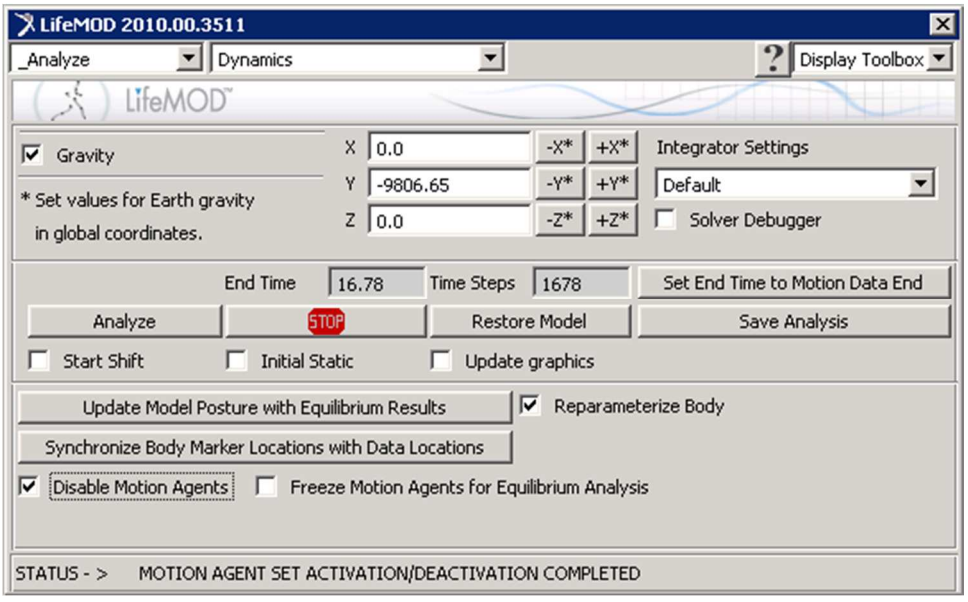

Figure 8. Panel to do analysis